Variation in ringed seal density, distribution, and diet across a latitudinal gradient of sea ice

by

Cody G. Carlyle

A Thesis submitted to the Faculty of Graduate Studies of

The University of Manitoba

in partial fulfilment of the requirements of the degree of

MASTER OF SCIENCE

Department of Biological Sciences

University of Manitoba

Table of Contents

Thesis Abstract i

Acknowledgements ii

List of Tables iii

List of Figures iv

Contributions of Authors vii

Chapter 1: General introduction 1

References 7

Chapter 2: Variation in ringed seal density along a latitudinal gradient of sea-ice dynamics 14

Abstract 14

Introduction 15

Methods 18

Survey design *18*

Digital survey protocol *19*

Image processing *20*

Density estimation *21*

Sea-ice concentration *22*

Statistical analysis *22*

Results 23

Discussion 24

References 40

Chapter 3: Ringed seal diet biomarkers identify spatial variation in carbon source and trophic dynamics across a latitudinal gradient of sea ice 46

Abstract 46

Introduction 47

Methods 50

Sample collection and study sites *50*

Stable isotope analysis *52*

Highly branched isoprenoid (HBI) analysis *54*

Statistical analysis *56*

Results........57

Stable isotope analysis........*57*

Relative carbon source and highly branched isoprenoids........*58*

Relative trophic position........*58*

Discussion........59

References........73

Chapter 4: Marine mammal biodiversity and rare narwhal (*Monodon monoceros*) observations near northern Ellesmere Island, Canada........82

Abstract........82

Acknowledgments........88

References........89

Chapter 5: General conclusion........94

References........98

Appendix A: Statistical tables and supplementary figures........102

Appendix B: Supporting tables and figures from Chapter 4........116

Thesis Abstract

Climate change is causing the poleward redistribution of species linked to abiotic factors such as temperature. The Arctic is warming three times faster than the global average and causing a rapid climate-driven recession of sea ice, which is an added stressor to Arctic species and ecosystems. As a mobile, generalist predator, ringed seals integrate resources spatially and trophically up the Arctic marine food web, which makes them a model indicator of how the Arctic marine ecosystem will respond to environmental change. Ringed seals are also vulnerable to loss of the sea-ice habitat they depend on for pupping, nursing, moulting, and prey from sea-ice derived food webs but experience a broad range of sea-ice conditions from the southern to northern edge of their range. The objectives of this thesis were to determine how the (1) density and (2) diet of ringed seals varied over the vastly different icescapes within their latitudinal range. Our results indicated latitudinal variation in ringed seal density potentially increased with availability of preferred first-year ice habitat. We also found a shift in ringed seals diets from primarily phytoplanktonic carbon in the low Arctic to a high proportion of ice-algal carbon in the high Arctic. The observed change in the base of food webs contributing to ringed seal diets may also have implications for trophic dynamics in these food webs. Overall, we show the potential of ringed seal density and diet to indicate large scale changes to the Arctic environment and Arctic food webs. We also provide insight into the potential responses to continued sea-ice recession of a key species for Arctic ecosystems and communities, important information for cooperative management of Arctic resources.

Acknowledgements

First, I want to thank my supervisors Dr. Steven Ferguson and Dr. James Roth. I will always appreciate the incredible opportunities Steve has afforded to me and the support he has provided while attempt to navigate academia. Jim has been amazing for welcoming me into his lab with open arms and giving me the same high level of commitment and support he gives all his students despite me unexpectedly becoming a part of his lab.

I also want to thank Dr. Dave Yurkowski, an *ex officio* member of my committee who has been essential to this project since day one and has been a vital source of advice, support, and mentorship these past few years.

Dr. Stephen Petersen and Dr. Jens Ehn also deserve recognition for their knowledge and contributions to this project.

I would not have succeeded without the help of many Biologists, technicians, and postdocs. Most of all Brent Young was and endless source of help when I came knocking and Dr. Doreen Kohlbach was great for teaching and making lab work more enjoyable. Bruno Rosenberg, Tera Edkins, Justine Hudson, Robyn Gervais, and Megan Wardekker also deserve mention. I also can’t forget the help and excellent conversations with Max Griffin.

I was fortunate to be able to participate in some incredible field seasons with the Last Ice Team in Alert and thank everyone that was involved for their friendship, support, and memories including Ben Lange, Pascal Tremblay, Melissa Galicia, Katie Florko, Uluriak Amarualik, Suupi Idlout, Steve Duerksen, Joannie Charette, Pierre Coupel, Constance Duffaud, Karley Campbell, Graham Underwood, Christine Michel, and my Finnish culture consultant Arttu Jutila.

Thanks to the Resolute, Arviat, Pond Inlet, Grise Fjord, and Qaannaaq communities and Hunters and Trappers Associations that made my research possible. Thanks also to CFS Alert, PCSP and Kenn Borek for making the surveys possible. Special mention to pilots Phil, Doug, Kelsey, Troy, Steve, Alex, Ollie, Hugh, Jorge and Genia. I also can’t forget engineer Cody 2.0.

Thank you to all the FWI and Roth Lab students who helped me survive this adventure. Especially Alexandra Mayette for helping me have fun and stay sane. Thanks Kevin Scharffenberg, Wesley Ogloff, Kasey Ryan, Chris Peck, Luke Storrie, Shu-Ting Zhao, Cassandra Debets, Kyle Lefort, Justine Hudson, Francis Beaudet, Lauren Wiens, Jillian St. George, Tommy Pontbriand, Kim Ovitz, Veronica Coppolaro, Emma Ausen, Sean Johnson-Bice, Morgan Dobroski, Alex Windsor, Chloe Rodrigues, Jess Lang, Megan Dudenhoeffer, Phil Shimel, Caila Kucheravy, and Annemarie van der Marel.

Finally, thank you to my family and friends back home, especially Lori and Colin Carlyle for always supporting my path in this strange journey of biology even if it is hard to understand at times. The rock I have in all of you gives me the motivation to take risks and follow my goals.

Thanks to DFO, NSERC, UM, and the Weston Foundation for financially supporting my research.

List of Tables

Table 2.1. Summary of digital-based aerial surveys from our low, intermediate and high-Arctic locations (2016-2019) (Young et al. 2019b, Yurkowski et al. 2019b) and past observer based aerial surveys for additional context (2007-2010, 2013) (Young et al. 2015b). 38

Table 3.1. Summary of means (SE) of $\delta^{15}N$, $\delta^{13}C$, sympagic carbon, relative carbon source, relative trophic position, and Carbon/Nitrogen ratio for each tissue type from biomarker analysis of ringed seals in this study. 71

Table 3.2. Means (SE) of $\delta^{15}N$, $\delta^{13}C$ for prey samples. $\delta^{13}C$ was corrected to account for decreasing $\delta^{13}C$ in the atmosphere over time according to de la Vega et al. (2019)(Chambellant et al. 2013a, Quay et al. 2017)(Chambellant et al. 2013a, Quay et al. 2017) and to remove a carbonate correction made by Chambellant et al. (2013)..72

List of Figures

Figure 2.1. A latitudinal gradient of sea-ice conditions in the Canadian Arctic. Arviat, Nunavut (61.1°N) in western Hudson Bay represents the low Arctic, Pond Inlet, Nunavut (72.7°N) in Eclipse Sound/Lancaster Sound represents the intermediate Arctic, and Alert, Nunavut (82.5°N) in the Lincoln Sea/Nares Strait represents the high Arctic. Right: Conceptual representation of the increase in sea-ice conditions from low to high Arctic that forms the basis for our selection of a latitudinal gradient for this study. 31

Figure 2.2. Aerial surveys of ringed seals hauled out on sea ice conducted in the low (D: 2017), intermediate (C: 2016, 2017), and high (B: 2018, 2019) Arctic used to calculate relative density across a latitudinal gradient in the Canadian Arctic (A). Solid lines represent transects that were successfully flown. 32

Figure 2.3. Ringed seal observations recorded by infrared and visual photography from digital based aerial surveys in low (2017: A), intermediate (2016: B, C 2017: D) and high (2018: E 2019: F) Arctic regions..33

Figure 2.4. Ringed seal density estimates (means and 95% confidence intervals) calculated by strip transect analysis from digital-based aerial surveys in low (2017), intermediate (2016-2017), and high (2018-2019) Arctic regions. 34

Figure 2.5. Ringed seal density estimates (means and 95% confidence intervals) related to A) total sea-ice concentration (β = -0.0048), B) first-year ice concentration (β = 0.0059), and C) multiyear ice concentration (β = -0.0057). Digital based aerial surveys were conducted in low (squares), intermediate (triangles), and high Arctic (circles) regions. 35

Figure 2.6. (A) Ringed seal observations (red points) from the high Arctic aerial survey carried out from 2-5 June, 2018 and (B) a close up of five ringed seal observations on 5 June, 2018 overlaid with Radarsat-2 imagery. These observations demonstrate ringed seal occurrence at limited areas likely consisting of first-year ice or cracks (dark/smooth) in an environment dominated by multiyear ice (light/rough). 36

Figure 2.7. Conceptual diagram of the approximate proportion of time spent hauled out by ringed seals during the ice-covered season for the low (solid lines; square), intermediate (dotted lines; triangles), and high Arctic (dashed lines; circles) regions. This diagram demonstrates the

latitudinal variation in peak haul-out timing compared to our survey dates and how both surveys in the high Arctic may have been early for peak haul out...37

Figure 3.1. Main: A latitudinal gradient of sea-ice conditions from the eastern Canadian and western Greenland Arctic. Arviat, Nunavut (61.1°N) represents low latitude western Hudson Bay, Pond Inlet, Nunavut (72.7°N) represents intermediate latitude Eclipse Sound/Lancaster Sound, and Grise Fjord, Nunavut (76.4°N) and Qaanaaq, Greenland (77.5°N) represent high latitude Smith Sound/Jones Sound. Right: Conceptual representation of the increase in sea-ice conditions from low to high Arctic that reflects the latitudinal gradient that is the basis for this study. 65

Figure 3.2. δ^{13}C and δ^{15}N for ringed seal liver samples collected in 2018 from Arviat, NU, Grise Fjord, NU, and Qaanaaq, GL, and in 2016-2017 from Pond Inlet, NU (Table 3.1). Main: biplot of δ^{13}C and δ^{15}N with dashed ellipses representing the 95% confidence intervals of multivariate t-distributions for each location. Top: Boxplot of δ^{13}C for each location. Letters represent separate groups determined by Tukey post-hoc analysis. Right: Boxplot of δ^{15}N for each location..........66

Figure 3.3. δ^{13}C and δ^{15}N for ringed seal muscle samples collected in 2018 from Arviat, NU, Grise Fjord, NU, and Qaanaaq, GL, and in 2016-2017 from Pond Inlet, NU (Table 3.1). Main: biplot of δ^{13}C and δ^{15}N with dashed ellipses representing the 95% confidence intervals of multivariate t-distributions for each location. Top: Boxplot of δ^{13}C for each location. Letters represent separate groups determined by Tukey post-hoc analysis. Right: Boxplot of δ^{15}N for each location. 67

Figure 3.4. Relative carbon source index from seal liver and muscle samples collected from each study area (higher values indicate relatively more phytoplanktonic feeding and lower values indicate more benthic/sympagic feeding). Letters represent separate groups determined by Tukey post-hoc analysis. 68

Figure 3.5. Boxplot of sympagic carbon (%) as a percentage of total marine carbon in ringed seal diets for each location in this study (Table 3.1). Letters represent separate groups determined by Tukey post-hoc analysis. 69

Figure 3.6. Relative trophic positions calculated (see Eq. 1 Methods) for ringed seal liver and muscle using *Calanus* literature values as a baseline (TP = 2) from Arviat, NU (Chambellant et al. 2013a), Lancaster Sound, NU for Pond Inlet (Hobson, Keith A., and Welch 1992), and the

North Water Polynya for Grise Fjord, NU and Qaanaaq, NU (Hobson et al. 2002) (Table 3.1). Letters represent separate groups determined by Tukey post-hoc analysis. 70

Figure 4.1. Close-up images of (A) a group of five narwhals including a yearling, (B) a bearded seal, and (C) six ringed seals taken in Archer Fjord and Lady Franklin Bay on 14 August 2019. (D) Close-up image of two Atlantic walruses taken in Archer Fjord on 18 August 2019............92

Figure 4.2. (A) The eastern Canadian and western Greenland Arctic. The area covered by the TMPA is indicated in red and the area covered by national parks is indicated in green (shapefiles from Natural Resources Canada at https://open.canada.ca/data). (B) Study region and place names mentioned in text. (C) Location of the marine mammals observed in Archer Fjord, Nunavut, Canada on 14 and18 August 2019. Map was generated using QGIS version 3.6.2 (http://www.qgis.org/en/site/)...93

Contributions of Authors

Chapter 4

Carlyle CG, Florko KRN, Young BG, Yurkowski DJ, Michel C, Ferguson SH (2021) Marine mammal biodiversity and rare narwhal (*Monodon monoceros*) observations near northern Ellesmere Island, Canada. Ecosphere 12(6):

CG Carlyle conceived the study, collected the data, analyzed the data, and wrote the manuscript. KRN Florko assisted with data collection and writing of the manuscript. BG Young, DJ Yurkowski, C Michel, and SH Ferguson provided guidance and reviewed the manuscript before submission.

Chapter 1: General introduction

Rising greenhouse gas emissions into the atmosphere have resulted in a 0.85°C increase in average global temperature since 1880 (IPCC 2014). This warming influences a variety of abiotic conditions and biotic interactions that organisms must respond to with movement, tolerance, adaptation, or extinction and is associated with the global poleward redistribution of species (Frainer et al. 2017, Pecl et al. 2017) and species tracking local climate velocities (Pinsky et al. 2013). Furthermore, variability in biogeography, species phenology, dispersal ability, and adaptive capacity has led to varying rates of redistribution by different species with major implications for species interactions and ecosystem function (Dey et al. 2017, Fossheim et al. 2015, Zarnetske et al. 2012). Understanding how species distributions, abundance, and food web interactions will respond to these stressors is necessary to inform conservation efforts in the face of continued environmental changes (Frainer et al. 2017, Pecl et al. 2017).

The rate of warming observed in the Arctic is three times the global average, threatening Arctic species with rapid environmental changes (Overland & Wang 2013, Laidre et al. 2015, Voosen 2020). One such change is recession of biologically important sea-ice characteristics, including a decline in total extent, thickness, age, and length of ice-covered season (Iverson et al., 2014; Laidre et al., 2015; Overland and Wang, 2013). This rapid climate-driven decline of sea ice can be a direct abiotic stressor through the loss of habitat to organisms that grow, reproduce, and feed on the sea ice but also has implications for changing interspecific interactions and food-web dynamics in the Arctic (Post et al. 2013, Dey et al. 2017; Iverson et al. 2014). For example, reduction in sea-ice extent has led to poleward range expansion and increased prevalence of sub-Arctic capelin (*Mallotus villosus*) and a concurrent decrease of

Arctic cod (*Boreogadus saida*) in the diet of thick billed murres (*Uria lomvia*), as well as causing changes in the timing and composition (phytoplankton versus sea-ice algae) of seasonal pulses in primary productivity in the Arctic (Provencher 2012, Arrigo & van Dijken 2015). Sea-ice recession is of special concern to ice-associated marine mammals that will be forced to respond to a northward shift in particular sea-ice conditions and phenology on which they depend (Laidre et al. 2015). Due to the remote and vast ranges of Arctic marine mammals, more knowledge on their distributions and ecology is needed to understand how they will respond to future sea-ice loss, especially in high latitudes expected to contain the last summer sea ice in the Arctic and function as a refuge for ice-associated species (Laidre 2015, Carlyle et al. 2021).

Ringed seal (*Phoca hispida*) are a vital link in Arctic ecosystem dynamics as a consumer of a variety of fish, crustaceans and benthic invertebrates, and as the main prey source for polar bears (*Ursus maritimus*) (Smith 1980, Stirling & Archibald 1977, Ferguson et al. 2005, Hamilton et al. 2015). Ringed seals are also key Arctic species that have a circumpolar distribution, are one of the most abundant Arctic pinnipeds, and are a vital target species for annual harvests by communities across the Arctic (Smith 1987, Mclaren 1958, Kovacs et al. 2011). Ringed seals can also be a prey source for walrus (*Odobenus rosmarus*) and Greenland shark (*Somniosus microcephalus*), as well as terrestrial scavengers such as Arctic foxes (*Vulpes lagopus*) during years of low primary prey abundance or food scarcity during winter months (Smith & Stirling 1978, Roth 2002). These many connections make ringed seals an indicator species of changing Arctic food webs (Laidre et al. 2008, Chambellant et al. 2012, de la Vega et al. 2021a b)

Ringed seals rely directly on sea ice as habitat for resting, pupping, and nursing in subnivean lairs, as well as for hauling out to undergo an annual moult (Mclaren 1958, Smith and Stirling 1975), and are therefore vulnerable to changes in sea-ice conditions and timing (Laidre et al. 2008, Kovacs et al. 2011). Ringed seals dig and maintain breathing holes in sea ice to remain in ice-covered areas throughout the winter and facilitate their critical life-history phases such as pupping and molting (Mclaren 1958, Kovacs et al. 2011). Due to the habitat requirements of the lairs and breathing holes ringed seals construct, they prefer thinner first-year landfast ice and areas of dense pack ice (Kovacs et al., 2011; McLaren, 1958; Smith and Harwood, 2001), or polynyas (Heide-Jørgensen et al. 2013, Stirling 1997). Ringed seals can also rely on sea-ice associated prey such as Arctic cod and in turn, experience predation pressure from polar bears that hunt on the sea ice (Stirling et al., 1993; Stirling and Lunn, 1997). However, changes in sea-ice conditions could alter the abundance and distribution of ice-associated prey and predators, while introducing novel interactions with more temperate species shifting poleward such as capelin and harp seals (Provencher 2012, Ogloff et al. 2020).

Ringed seals occupy a broad latitudinal range that experiences a large variation in sea-ice conditions from transient and first-year ice in the low Arctic to year-round coverage of first-year and multi-year sea ice in the high Arctic. The varying sea-ice conditions in these regions also influence the prey availability and foraging interactions that ringed seals experience across their range (Yurkowski et al. 2016a). Therefore, the abundance, distribution, and diet of ringed seals likely varies with regional sea-ice conditions and their responses to future change are likely not uniform across their range (Yurkowski et al. 2016c, Laidre et al. 2020). Ringed seals at the southern extremes of their range will likely be the first to experience the impacts of sea-ice recession via demographic shifts, diet changes, and range contraction, but the northern region of their range is seldom studied (Ferguson et al. 2017, Ferguson et al. 2020, Laidre et al. 2018, Reimer et al. 2019). This study intended to address this knowledge gap using a combination of aerial surveys and diet biomarker analyses.

Aerial surveys can be costly in remote areas of the Arctic, but are an effective tool to study Arctic marine mammals over their vast distributions (Valcroze et al. 2020). When systematically designed, aerial surveys are used to estimate abundance or densities of marine mammals using strip transect or distance sampling analysis and can be consistently repeated over time to monitor long-term changes in population abundance and distribution. For example, aerial surveys have commonly been used to observe and estimate the relative abundance of ringed seals in the Canadian Arctic during the moulting season when the highest proportion of ringed seals are basking on ice and available to count (Finley 1979, Bengtson et al. 2005, Young et al. 2015). However, aerial surveys are subject to availability bias when Arctic marine mammals are present but undetectable (submerged under water or ice), and visibility bias from poor detection by observers due to factors such as aircraft speed, altitude, and observer fatigue (Young et al. 2019a, Florko et al. 2021). Biotelemetry tools can be used to estimate proportion of time spent above the water or ice to correct for availability bias and obtain more accurate estimates of abundance (Bengtson et al. 2005, Conn et al. 2014). Recent technological advancements have allowed aircraft to collect visible light and infrared images of survey transects to improve detection, eliminate visibility bias, and reduce costs and logistical constraints of observer based aerial surveys (Conn et al. 2014, Cameron et al. 2015, Young et al. 2019). These digital survey methods have been applied successfully to improve abundance estimates from aerial surveys of ringed seals while hauled out (Cameron et al. 2015, Young et al. 2019b). Correcting for availability and visibility bias, improves the usefulness of aerial surveys as a tool to estimate the relative abundance of ringed seals over large areas throughout the Arctic.

Stable isotope analysis is commonly used to identify feeding relationships and food web dynamics for consumers (Layman et al. 2012, Petersen and Fry 1987, Yurkowski et al. 2016b).

Specifically, $\delta^{15}N$ increases with trophic position and can identify spatial variation in trophic changes of a consumer's diet or food web when combined with baseline $\delta^{15}N$ tissue- and taxon-specific discrimination factors ($\Delta^{15}N$) (Minagawa & Wada 1984, Hobson et al. 1996, Caut et al. 2009, Yurkowski et al. 2016b). Further, $\delta^{13}C$ can be used to identify relative source of diet, and is often used in the marine environment to infer the relative contribution of pelagic versus benthic production in a consumer's diet (DeNiro & Epstein 1978, McMeans et al. 2013a, Pedro et al. 2020). However, in polar ecosystems, ^{13}C enrichment similar to benthic feeding is observed in sea-ice algae, making it difficult to infer whether an increase in $\delta^{13}C$ over a gradient is due to an increase in benthic or sympagic (sea-ice associated) carbon in the diet of polar consumers (Kohlbach et al. 2019, Pedro et al. 2020). Highly branched isoprenoids (HBIs) are lipids found in diatoms that are differentially produced in sea-ice algae compared to pelagic phytoplankton, and these HBIs transfer predictably up the food chain into fish and marine mammals (Belt et al. 2012, Brown et al. 2014b). We can then use HBIs as an indicator of the relative importance of sympagic versus pelagic production in Arctic consumer diets to characterize and understand the ecosystems that these animals rely on for energy (Brown et al. 2014b a, 2017, 2018). Therefore, HBIs and stable isotope analysis could be compared over a spatial or environmental gradient as complementary tools for greater insight into feeding relationships and carbon sources in the diet of Arctic consumers (Brown et al. 2014a, Yurkowski et al. 2020a).

The objectives of this thesis were to investigate how 1) the density, distribution, and 2) the diet of ringed seals varied with spatial variation in regional sea-ice conditions across their latitudinal range. With an unprecedented opportunity to conduct aerial surveys in the high Arctic, we also investigated 3) the biodiversity and distribution of marine mammals in the high Arctic. To accomplish these objectives, we estimated the density of ringed seals from aerial surveys across their latitudinal range in the low (Arviat, Nunavut, Canada), intermediate (Pond Inlet, Nunavut, Canada), and high (Alert, Nunavut, Canada) Arctic and explored how density was correlated to the sea-ice conditions (concentration of first-year ice and multi-year ice) in each region (Chapter 2). We also analyzed stable isotope and HBI diet biomarkers in ringed seal muscle and liver tissues to determine the relative contribution of different primary production sources, and the relative trophic position of ringed seals across the low (Arviat, Nunavut), intermediate (Pond Inlet, Nunavut), and high (Grise Fjord, Nunavut and Qaanaaq, Greenland) Arctic (Chapter 3). Lastly, we documented the occurrence and location of ringed seals and other marine mammals from aerial surveys in the high Arctic (northern Ellesmere Island, Nunavut, Canada) to better understand the use of this seldom studied region by ice-associated marine mammals (Chapter 4). We have provided information on how ringed seals respond to regional variation in sea-ice conditions, which in a space-for-time study format (Hayden et al. 2019) is important context given continued environmental change in the Arctic. Overall, this thesis will help identify the mechanism of range and diet shifts in ringed seals that experience vastly different regional environmental conditions and could inform management and conservation.

References

Amstrup SC, York G, McDonald TL, Nielson R, Simac K (2004) Detecting denning polar bears with forward-looking infrared (FLIR) imagery. Bioscience 54:337–344.

Arrigo KR, van Dijken GL (2015) Continued increases in Arctic Ocean primary production. Prog Oceanogr 136:60–70.

Belt ST, Brown TA, Rodriguez AN, Sanz PC, Tonkin A, Ingle R (2012) A reproducible method for the extraction, identification and quantification of the Arctic sea ice proxy IP 25 from marine sediments. Anal Methods 4:705–713.

Bengtson JL, Hiruki-Raring LM, Simpkins MA, Boveng PL (2005) Ringed and bearded seal densities in the eastern Chukchi Sea, 1999–2000. Polar Biol 28:833–845.

Brown TA, Alexander C, Yurkowski DJ, Ferguson SH, Belt ST (2014a) Identifying variable sea ice carbon contributions to the Arctic ecosystem: A case study using highly branched isoprenoid lipid biomarkers in Cumberland Sound ringed seals. Limnol Oceanogr 59:1581–1589.

Brown TA, Chrystal E, Ferguson SH, Yurkowski DJ, Watt C, Hussey NE, Kelley TC, Belt ST (2017) Coupled changes between the H-Print biomarker and δ15N indicates a variable sea ice carbon contribution to the diet of Cumberland Sound beluga whales. Limnol Oceanogr 62:1606–1619.

Brown TA, Galicia MP, Thiemann GW, Belt ST, Yurkowski J, Dyck MG (2018) High contributions of sea ice derived carbon in polar bear (*Ursus maritimus*) tissue. PLoS ONE 13:e0191631.

Brown TA, Yurkowski DJ, Ferguson SH, Alexander C, Belt ST (2014b) H-Print: A new chemical fingerprinting approach for distinguishing primary production sources in Arctic ecosystems. Environ Chem Lett 12:387–392.

Cameron M, Sigler M, Moreland E, Towler R (2015) Advances in Methods for Marine Mammal.

Carlyle CG, Florko KRN, Young BG, Yurkowski DJ, Michel C, Ferguson SH (2021) Marine mammal biodiversity and rare narwhal (*Monodon Monoceros*) observations near northern Ellesmere Island, Canada. Ecosphere 12: e03534.

Caut S, Angulo E, Courchamp F (2009) Variation in discrimination factors (Δ^{15}N and Δ^{13}C): The effect of diet isotopic values and applications for diet reconstruction. J Appl Ecol 46:443–453.

Chambellant M, Lunn NJ, Ferguson SH (2012) Temporal variation in distribution and density of ice-obligated seals in western Hudson Bay, Canada. Polar Biol 35:1105–1117.

Conn PB, Ver Hoef JM, Mcclintock BT, Moreland EE, London JM, Cameron MF, Dahle SP, Boveng PL (2014) Estimating multispecies abundance using automated detection systems: Ice-associated seals in the Bering Sea. Methods Ecol Evol 5:1280–1293.

DeNiro M, Epstein S (1978) Influence of diet on the distribution in animals. Geochim Cosmochim Acta 42:495–506.

Ferguson SH, Stirling I, McLoughlin P (2005) Climate change and ringed seal (*Phoca hispida*) recruitment in western Hudson Bay. Mar Mammal Sci 21:121–135.

Ferguson SH, Young BG, Yurkowski DJ, Anderson R, Willing C, Nielsen, O (2017) Demographic, ecological and physiological responses of ringed seals to an abrupt decline in sea ice availability. PeerJ 5:e2957.

Ferguson SH, Yurkowski DJ, Young BG, Fisk AT, Muir DCG, Zhu X, Thiemann GW (2020) Comparing temporal patterns in body condition of ringed seals living within their core geographic range with those living at the edge. Ecography 43:1-15.

Finley KJ (1979) Haul-out behaviour and densities of ringed seals (*Phoca hispida*) in the Barrow Strait area, N.W.T. Can J Zool 57:1985–1997.

Florko KRN, Carlyle CG, Young BG, Yurkowski DJ, Michel C, Ferguson SH (2021) Narwhal (*Monodon monoceros*) detection by infrared flukeprints from aerial survey imagery. Ecosphere 12: e03698.

Fossheim M, Primicerio R, Johannesen E, Ingvaldsen RB, Aschan MM, Dolgov A V. (2015) Recent warming leads to a rapid borealization of fish communities in the Arctic. Nat Clim Chang 5:673–677.

Frainer A, Primicerio R, Kortsch S, Aune M, Dolgov A V., Fossheim M, Aschan MM (2017) Climate-driven changes in functional biogeography of Arctic marine fish communities. Proc Natl Acad Sci U S A 114:12202–12207.

Hamilton CD, Lydersen C, Ims RA, Kovacs KM, Kovacs KM (2015) Predictions replaced by facts : a keystone species ' behavioural responses to declining arctic sea-ice. Biol Lett 11: 20150803.

Hayden B, Harrod C, Thomas SM, Eloranta AP, Myllykangas JP, Siwertsson A, Præbel K, Knudsen R, Amundsen PA, Kahilainen KK (2019) From clear lakes to murky waters – tracing the functional response of high-latitude lake communities to concurrent 'greening' and 'browning'. Ecol Lett 22:807–816.

Heide-Jørgensen MP, Burt LM, Guldborg R, Nielsen NH, Rasmussen M, Fossette S, Stern H (2013) The significance of the North Water Polynya to Arctic Top Predators. Ambio 42:596-610.

Hobson KA, Schell DM, Renouf D, Noseworthy E (1996) Stable carbon and nitrogen isotopic fractionation between diet and tissues of captive seals. Can J Fish Aquat Sci 53:528–533.

Kohlbach D, Ferguson SH, Brown TA, Michel C (2019) Landfast sea ice−benthic coupling during spring and potential impacts of system changes on food web dynamics in Eclipse Sound, Canadian Arctic. Mar Ecol Prog Ser 627:33–48.

Kovacs KM, Lydersen C, Overland JE, Moore SE (2011) Impacts of changing sea-ice conditions on Arctic marine mammals. 181–194.

de la Vega C, Mahaffey C, Tuerena RE, Yurkowski DJ, Ferguson SH, Stenson GB, Nordøy ES, Haug T, Biuw M, Smout S, Hopkins J, Tagliabue A, Jeffreys RM (2021a) Arctic seals as tracers of environmental and ecological change. Limnol Oceanogr Lett 6:24–32.

de la Vega C, Mahaffey C, Yurkowski DJ, Norman L, Simpson E, Smout S, Ferguson SH, Jeffreys RM (2021b) Biomarkers in Ringed Seals Reveal Recent Onset of Borealization in the High- Compared to the Mid-Latitude Canadian Arctic. Front Mar Sci 8:700687.

Laidre KL, Atkinson SN, Regehr E V, Stern HL, Born EW, Wiig Ø, Lunn NJ, Dyck M, Heagerty P, Cohen BR (2020) Transient benefits of climate change for a high-Arctic polar bear (*Ursus maritimus*) subpopulation. Glob Chang Biol 1–15.

Laidre KL, Stern H, Kovacs KM, Lowry L, Moore SE, Regehr EV, Ferguson SH, Wiig Ø, Boveng P, Angliss RP, Born EW, Litovka D, Quakenbush L, Lydersen C, Vongraven D, Ugarte F (2015) Arctic marine mammal population status , sea ice habitat loss , and conservation recommendations for the 21st century. Cons Biol 29:724–737.

Laidre KL, Stirling I, Lowry LF, Wiig Ø, Heide-Jørgensen MP, Ferguson SH (2008) Quantifying the sensitivity of Arctic marine mammals to climate-induced habitat change. Ecol Appl 18:97–125.

Layman CA, Araujo MS, Boucek R, Hammerschlag-Peyer CM, Harrison E, Jud ZR, Matich P, Rosenblatt AE, Vaudo JJ, Yeager LA, Post DM, Bearhop S (2012) Applying stable isotopes to examine food-web structure: An overview of analytical tools. Biol Rev 87:545–562.

Mallory ML, Gilchrist HG, Janssen M, Major HL, Merkel F, Provencher JF, Strøm H (2018) Financial costs of conducting science in the Arctic: examples from seabird research. Arct Sci 4:624–633.

Mclaren IA (1958) The Biology of the Ringed Seal (*Phoca hispida Schreber*) in the Eastern Canadian Arctic. Ottawa, Fisheries Research Board of Canada. 97 pp.

McMeans BC, Rooney N, Arts MT, Fisk AT (2013) Food web structure of a coastal Arctic marine ecosystem and implications for stability. Mar Ecol Prog Ser 482:17–28.

Minagawa M, Wada E (1984) Stepwise enrichment of 15N along food chains: Further evidence and the relation between δ15N and animal age. Geochim Cosmochim Acta 48:1135–1140.

Ogloff WR, Ferguson SH, Tallman RF, Davoren GK (2020) Diet of capelin (*Mallotus villosus*) in the Eastern Canadian Arctic inferred from stomach contents and stable isotopes. Polar Biol 43:1273–1285.

Overland JE, Wang M (2013) When will the summer Arctic be nearly sea ice free? Geo Res Lett 40:2097–2101.

Pecl GT, Araújo MB, Bell JD, Blanchard J, Bonebrake TC, Chen IC, Clark TD, Colwell RK, Danielsen F, Evengård B, Falconi L, Ferrier S, Frusher S, Garcia RA, Griffis RB, Hobday AJ, Janion-Scheepers C, Jarzyna MA, Jennings S, Lenoir J, Linnetved HI, Martin VY, McCormack PC, McDonald J, Mitchell NJ, Mustonen T, Pandolfi JM, Pettorelli N, Popova E, Robinson SA, Scheffers BR, Shaw JD, Sorte CJB, Strugnell JM, Sunday JM, Tuanmu MN, Vergés A, Villanueva C, Wernberg T, Wapstra E, Williams SE (2017) Biodiversity redistribution under climate change: Impacts on ecosystems and human well-being. Science 355: eaai9214.

Pedro S, Fisk AT, Ferguson SH, Hussey NE, Kessel ST, McKinney MA (2020) Broad feeding niches of capelin and sand lance may overlap those of polar cod and other native fish in the eastern Canadian Arctic. Polar Biol 43:1707–1724.

Pinksy ML, Worm, B, Fogarty MJ, Sarmiento JL, Levin SA (2013) Marine Taxa Track Local Climate Velocities. Science 341: 1239-1242.

Post E, Bhatt US, Bitz CM, Brodie JF, Fulton TL, Hebblewhite M, Kerby JT, Kutz S, Stirling I, Walker DA (2013) Ecological Consequences of Sea-Ice Decline. Science 341:519–524.

Provencher JF (2012) Seabird diet indicates changing Arctic marine communities in eastern Canada. Mar Ecol Prog Ser 454:171-182.

Roth JD (2002) Temporal variability in Arctic fox diet as reflected in stable-carbon isotopes ; the importance of sea ice. Oecologia 133:70–77.

Smith TG (1980) Polar bear predation of ringed and bearded seals in the land-fast sea ice habitat. Can J Zool 58:2201–2209.

Smith TG, Stirling I (1978) Variation in the density of ringed seal (*Phoca hispida*) birth lairs in the Amundsen Gulf, Northwest Territories. Can J Zool 56:1066–1070.

Stirling I. (1997) The importance of polynyas, ice edges, and leads to marine mammals and birds. J Mar Syst 10:9-21.

Stirling I, Archibald R (1977) Aspects of predation of seals by polar bears. J Fish Res Board Can 34:1126–1129.

Doniol-Valcroze, T., Gosselin, J.-F., Pike, D.G., Lawson, J.W., Asselin, N.C., Hedges, K. & Ferguson S.H. (2020). Narwhal Abundance in the Eastern Canadian High Arctic in 2013. NAMMCO Scientific Publications 11. https://doi.org/10.7557/3.5100

Voosen P (2020) New feedbacks speed up the demise of Arctic sea ice. Science 369:1043–1044.

Young BG, Ferguson SH, Lunn NJ (2015) Variation in ringed seal density and abundance in western Hudson Bay estimated from aerial surveys, 1995 to 2013. Arctic 68:301–309.

Young BG, Yurkowski DJ, Dunn JB, Ferguson SH (2019a) Comparing infrared imagery to traditional methods for estimating ringed seal density. Wildl Soc Bull 43:121–130.

Yurkowski DJ, Brown TA, Blanchfield PJ, Ferguson SH (2020) Atlantic walrus signal latitudinal differences in the long-term decline of sea ice-derived carbon to benthic fauna in the Canadian Arctic: Climate change and imperiled ice carbon. Proc R Soc B Biol Sci 287.

Yurkowski DJ, Ferguson SH, Semeniuk CAD, Brown TM, Muir DCG, Fisk AT (2016a) Spatial and temporal variation of an ice-adapted predator's feeding ecology in a changing Arctic marine ecosystem. Oecologia 180:631–644.

Yurkowski DJ, Semeniuk CAD, Harwood LA, Rosing-Asvid A, Dietz R, Brown TM, Clackett S, Grgicak-Mannion A, Fisk AT, Ferguson SH (2016b) Influence of sea ice phenology on the movement ecology of ringed seals across their latitudinal range. Mar Ecol Prog Ser 562:237–250.

Chapter 2: Variation in ringed seal density along a latitudinal gradient of sea-ice dynamics

Abstract

Anthropogenic climate warming is triggering northward species redistributions and range shifts, highlighting the importance of understanding how species distributions and abundance vary over latitude. In the rapidly warming Arctic, northward retreating sea-ice conditions are an added stressor to ice-adapted species from ice algae to marine mammals. Ringed seals rely on sea ice as habitat throughout their life history and occupy a broad latitudinal range with large variation in sea-ice conditions. Therefore, ringed seals provide a useful model to study patterns in distribution and abundance over a spatial-environmental gradient. We estimated the density of ringed seals from systematic aerial surveys completed in the low, intermediate, and high Arctic to investigate latitudinal trends in ringed seal distribution that could be linked to regional variation in sea-ice dynamics. Ringed seal densities were similar in the low (2017: 0.46 ± 0.11 seals/km^2) and intermediate (2016: 0.70 ± 0.14 seals/km^2; 2017: 0.45 ± 0.07 seals/km^2) Arctic, but approximately an order of magnitude lower in the high (2018: 0.05 ± 0.01 seals/km^2; 2019: 0.09 ± 0.01 seals/km^2) Arctic, coincident with a decrease in first-year ice and increase in multiyear ice concentrations from low (First-year ice concentration: 85.0%; Multiyear ice concentration: 0.0%) to high (First-year ice concentration 13.2%: ;Multiyear ice concentration: 86.8%) Arctic. Our results suggest that ringed seals in the high Arctic are limited by a lack of first-year ice preferred for maintaining holes in the sea ice during critical life-history stages. These findings indicate that the vastly different icescapes across the ringed seal's range influences their density and highlights that the response of ringed seals to continued climate change and sea-ice recession will likely not be uniform.

Introduction

Species distributions and range limits are strongly linked to latitude in association with abiotic factors such as light and temperature (MacArthur 1965, Stevens 1989, Pecl et al. 2017). Anthropogenic climate change is altering these abiotic conditions, primarily temperature, which species must respond to by movement, tolerance, adaptation, or extinction. For example, climate warming is causing the poleward shifts of many species globally (Hof et al. 2012, Jenouvrier 2012). Understanding how species distributions and abundance vary over latitude will help predict how species respond to these stressors and detect changes in ecosystem function to inform conservation efforts trying to manage biological and socioeconomic impacts of continued environmental change (Pecl et al. 2017).

The rate of warming in the Arctic is three times faster than the global average, and is causing a reduction in the extent of sea ice as well as changes to its annual phenology (Voosen 2020). Sea ice is a fundamental characteristic of Arctic marine food webs that is strongly linked to latitude and temperature. The high Arctic experiences higher concentrations of ice, longer ice-covered seasons, and thicker and older sea ice in the high Arctic compared to the low Arctic. Ice-adapted species from sea-ice algae to polar bears (*Ursus maritimus*) rely on specific sea-ice dynamics and phenology for energy acquisition and habitat (Post et al. 2013). Sea-ice recession is one of the main drivers of the poleward redistribution of Arctic marine species, as well as an expansion of temperate species into the Arctic exploiting the reduction of sea ice (Fossheim et al. 2015, Frainer et al. 2017). Information on how latitudinal variation in sea-ice conditions influences the distributions of Arctic species will give insight into how biogeographic patterns may shift in the context of global change (Frainer et al. 2017).

Ringed seals are a key species in Arctic marine food webs as a mobile, opportunistic predator that provides an integral link between lower trophic levels and polar bears (Mclaren 1958). With a circumpolar distribution and as the most abundant Arctic pinniped, they are also an important species in annual subsistence hunts by northern people. Therefore, understanding the abundance and distribution of ringed seals throughout the Arctic, and the factors influencing them, is vital to understanding the impacts of climate change on Arctic ecosystems and humans. Ringed seals prefer first-year stable landfast or consolidated pack ice for construction and maintenance of their subnivean (under snow) lairs and breathing holes for breeding, pupping, and nursing (Mclaren 1958, Smith & Hammill 1981). After the subnivean period, ringed seals still require stable landfast or consolidated first-year ice while they undergo an energetically costly annual moult (replacement of epidermal tissue) (Mclaren 1958, Thometz et al. 2020). For this reason, ringed seals as a species depend on ice habitat, and specific conditions and phenology to facilitate the requirements of each life-history phase. However, ringed seals occupy a broad latitudinal range with large variation in sea-ice conditions, from the transient coverage in the low Arctic, to year-round high concentrations in the high Arctic. This variation makes ringed seals an interesting model to investigate changes in density and distribution over a large scale latitudinal and environmental gradient related to sea-ice conditions and phenology.

Extremely long ice-covered seasons have been linked to poor breeding success and body condition in ringed seals, potentially due to their habitat requirements for maintaining subnivean lairs and breathing holes, which ringed seals use for breeding, pupping, and moulting (Harwood et al. 2012). Conversely, ringed seals experience increased pup mortality during years of light sea-ice conditions, a shorter ice-covered season, and associated environmental conditions such as a lack of snow on ice (Ferguson et al. 2005, Iacozza & Ferguson 2014, Reimer et al. 2019).

Further, lighter sea-ice conditions with a shorter ice-covered season may lead to a decrease in preferred dense pack ice and more unstable loose pack ice with larger cracks and leads, which could affect energetic costs of the moulting process (Mclaren 1958, Kovacs et al. 2011, Thometz et al. 2020). Therefore, the large spatiotemporal variation in sea-ice conditions and phenology that ringed seals experience likely affects their regional abundance and distributions, and suggests that responses to changes in sea-ice conditions may not be uniform across their range (Yurkowski et al. 2016c, Laidre et al. 2020). In the well-studied southern end of their range, ringed seals are expected to experience the impacts of sea-ice recession via demographic shifts, diet changes, and range contraction (Ferguson et al. 2005, 2017a, Young & Ferguson 2013b). The higher latitudes of the ringed seals range are seldom studied, due to their remote range and the logistical challenges of conducting research in the high Arctic (Laidre et al. 2008, Mallory et al. 2018).

The aims of this study were to investigate 1) how the density of ringed seals varies across the latitudinal gradient of their range, and 2) the potential link between variation in ringed seal densities and the different sea-ice conditions experienced across this latitudinal gradient. We hypothesized that latitudinal variation in ringed seal density will reflect availability of first-year landfast or consolidated pack ice preferred for hauling out. At low latitudes, more abundant first-year ice will permit higher spring densities of ringed seals, while in the high Arctic, high concentrations of multiyear ice with limited first-year ice will limit ringed seal densities. Under this hypothesis, the intermediate Arctic should display first-year ice availability and ringed seal densities in between the low and high Arctic. Alternatively, a shorter ice-covered season with more open water in the low Arctic may limit stable first-year landfast and consolidated ice. Therefore, ringed seal density estimates may be highest in the intermediate Arctic.

Methods

Survey design

Aerial surveys were conducted in the low Arctic (near Arviat, Nunavut, Canada: 61.1°N), intermediate Arctic (near Pond Inlet, Nunavut, Canada: 72.7°N), and high Arctic (near Alert, Nunavut, Canada: 82.5°N) (Fig. 2.1). Western Hudson Bay, near the southern end of the ringed seals' range, experiences seasonal first-year sea-ice coverage and no multiyear ice. Complete ice coverage is from December until break up in June and open water is from July until freeze up begins in late October and November (Wang et al. 1994, Laidre et al. 2020). At more intermediate latitudes around Pond Inlet, first-year ice primarily occurs with some multiyear sea ice present. Sea-ice break-up begins later in June or early July with a shorter open-water period, and freeze-up begins earlier for complete ice coverage in November (Welch et al. 1992, Galley et al. 2012). Near the northern extent of the ringed seals' range, in the Lincoln Sea and Nares Strait region, sea-ice coverage is predominantly multiyear sea ice and is heavy year-round, although coverage in summer can be dynamic and shift between dense pack ice and open water on daily to weekly time scales (Moore et al. 2019). These three regions form a spatial and environmental gradient of low, intermediate, and high Arctic that covers a broad variation in sea-ice conditions across the latitudinal range of ringed seals (Fig. 2.1).

For each survey, strata were of an equal-interval systematic strip-transect design with a random start to create uniform coverage probability for robust estimation of relative density (Lunn et al. 1997, Chambellant et al. 2012b, Thomas et al. 2013, Young et al. 2015b). The low-Arctic survey consisted of ten parallel transects totalling 3074 km at a spacing of 27.8 km (0.25° of latitude; 1.8% coverage) from the western Hudson Bay shoreline to 89° W longitude in the east and from Arviat (61.1°N) in the north to just south of Churchill, Manitoba, Canada (58.8°N)

(Fig. 2.2) (Lunn et al. 1997, Chambellant et al. 2012b, Young et al. 2015b). The intermediate Arctic surveys consisted of 35 parallel transects totaling 874 km at a spacing of 5 km (5% coverage) covering Eclipse Sound on northern Baffin Island (Fig. 2.2) (Young et al. 2019b, Yurkowski et al. 2019b). The high-Arctic surveys consisted of 51 parallel transects totalling 4074 km at a spacing of 5 km (5% coverage) along the northern coast of Ellesmere Island up to 131 km offshore in the surrounding Nares Strait and Lincoln Sea (Fig. 2.2) (Yurkowski et al. 2019a, Carlyle et al. 2021).

The surveys were conducted from late May to mid-June (Table 2.1), when ringed seals haul out on the sea ice for moulting (Mclaren 1958). We targeted this peak haul-out period for timing our surveys to produce comparable estimates of ringed seal density between locations. All surveys were flown between 0800 and 1800 and in low wind, cloud cover, fog, and precipitation, as adverse weather such as wind and cloud cover can reduce the haul-out proportion and visibility of ringed seals (Bengtson et al. 2005, Carlens et al. 2006). For the low-Arctic survey in 2017, weather allowed for completion of only four of the ten transects used for density estimation (Fig. 2.2D; Table 2.1). For the intermediate Arctic, every transect line could be completed twice in 2016 and once in 2017 (Fig. 2.2C; Table 2.1). For the high Arctic, we could fly every transect line in 2018 and 2019 (Fig. 2.2B; Table 2.1).

Digital survey protocol

We used digital survey methods to detect seals due to the improved detection, and more simplified data collection, processing, and analysis of digital methods over traditional visual-observer methods (Conn et al. 2014, Cameron et al. 2015, Young et al. 2019b). Surveys were flown in a DeHavilland Twin Otter (DH-6) aircraft at a target altitude of 305 m (1000 feet) and speed of 204 km/h (110 knots). A custom hole and mounting bracket in the belly of the aircraft was equipped with a Nikon (Tokyo, Japan) D810 digital single-lens reflex (DSLR) camera with a 35mm lens and a Forward Looking Infrared (FLIR; FLIR Systems, Inc., Wilsonville, OR, USA) T1030sc camera with a 45° lens. The DSLR took images every two seconds for an approximate 30% overlap between each successive image and the FLIR took video at a rate of 5 Hz. This continuous collection of visible and infrared imagery of the area beneath the plane allowed a transect strip width of 312 m at a resolution of 7360x4912 pixels for the digital imagery and a strip width of 250m at a resolution of 1024x768 pixels for infrared imagery. The 2019 high-Arctic survey used an array of two DSLR cameras instead of a DSLR and FLIR camera. A Bad Elf (West Hartford, CT, USA) global positions system (GPS) was mounted in the plane and recorded the position, altitude, speed, and heading of the aircraft every second and connected to the Nikon through a Foolography (Berlin, Germany) Bluetooth unit, which allowed geotagging of every photo along the transect line. For each transect, the camera operator recorded the starting and ending image for the Nikon, the starting file and duration of each FLIR video, and a time stamp that linked each infrared image to each geotagged visible image. A visual observer also documented environmental conditions such as ice concentration in tenths, cloud cover (%), fog, and precipitation.

Image processing

Collected imagery was analyzed by a trained observer for seals hauled out on sea ice. The infrared video using FLIR Research IR Max software version 4.30.1.70 (FLIR Systems, Inc., Wilsonville, OR, USA) was scanned to detect heat signatures corresponding to potential animals. Then the observer checked the GPS-matched visible image from the DSLR camera to validate the presence of ringed seal(s). Validation with images also allowed accurate recording of the number of seals associated with each observation. The low-Arctic survey in 2019 without FLIR video was analyzed for seals by individually scanning each image, which increased processing time but has a comparable success rate to infrared processing (Young et al. 2019b). GPS data associated with each image allowed a time and geographic position to be applied to all observations.

Density estimation

Ringed seal detections on each transect were used in strip-transect analysis of the 250m strip below the plane covered by the FLIR camera. For the 2019 high-Arctic survey with only DSLR images, the 312 m strip captured by the DSLR camera was used. Strip-transect analysis was performed according to Young et al. (2019) adapted from previously established methods for observer-based aerial surveys (Chambellant et al. 2012a, Young et al. 2015b). Ringed seal density (seals/km^2) was calculated using the standard ratio estimate according to Buckland et al. (2001).

$$\widehat{D} = \sum_{i=l}^{k} n_i \,/\, \omega \sum_{i=l}^{k} l_i$$

In this equation k is the number of transects flown, n_i is the number of ringed seal observations for the ith transect, ω is the strip width, and l_i is the length of the ith transect. The length of the transects were calculated using the GPS locations attached to images collected to ensure density was calculated based off the realized flown survey effort. The variance, coefficient of variation (CV), and 95% confidence intervals of the density were also calculated according to Young et al. (2019) adapted from methods developed for observer-based aerial surveys (Kingsley and Smith 1981; Buckland et al. 2001; Chambellant et al. 2012). Past results from observer-based aerial surveys in our low-Arctic region (2007-2010, 2013) were also compared to our findings (Lunn et al. 1997, Chambellant et al. 2012b, Young et al. 2015b) to provide context to our limited digital survey estimates.

Sea-ice concentration

We accessed the Canadian Ice Service weekly regional ice data product (https://iceweb1.cis.ec.gc.ca) that corresponded with each aerial survey. Using the geotagged survey coverage and the known strip width captured by the survey cameras, we extracted the sea-ice concentration and type along each transect line using R version 3.4.2 and QGIS version 3.12.2 (R Core Team 2020). We then calculated concentration (%) of total sea ice, first-year ice, and multiyear ice for each survey.

Statistical analysis

We used a generalized linear model (GLM) with a Gamma distribution and an inverse link function for zero-truncated continuous data to investigate spatial differences in ringed seal density. Density was compared among regions using Tukey post-hoc analysis. To explore the role that our limited sample size ($n = 5$ surveys) may have had in a lack of significance in the GLM performed, we conducted post-hoc power analyses for our desired α and a suggested power ($1-\beta$) of 0.8 (Cohen 1988). To investigate the relationship between the variation in seal density and sea-ice, we used three separate simple linear regressions for total, first year, and multiyear ice concentration calculated for each survey. P-values were determined with the F-statistic.

Results for all tests were considered significant at $\alpha = 0.05$. Models were validated and model assumptions were tested by examining the residuals against the fitted values for covariates of interest to ensure valid model specification (e.g. location, survey date, proportional effort) (Zuur & Ieno 2016, Hartig 2020). All statistical analyses were performed using R version 3.4.2, except for the power analysis, which was performed using GPower 3.1 (Faul et al. 2007, Erdfelder et al. 2009, R Core Team 2020).

Results

During the low-Arctic survey in 2017, 191 ringed seals were counted from 150 observations (Fig. 2.3; Table 2.1). In the 2016 intermediate Arctic survey, there were a total of 320 seals (June 17: 97, June 19/22: 223) from 288 observations (June 17: 89, June 19/22: 199) during the two completions of the transect lines (Fig. 2.3; Table 2.1). We counted 109 ringed seals in 95 observations during the 2017 survey in the intermediate Arctic (Fig. 2.3; Table 2.1). In the high Arctic surveys, we counted 49 ringed seals from 44 observations in 2018 and 116 ringed seals from 100 observations during in 2019 (Fig. 2.3; Table 2.1).

Densities in the high Arctic (2018: 0.05 ± 0.01 seals/km^2, 2019: 0.09 ± 0.01 seals/km^2) were approximately an order of magnitude lower than in the intermediate (2016: 0.70 ± 0.14 seals/km^2, 2017: 0.45 ± 0.07 seals/km^2) and low (2017: 0.46 ± 0.11 seals/km^2) Arctic (Fig. 2.4; Table 2.1). Although location was not a statistically significant predictor of density as determined by GLM ($F_{2,4} = 13.7$, $p = 0.068$), a post-hoc power analysis revealed that with the effect size from our study, only two more samples ($n = 7$) would have been needed to achieve significance. Moreover, a Tukey post-hoc test indicated that ringed seal densities in the high Arctic were in fact lower than the intermediate ($z = 3.262$, $p < 0.005$) and low ($z = 3.091$, $p <$

0.005) Arctic, whereas densities in the low and intermediate Arctic were not different from each other ($z = -0.498$, $p = 0.861$). There was also high interannual variation within locations, with the intermediate-Arctic density estimate in 2016 approximately 1.5x higher than 2017, and the high Arctic having almost twice the estimated density in 2019 than in 2018. Ringed seal density significantly increased with first-year ice concentration ($R^2 = 0.91$, $F_{1,3} = 31.37$, $p = 0.011$) and significantly decreased with multiyear ice concentration ($R^2 = 0.88$, $F_{1,3} = 21.2$, $p = 0.019$), while total sea-ice concentration ($R^2 = 0.012$, $F_{1,3} = 0.036$, $p = 0.862$) was not a significant predictor of ringed seal density (Fig. 2.5).

Discussion

This study is the first to investigate variation in ringed seal density over their large latitudinal range (approximately 61° N to 83° N across our study sites) and in relation to varying sea-ice characteristics using consistent aerial survey methods. Ringed seal densities were similar at our low and intermediate-latitude regions but were significantly lower at the high-latitude region. Interestingly, there was no discernable relationship between ringed seal density and total ice concentration, but relationships were observed when split into ice type (first year versus multiyear). This result supports our hypothesis that the different icescapes between low, intermediate, and high-latitude regions in the Arctic influence the densities of ringed seals at a large spatial scale. Specifically, a decrease in ringed seal density in our high-latitude region parallels limited preferred first-year ice and dominance of multiyear ice in the region.

The high-Arctic environment is dominated by multiyear ice and a longer ice-covered period. Ringed seal densities in the high Arctic are limited by a lack of suitable first-year ice or thinner ice habitat necessary to construct subnivean lairs and breathing holes, and for the formation of small holes and cracks taken advantage of by ringed seals (Fig. 2.6) (Mclaren 1958, Harwood et al. 2012). Furthermore, changes in ice coverage and length of open water season can impact the base of Arctic food webs especially during a burst of productivity with increased sunlight in spring. Changes to spring productivity are of particular interest since ringed seals rely on the seasonal resource pulse to rebuild energy stores after the energetically expensive moult (Young & Ferguson 2013b, Thometz et al. 2020). Likely a combination of these factors explains the density decrease in the high Arctic where overall heavier ice conditions are a part of a less suitable environment that supports lower densities of ringed seals.

Comparing our results with past observer surveys from the low Arctic region (Lunn et al., 1997; Young et al, 2015) supports our conclusion that ringed seal densities are higher in our low Arctic region than our high-Arctic region, coincident with increasing first-year sea-ice availability and a lack of multiyear sea-ice availability (Table 2.1). This conclusion is strengthened by considering that the observer surveys likely underestimate densities compared to our digital surveys (Young et al. 2019a). We also note that a potential decline in ringed seal densities in the low-Arctic proposed by Young et al. (2015) may be continuing. Considering that our digital-based estimate in 2017 (0.46 seals/km^2) was likely biased to be higher than the observer estimates, and Young et al. (2019) estimated the traditional observer-based density more consistent with the past surveys at 0.2 seals/km^2 for the 2017 low Arctic survey. This lends more support for the potential decreasing trend. Every single survey from prior to 2007 was estimated to be 0.6 seals/km^2 or higher, while in five subsequent surveys between 2008 and 2017, only one (0.73 seals/km^2 in 2010) was over 0.5 seals/km^2. A decline in low Arctic ringed seal densities would parallel recent observed demographic and diet shifts in ringed seals in the region and may reflect the impact of an extended open-water season as suggested in our alternative hypothesis (Ferguson et al. 2017a).

The use of digital survey methods is a significant improvement on detection of ringed seals that are hauled out compared to observer methods (Young et al. 2019a), but it does not eliminate variation in proportion of time ringed seals spend hauled out and available for detection. Although best efforts are made to target the peak moulting season of ringed seals, many factors could affect the timing of peak haul out and the proportion of seals hauled out in the region during our surveys. All surveys were flown at similar times of day and in similar weather conditions, which controls for some potential influences of haul-out probability, but other factors such as survey timing (e.g. month), location, ice conditions, sex, and age class could introduce bias to the estimates (Smith & Hammill 1981, Bengtson et al. 2005, Carlens et al. 2006, Kelly et al. 2010). Some studies have attempted to quantify haul-out rates of seals to correct survey estimates for proportion of ringed seals not available to be counted (Bengtson et al. 2005). However, since haul-out proportion varies spatially and temporally, information that matches better with our survey locations and timing is required to apply reliable corrections to our data. For this reason, our estimates are relative indices and not absolute densities. Still, these standardized surveys are useful to understand ringed seal densities and distributions during the spring ice-covered season and early breakup and can be replicated over time to document the response of ringed seals to continued environmental and ecological change.

Spatial variation in ringed seal haul-out proportion and timing of peak haul out during moulting suggests the target peak haul-out period for our aerial surveys likely varies by region (Fig. 2.7). Although the moult usually occurs from mid-May to mid-July, the peak likely occurs earlier at lower latitudes and later at high latitudes to correspond with the timing of sea-ice breakup (Mclaren 1958, Smith & Hammill 1981, Kelly et al. 2010). Peak haul out generally occurs in late May or early June for seals in our low-Arctic region according to local knowledge and surveys flown in mid-June in western Hudson Bay found it was too late to observe seals on the sea ice (Lunn et al. 1997). For seals in our intermediate-Arctic region, peak haul out likely occurs closer to mid or late June, and potentially later in June or early July for seals in our high-Arctic region. Due to logistics, 2018 (2-5 June) and 2019 (8-12 June) surveys in the high Arctic may have been too early to capture the peak haul-out period and could be underestimates. However, a several-fold increase in ringed seal density, even for the higher density 2019 survey, would be needed to be statistically similar to the intermediate and low Arctic.

The considerable interannual variation in ringed seal densities we observed within our sites may also be explained by sea-ice conditions. The interannual variation in the intermediate Arctic surveys in 2016 and 2017 fit with our predictions of increasing densities with increasing first-year ice and decreasing multiyear ice. However, the high and low Arctic surveys did not fit the large-scale trend we observed. In 2019, ringed seals in the high Arctic had higher densities than 2018 despite slightly less first-year ice, and the low Arctic surveys in 2013 (0.20 seals/km^2) indicated much lower ringed seal densities than 2007 (0.92 seals/km^2) despite similar first year ice concentrations (89.8% in 2017 vs. 90.2% in 2007). Small-scale variation and dynamic sea-ice conditions (Moore et al. 2019) did not impact the large-scale pattern we observed between our locations but may introduce interannual variation in ringed seal densities within our locations (Fig. 2.6).

In the low Arctic, even though 2013 had a first-year ice concentration comparable to 2007, this measurement did not capture that this first-year ice was an above average proportion of unstable loose pack and below average proportion of dense pack preferred for nursing and moulting which could have driven the low ringed seal density measurement in 2013 (Young & Ferguson 2015). In the high Arctic, congestion of sea ice creates reliable annual formation of a southern blockage in Smith Sound and/or a northern blockage in the Lincoln Sea known as ice arches. The interannual variation in phenology of these ice arches have implications for sea-ice export, especially thicker and older ice, out of our study site, and therefore the sea-ice conditions in the region. In 2019 the southern ice arch did not form, and although the more northern ice arch formed, it broke apart on March 20, 2019, after only 32 days (1979-2019 average: 161 ± 77 days) of formation and a total of 100 days earlier than the 1979-2019 average ice arch breakdown (June 28 ± 39 days) (Vincent 2019). In 2018, southern arch formed for more typical 118 days and broke down two days later than average on June 30. Indeed, in 2018 sea-ice concentrations of 80-100% with sparse leads were observed throughout the survey, while in 2019 only the western most transects had sea-ice concentrations of 80-100%. In 2019, the more central transects ranged from 40-100% sea-ice concentration with even small amounts of open water (0-10%). The easternmost transects overlapping and adjacent to the Nares Strait had a mix of areas with 70-100% ice concentration and areas of open-water or drift ice from 0-60% ice concentration in 2019. The difference in sea ice conditions between the two years may have played a role in the differences in ringed seal densities we observed between 2018 and 2019. Relating interannual variation in ringed seal density to ice conditions is important to better understand the relationships that influence ringed seals in these vastly different icescapes. Future research quantifying the distribution of ringed seals in relation to sea-ice variables (concentration, ice type, floe velocity) at finer spatial and temporal resolution than this study to is needed to understand variation in ringed seal density in these dynamic sea-ice environments.

Our density estimates could also be influenced by interannual variation in ringed seal distribution and movement into and out of our study areas (Finley 1979, Carlens et al. 2006). However, this effect is likely minimal as ringed seals display restricted home ranges and movement during the ice-covered season (Born et al. 2004, Kelly et al. 2010, Luque et al. 2014). The increase in ringed seal density in the high Arctic in 2019 could be partially attributed to an increase of seals coming from outside of the study area due to the unusually early breakdown of the northern ice arch increasing ice export and access to the region for seals retreating from unusually unstable ice areas (Carlyle et al. 2021; Higdon and Ferguson, 2009). A distribution shift into the study area would suggest that certain areas of increased stable or landfast ice in our high-Arctic region may become important in increasingly frequent years where a southern and/or northern ice arch does not form or breaks down early and as sea-ice loss impacts even the high Arctic "Last Ice Area" (Vincent 2019, Schweiger et al. 2020). More information on the movements and haul-out behavior of ringed seals within and between each study region is required to better interpret inter-annual variation in density estimates and provide insights into potential distribution shifts in the face of continued sea-ice recession.

As a species dependent on sea-ice habitat for mating, pupping, nursing, moulting, and for feeding on ice-associated prey, it is important to understand ringed seal responses to the highly variable icescapes they inhabit for insights into their response to continued environmental change. Our data demonstrates the plasticity of ringed seals to respond to spatiotemporal variation in their environment, although there is likely a limit to their plasticity. We highlight that changes in ringed seal density may not be uniform as ringed seals in the high Arctic may increase in density over time with a presumed increase in availability of first year sea ice and productivity in this region compared to the current limitation of inhabiting an area with heavy year-round multi-year sea conditions (Laidre et al. 2020). On the other hand, in the low Arctic continued sea-ice loss will lead to less preferred first-year ice and earlier break up during the spring, which could reduce ringed seal densities of which we may already be seeing the initial impacts (Young et al. 2015b, this study). It is important to note that any early benefits of multiyear sea-ice loss to ringed seals in the high Arctic may not continue after the complete replacement of multiyear ice by first-year ice projected to happen by the middle of the century (Laidre et al. 2020). Changing environmental conditions can have immediate beneficial or deleterious impacts on species distributions but responses are not necessarily linear or uniform in space and time. Our results highlight the importance of understanding critical factors influencing species distributions.

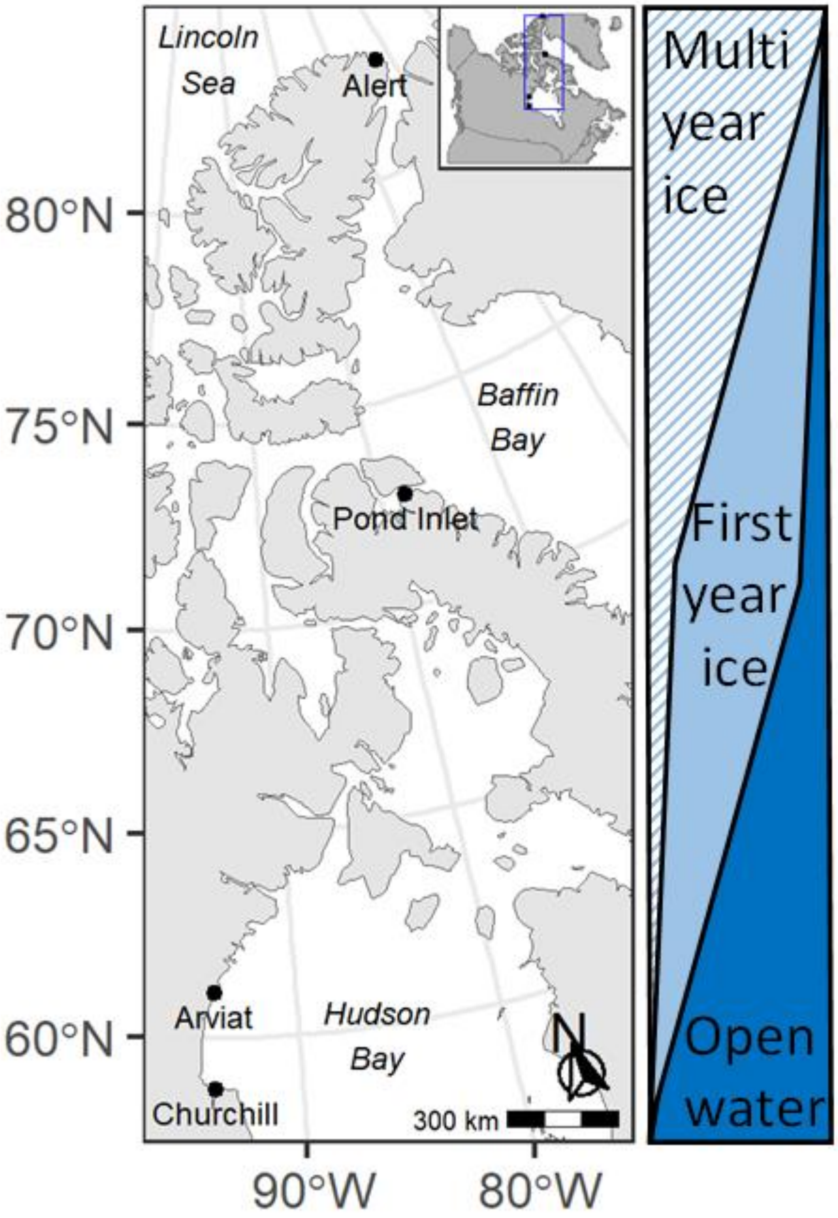

Figure 2.1. A latitudinal gradient of sea-ice conditions in the Canadian Arctic. Arviat, Nunavut (61.1°N) in western Hudson Bay represents the low Arctic, Pond Inlet, Nunavut (72.7°N) in Eclipse Sound/Lancaster Sound represents the intermediate Arctic, and Alert, Nunavut (82.5°N) in the Lincoln Sea/Nares Strait represents the high Arctic. Right: Conceptual representation of the increase in sea-ice conditions from low to high Arctic that forms the basis for our selection of a latitudinal gradient for this study.

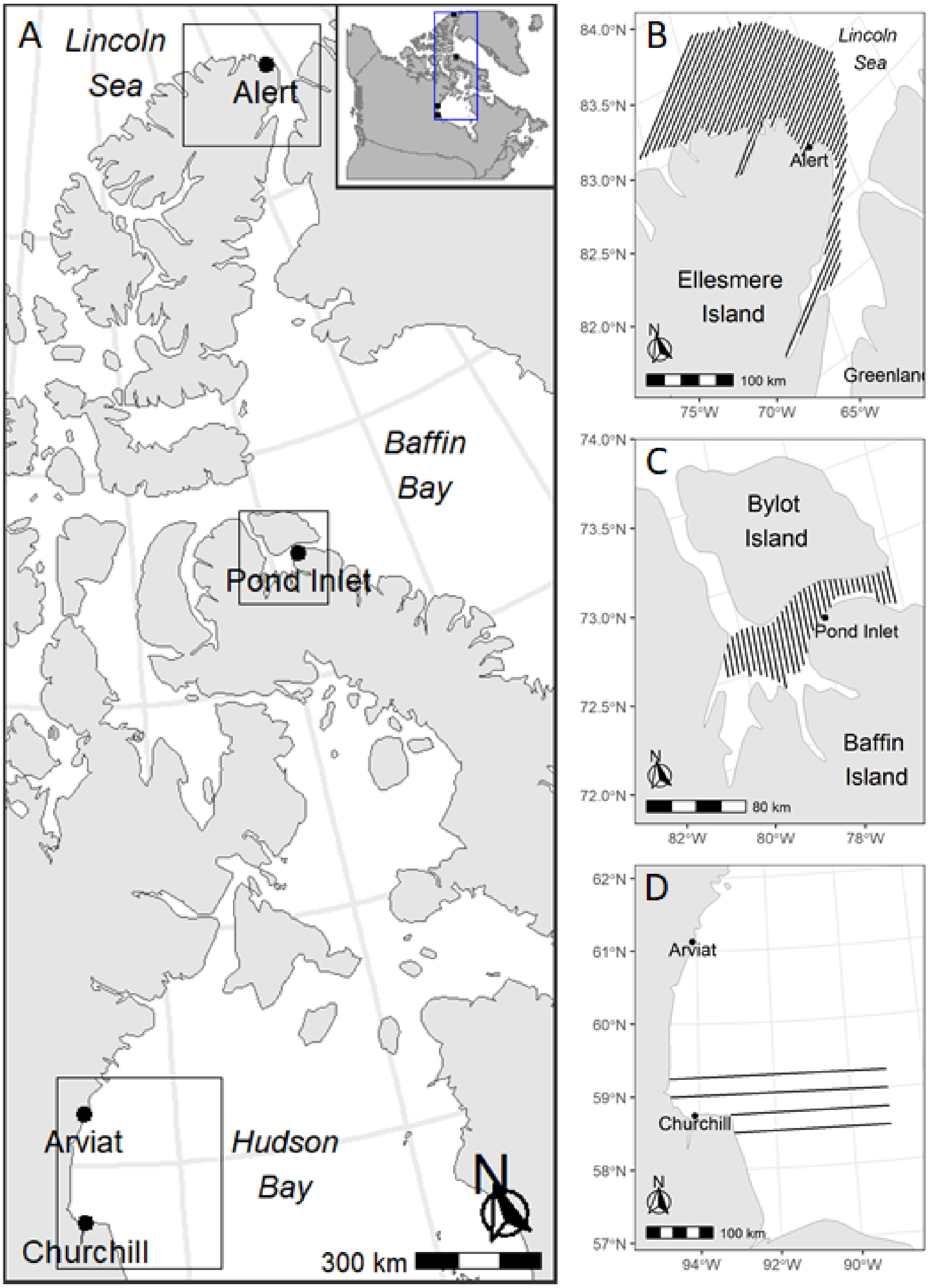

Figure 2.2. Aerial surveys of ringed seals hauled out on sea ice conducted in the low (D: 2017), intermediate (C: 2016, 2017), and high (B: 2018, 2019) Arctic used to calculate relative density across a latitudinal gradient in the Canadian Arctic (A). Solid lines represent transects that were successfully flown.

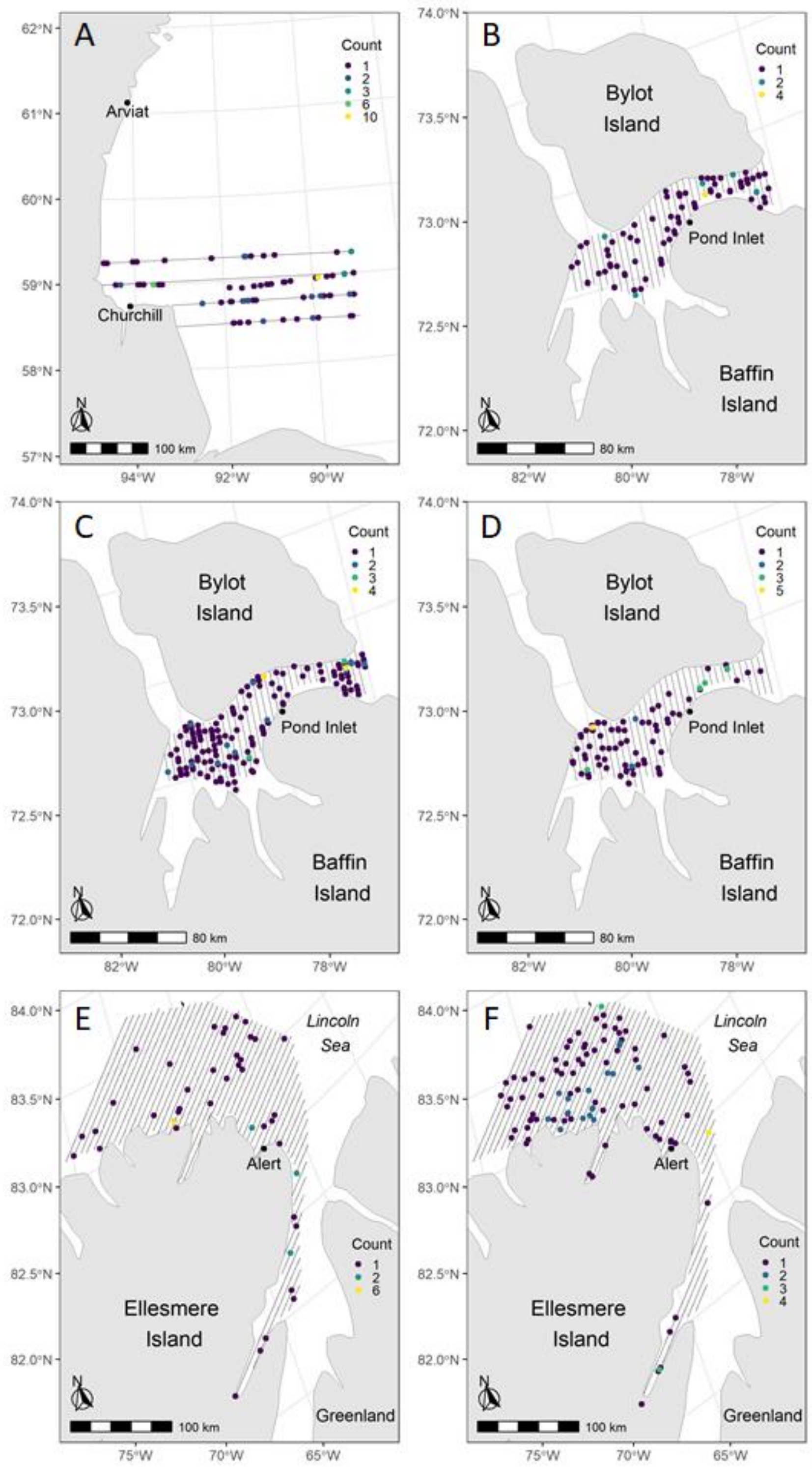

Figure 2.3. Ringed seal observations recorded by infrared and visual photography from digital based aerial surveys in low (2017: A), intermediate (2016: B, C 2017: D) and high (2018: E 2019: F) Arctic regions.

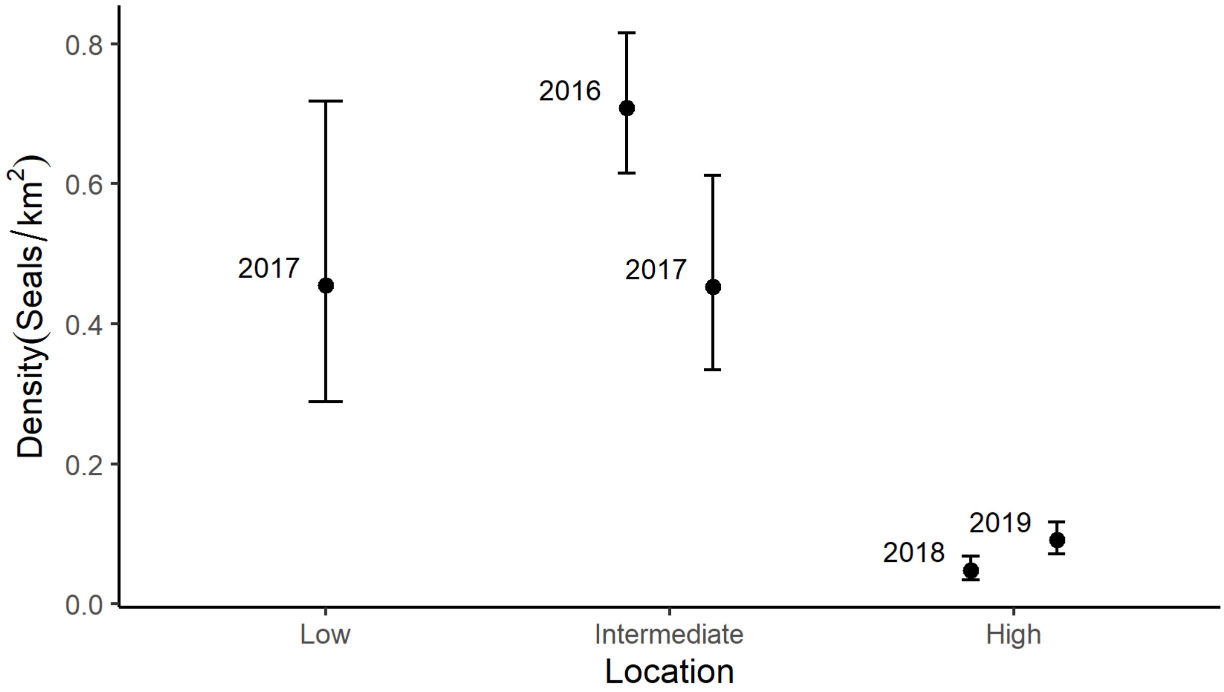

Figure 2.4. Ringed seal density estimates (means and 95% confidence intervals) calculated by strip transect analysis from digital-based aerial surveys in low (2017), intermediate (2016-2017), and high (2018-2019) Arctic regions.

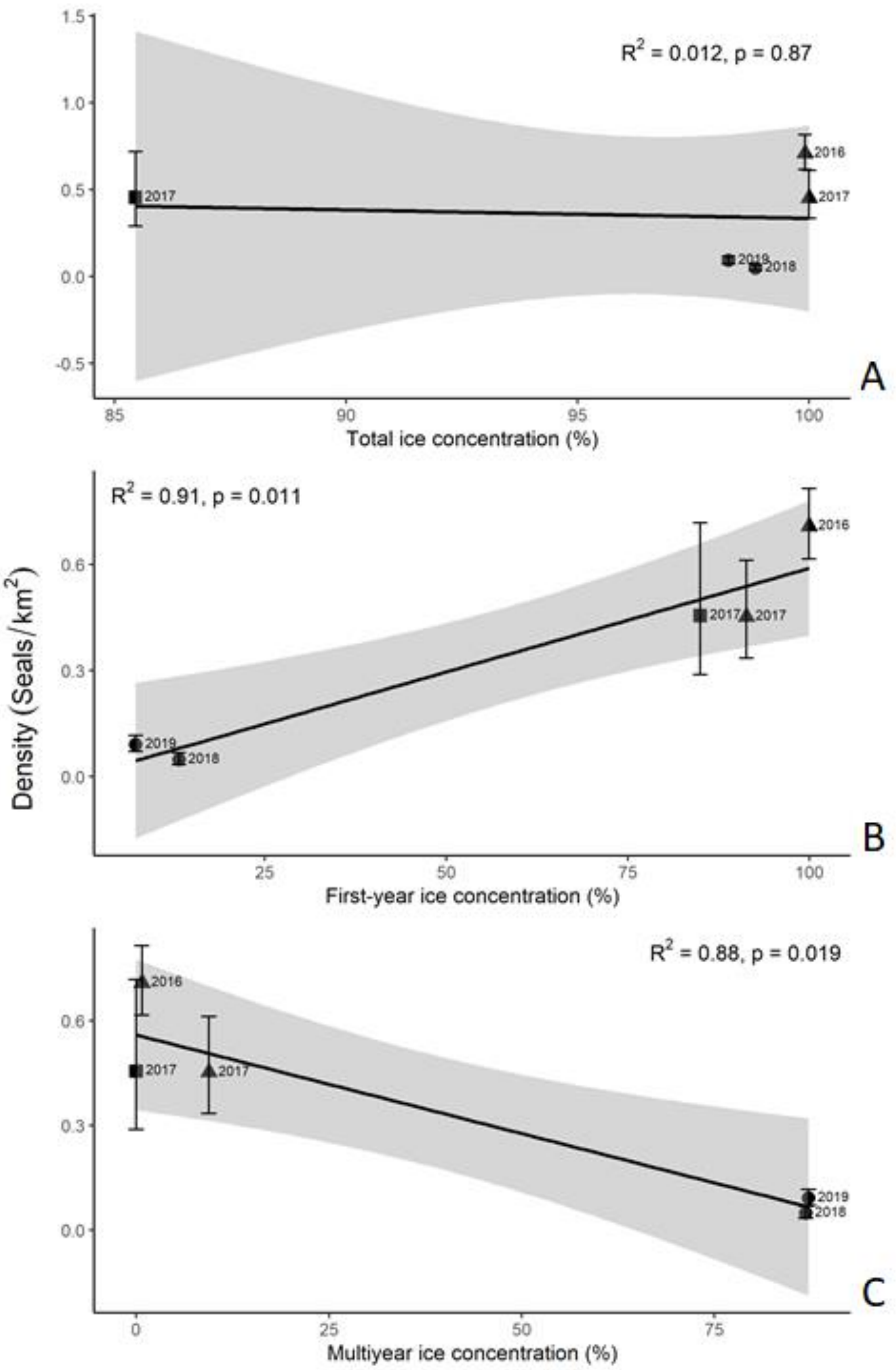

Figure 2.5. Ringed seal density estimates (means and 95% confidence intervals) related to A) total sea-ice concentration (β = -0.0048), B) first-year ice concentration (β = 0.0059), and C) multiyear ice concentration (β = -0.0057). Digital based aerial surveys were conducted in low (squares), intermediate (triangles), and high Arctic (circles) regions.

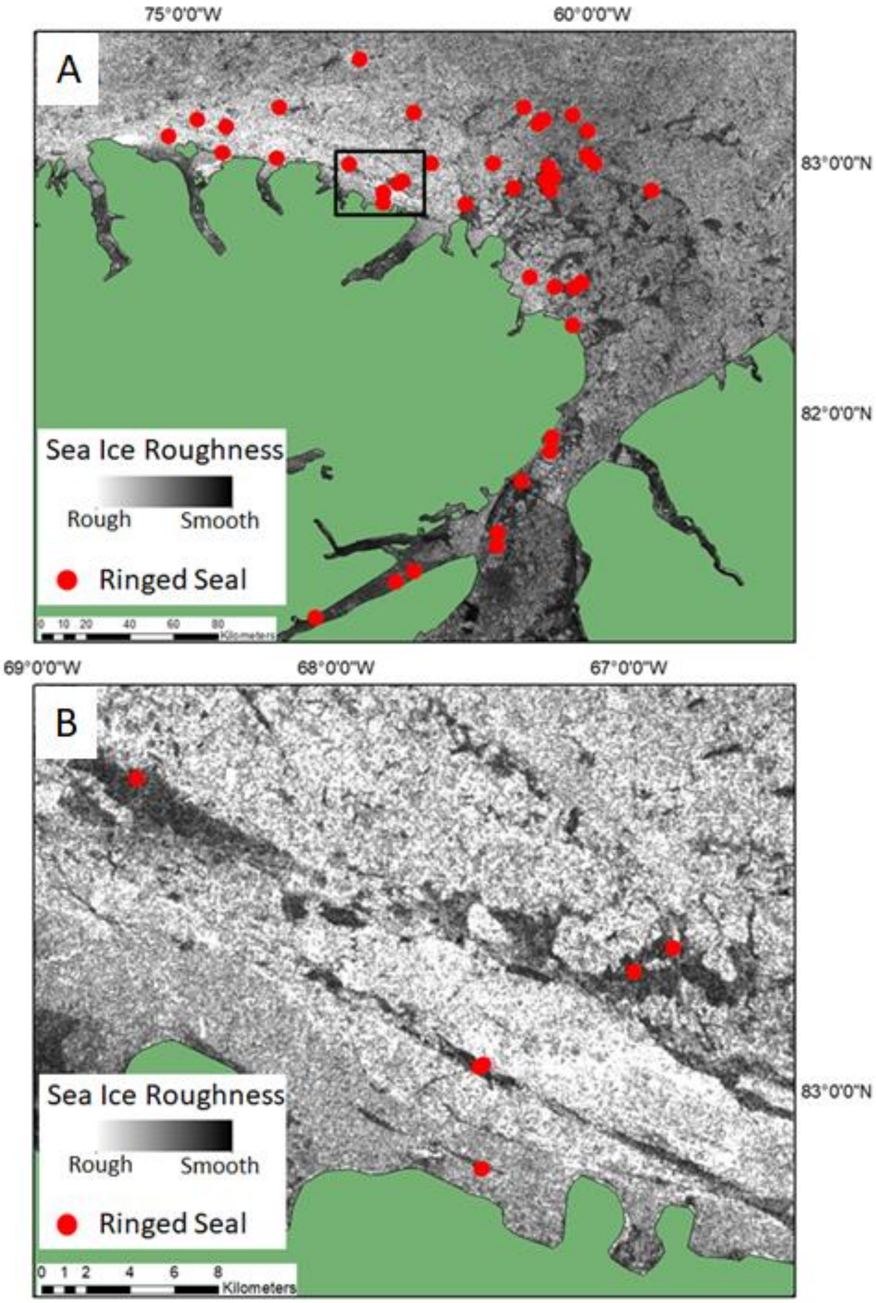

Figure 2.6. (A) Ringed seal observations (red points) from the high Arctic aerial survey carried out from 2-5 June, 2018 and (B) a close up of five ringed seal observations on 5 June, 2018 overlaid with Radarsat-2 imagery. These observations demonstrate ringed seal occurrence at limited areas likely consisting of first-year ice or cracks (dark/smooth) in an environment dominated by multiyear ice (light/rough).

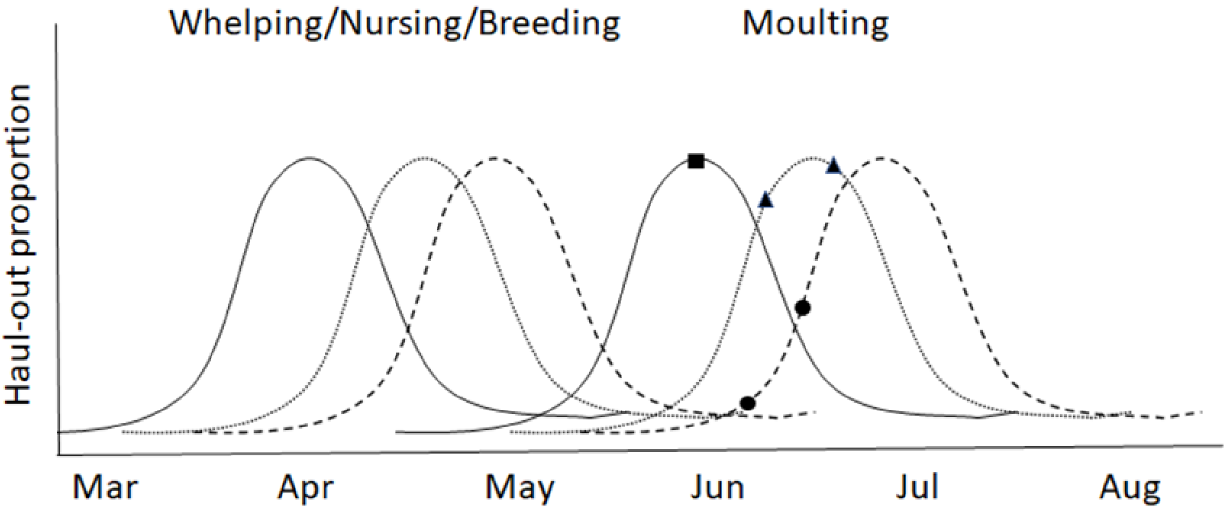

Figure 2.7. Conceptual diagram of the approximate proportion of time spent hauled out by ringed seals during the ice-covered season for the low (solid lines; square), intermediate (dotted lines; triangles), and high Arctic (dashed lines; circles) regions. This diagram demonstrates the latitudinal variation in peak haul-out timing compared to our survey dates and how both surveys in the high Arctic may have been early for peak haul out.

Table 2.1. Summary of digital-based aerial surveys from our low, intermediate and high-Arctic locations (2016-2019) (Young et al. 2019b, Yurkowski et al. 2019b) and past observer based aerial surveys for additional context (2007-2010, 2013) (Young et al. 2015b).

Latitude	Year	Date	Method (km)	Effort	Proportion Completed	Observations	# of Seals	Density (SE)	CV*	95% CI	Sea-ice Conc.	First-year ice Conc.	Old-ice Conc.
High	2019	June 8-12	Digital	4073.8	1.0	100	116	0.09 (0.01)	12.6	0.07-0.12	98.3	7.2	87.2
High	2018	June 2-5	Digital	4067	1.0	44	49	0.05 (0.01)	17.6	0.03-0.07	98.8	13.2	86.8
Intermediate	2017	June 6-8	Digital	857.7	1.0	95	109	0.45 (0.07)	15.5	0.33-0.61	100	91.3	9.43
Intermediate	2016	June 17-22	Digital	1665.7	1.0	288 (June 17: 89, June 19/22: 199)	320 (June 17: 97, June 19/22: 223)	0.71 (0.05)	7.18	0.62-0.82	99.9	99.9	0.73
Low	2017	May 26-June 1	Digital	1133.5	0.37	150	191	0.46 (0.11)	23.6	0.29-0.72	85.5	85.0	0

Low	2013	May 28-June 5	Observer	3074.3	1.0	N/A	N/A	0.20	5.8	0.18-0.22	90.9	89.8	0
Low	2010	June 5-9	Observer	3074.3	1.0	N/A	N/A	0.73	10.5	0.59-0.89	64.6	64.4	0
Low	2009	June 2-8	Observer	546.4	0.18	N/A	N/A	0.28	34.2	0.14-0.53	63.7	63.7	0
Low	2008	May 28-31	Observer	2764.8	0.90	N/A	N/A	0.44	10.6	0.36-0.54	72.9	72.3	0
Low	2007	May 26-29	Observer	2869.5	0.93	N/A	N/A	0.92	8.0	0.78-1.07	90.3	90.2	0

* The coefficient of variation (CV) was calculated according to Young et al. (2019) adapted from methods developed for observer-based aerial surveys (Kingsley and Smith 1981; Buckland et al. 2001; Chambellant et al. 2012)

References

Buckland, ST, Anderson DR, Burnham KP, Laake JL, Borchers DL, Thomas L (2001) Introduction to distance sampling: estimating abundance of wildlife populations. Oxford University Press, New York, New York, USA.

Bengtson JL, Hiruki-Raring LM, Simpkins MA, Boveng PL (2005) Ringed and bearded seal densities in the eastern Chukchi Sea, 1999–2000. Polar Biol 28:833–845.

Born EW, Teilmann J, Acquarone M, Riget FF (2004) Habitat use of ringed seals (*Phoca hispida*) in the North Water area (North Baffin Bay). Arctic 57:129–142.

Cameron M, Sigler M, Moreland E, Towler R (2015) Advances in Methods for Marine Mammal and Fish Stock Assessments: Thermal Imagery and CamTrawl. Mar Tech Soc J 49:99-106.

Carlens H, Lydersen C, Krafft BA, Kovacs KM (2006) Spring Haul-Out Behaviour Of Ringed Seals (*Pusa Hispida*) In Kongsfjorden, Svalbard. Mar Mammal Sci 22:379–393.

Carlyle CG, Florko KRN, Young BG, Yurkowski DJ, Michel C, Ferguson SH (2021) Marine mammal biodiversity and rare narwhal (*Monodon monoceros*) observations near northern Ellesmere Island, Canada. Ecosphere 12: e03534.

Chambellant M, Lunn NJ, Ferguson SH (2012) Temporal variation in distribution and density of ice-obligated seals in western Hudson Bay, Canada. Polar Biol 35:1105–1117.

Conn PB, Ver Hoef JM, Mcclintock BT, Moreland EE, London JM, Cameron MF, Dahle SP, Boveng PL (2014) Estimating multispecies abundance using automated detection systems: Ice-associated seals in the Bering Sea. Methods Ecol Evol 5:1280–1293.

Erdfelder E, FAul F, Buchner A, Lang AG (2009) Statistical power analyses using G*Power 3.1: Tests for correlation and regression analyses. Behav Res Methods 41:1149–1160.

Faul F, Erdfelder E, Lang AG, Buchner A (2007) G*Power 3: A flexible statistical power analysis program for the social, behavioral, and biomedical sciences. Behav Res Methods 39:175–191.

Ferguson SH, Stirling I, McLoughlin P (2005) Climate change and ringed seal (*Phoca hispida*) recruitment in western Hudson Bay. Mar Mammal Sci 21:121–135.

Ferguson SH, Young BG, Yurkowski DJ, Anderson R, Willing C, Nielsen O (2017) Demographic, ecological, and physiological responses of ringed seals to an abrupt decline in sea ice availability. PeerJ 5:e2957.

Finley KJ (1979) Haul-out behaviour and densities of ringed seals (*Phoca hispida*) in the Barrow Strait area, N.W.T. Can J Zool 57:1985–1997.

Fossheim M, Primicerio R, Johannesen E, Ingvaldsen RB, Aschan MM, Dolgov A V. (2015) Recent warming leads to a rapid borealization of fish communities in the Arctic. Nat Clim Chang 5:673–677.

Frainer A, Primicerio R, Kortsch S, Aune M, Dolgov A V., Fossheim M, Aschan MM (2017) Climate-driven changes in functional biogeography of Arctic marine fish communities. Proc Natl Acad Sci 114:12202–12207.

Galley RJ, Else BGT, Howell SEL, Jennifer V, Galley RJ, Else BGT, Howell SEL, Lukovich J V, Barber DG (2012) Landfast Sea Ice Conditions in the Canadian Arctic: 1983-2009. Arctic 65:133–144.

Harwood LA, Smith TG, Melling H, Alikamik J, Kingsley MCS (2012) Ringed Seals and Sea Ice in Canada’s Western Arctic : Harvest-Based Monitoring 1992 – 2011. Arctic 65:377–390.

Iacozza J, Ferguson SH (2014) Spatio-temporal variability of snow over sea ice in western Hudson Bay, with reference to ringed seal pup survival. Polar Biol 37:817–832.

Kelly BP, Badajos OH, Kunnasranta M, Moran JR, Martinez-Bakker M, Wartzok D, Boveng P (2010) Seasonal home ranges and fidelity to breeding sites among ringed seals. Polar Biol 33:1095–1109.

Kingsley MCS (1987) The numbers of ringed seals (*Phoca hispida*) in Baffin Bay and associated waters. NAAMCO Scientific Publications I:181–196.

Kovacs KM, Lydersen C, Overland JE, Moore SE (2011) Impacts of changing sea-ice conditions on Arctic marine mammals. Mar Biodiv 41:181–194.

Laidre KL, Atkinson SN, Regehr E V, Stern HL, Born EW, Wiig Ø, Lunn NJ, Dyck M, Heagerty P, Cohen BR (2020) Transient benefits of climate change for a high-Arctic polar bear (*Ursus maritimus*) subpopulation. Glob Chang Biol 1–15.

Laidre KL, Stirling I, Lowry LF, Wiig Ø, Heide-Jørgensen MP, Ferguson SH (2008) Quantifying the sensitivity of Arctic marine mammals to climate-induced habitat change. Ecol Appl 18:97–125.

Lenth RV (2021) emmeans: Estimated Marginal Means, aka Least-Squares Means. R package version 1.5.4. https://CRAN.R-project.org/package=emmeans.

Lunn NJ, Stirling I, Nowicki SN (1997) Distribution and abundance of ringed (*Phoca hispida*) and bearded seals (*Erignathus barbatus*) in western Hudson Bay. Can. J. Fish. Aquat. Sci. 54:914–921.

Luque SP, Ferguson SH, Breed GA (2014) Spatial behaviour of a keystone Arctic marine predator and implications of climate warming in Hudson Bay. J Exp Mar Bio Ecol 461:504–515.

MacArthur RH (1965) Patterns of Species Diversity. Biol Rev 40:510–533.

Mallory ML, Gilchrist HG, Janssen M, Major HL, Merkel F, Provencher JF, Strøm H (2018)

Financial costs of conducting science in the Arctic: examples from seabird research. Arct Sci 4:624–633.

Mclaren IA (1958) The Biology of the Ringed Seal (*Phoca hispida Schreber*) in the Eastern Canadian Arctic. Ottawa, Fisheries Research Board of Canada. 97 pp.

Moore GWK, Schweiger A, Zhang J, Steele M (2019) Spatiotemporal Variability of Sea Ice in the Arctic's Last Ice Area. Geophys Res Lett 46:11237–11243.

Pecl GT, Araújo MB, Bell JD, Blanchard J, Bonebrake TC, Chen IC, Clark TD, Colwell RK, Danielsen F, Evengård B, Falconi L, Ferrier S, Frusher S, Garcia RA, Griffis RB, Hobday AJ, Janion-Scheepers C, Jarzyna MA, Jennings S, Lenoir J, Linnetved HI, Martin VY, McCormack PC, McDonald J, Mitchell NJ, Mustonen T, Pandolfi JM, Pettorelli N, Popova E, Robinson SA, Scheffers BR, Shaw JD, Sorte CJB, Strugnell JM, Sunday JM, Tuanmu MN, Vergés A, Villanueva C, Wernberg T, Wapstra E, Williams SE (2017) Biodiversity redistribution under climate change: Impacts on ecosystems and human well-being. Science 355: eaai9214.

Post E, Bhatt US, Bitz CM, Brodie JF, Fulton TL, Hebblewhite M, Kerby JT, Kutz S, Stirling I, Walker DA (2013) Ecological Consequences of Sea-Ice Decline. Science 341:519–524.

Reimer JR, Caswell H, Derocher AE, Lewis MA (2019) Ringed seal demography in a changing climate. Ecol Appl 29:1–16.

R Core Team (2020) R: A language and environment for statistical computing. R Foundation for Statistical Computing, Vienna, Austria. URL https://www.R-project.org/.

Schweiger AJ, Steele M, Zhang J, Moore GWK, Laidre KL (2020) Accelerated sea ice loss in the Wandel Sea points to a change in the Arctic's Last Ice Area. Commun Earth Environ:1–11.

Smith TG, Hammill MO (1981) Ecology of the ringed seal, *Phoca hispida*, in its fast ice breeding habitat. Can J Zool 59:966-981.

Stevens GC (1989) The Latitudinal Gradient in Geographical Range : How so Many Species Coexist in the Tropics. The Univer. Am Nat 133:240–256.

Thometz NM, Hermann-Sorensen H, Russell B, Rosen DAS, Reichmuth C (2020) Molting strategies of Arctic seals drive annual patterns in metabolism. Conserv Physiol 9: coaa112; doi:10.1093/conphys/coaa112.

Vincent RF (2019) A Study of the North Water Polynya Ice Arch using Four Decades of Satellite Data. Sci Rep 9:1–12.

Voosen P (2020) New feedbacks speed up the demise of Arctic sea ice. Science 369:1043–1044.

Wang J, Mysak LA, Grant Ingram R (1994) Interannual variability of sea-ice cover in hudson bay, baffin bay and the Labrador sea. Atmos - Ocean 32:421–447.

Welch HE, Bergmann MA, Siferd TD, Martin KA, Curtis MF, Crawford RE, Conover RJ, Hop H (1992) Energy Flow through the Marine Ecosystem of the Lancaster Sound Region , Arctic Canada. Arctic 45:343–357.

Wickham H (2016) ggplot2: Elegant Graphics for Data Analysis. Springer-Verlag New York.

Young BG, Ferguson SH (2013) Seasons of the ringed seal : pelagic open-water hyperphagy , benthic feeding over winter and spring fasting during molt. Wild Res 40:52–60.

Young BG, Ferguson SH, Lunn NJ (2015) Variation in ringed seal density and abundance in western Hudson Bay estimated from aerial surveys, 1995 to 2013. Arctic 68:301–309.

Young BG, Yurkowski DJ, Dunn JB, Ferguson SH (2019) Comparing infrared imagery to traditional methods for estimating ringed seal density. Wildl Soc Bull 43:121–130.

Yurkowski DJ, Carlyle CG, Amarualik U, Lange BA, Platt A, Higdon JW, Stewart DB, Ferguson A, Ferguson SH, Michel C (2019a) Novel observations of Atlantic walruses (*Odobenus rosmarus rosmarus*) in Archer Fjord , northern Ellesmere Island , Nunavut , Canada. Polar Biol. 42:1193–1198.

Yurkowski DJ, Semeniuk CAD, Harwood LA, Rosing-Asvid A, Dietz R, Brown TM, Clackett S, Grgicak-Mannion A, Fisk AT, Ferguson SH (2016) Influence of sea ice phenology on the movement ecology of ringed seals across their latitudinal range. Mar Ecol Prog Ser 562:237–250.

Yurkowski DJ, Young BG, Dunn JB, Ferguson SH (2019b) Spring distribution of ringed seals (*Pusa hispida*) in eclipse sound and Milne Inlet, Nunavut: Implications for potential ice-breaking activities. Arct Sci 5:54–61.

Zuur AF, Ieno EN (2016) A protocol for conducting and presenting results of regression-type analyses. Methods Ecol Evol 7:636–645.

Chapter 3: Ringed seal diet biomarkers identify spatial variation in carbon source and trophic dynamics across a latitudinal gradient of sea ice

Abstract

Anthropogenic climate change is causing changes to abiotic factors such as temperature and sea-ice dynamics. These environmental changes influence the latitudinal organization of primary production, species interactions, and ecosystem function with major implications for Arctic food webs. Ringed seals are a mobile, generalist predator species with many links in the Arctic marine food web. These characteristics allow ringed seals to function as an indicator of changes in food web structure across the spatial-environmental gradient that coincides with their broad latitudinal range in the Arctic. We conducted diet biomarker analysis using ringed seal muscle and liver tissue from the low, intermediate, and high Arctic to investigate changes in ringed seal diet that could be linked to variation in sea-ice dynamics across a latitudinal gradient. Highly branched isoprenoids showed an increase in sympagic carbon in ringed seal diets from low (22.0 ± 2.73%) to high (89.9 ± 2.08%) Arctic, while stable carbon isotope analysis similarly indicated a decrease in pelagic carbon with increasing latitude (Low Arctic: 1.05 ± 0.003; High Arctic: 0.88 ± 0.009). These patterns are likely linked to the vastly different icescapes in these environments. Relative trophic position also increased from low (3.78 ± 0.02) to high (4.76 ± 0.03) Arctic, suggesting increased fish consumption or changing trophic dynamics paralleling the latitudinal change in carbon source. Ringed seals demonstrate considerable dietary flexibility, with a clear shift from low to high Arctic in the relative contribution of sympagic versus primary production. Our results establish the potential of ringed seal diets to indicate changes to Arctic ecosystem structure and function with continued sea-ice decline.

Introduction

Globally, species are undergoing poleward shifts to their distributions in response to anthropogenic climate warming (IPCC 2014, Pecl et al. 2017). Idiosyncratic responses of these species distribution shifts due to biogeography, species phenology, dispersal ability, and adaptive capacity has led to changes in species interactions as primary producers, prey, and predators shift their distributions at varying spatial and temporal scales (Wisz et al. 2013, Dey et al. 2017). Changes to species interactions are likely to have profound impacts to the structure and function of ecosystems (Frainer et al. 2017). In the Arctic, climate warming is also causing a rapid poleward retreat of biologically important sea-ice characteristics including extent, thickness, and length of ice-covered season (Overland & Wang 2013, IPCC 2014). Sea-ice loss further threatens Arctic species and their interactions through direct habitat loss, changes to food-wed dynamics, and invasion from more temperate species, with consequences on ecosystem structure and function (Post et al. 2013, Fossheim et al. 2015, Frainier eat al. 2017).

Latitudinal differences in sea-ice dynamics and phenology drive spatiotemporal variation in Arctic primary production and food web composition. In the high Arctic, sea ice is often present year round, with a high proportion of multi-year sea ice mixed with thinner first-year sea ice (Born et al. 2004, Laidre et al. 2020). Phytoplankton productivity is often lower in areas with heavy sea ice and longer sea-ice coverage because of limited light availability in the water column. Therefore, biological activity in these areas is skewed towards sea-ice associated (sympagic) algae, especially when heavy snow and sea-ice conditions overlap with increased sunlight, temperature and nutrients in spring (Brown et al. 2014a, Yurkowski et al. 2020a). At lower Arctic latitudes, seasonal ice ecoregions are present with first-year sea ice and longer open-water seasons in summer and fall (Wang et al. 1994). Lighter sea-ice conditions and longer open-water seasons are associated with increases in seasonal phytoplankton blooms and a shift to more phytoplanktonic primary production (Arrigo & van Dijken 2015, Yurkowski et al. 2020a). Overall, there is a potential difference in the base of food webs between high and low Arctic regions related to large-scale patterns in sea-ice coverage and phenology.

Heavy sea-ice conditions also favour more sympagic grazers of sea-ice diatoms and sea-ice associated forage fish such as Arctic cod (*Boreogadus saida*) (Hobson et al. 2002). High export of ice-derived organic matter to the benthic environment, especially during the spring melt, also drives tight benthic-sympagic coupling, which can produce species-rich and productive benthic communities in regions with heavy sea ice (Kohlbach et al. 2019). On the other hand, lighter sea-ice conditions in the southern Arctic may favour more temperate-associated species that are expanding their range northward (Kortsch et al. 2015) and feed on pelagic phytoplankton, such as capelin (*Mallotus villosus*). Even if primary productivity increases with reduced sea ice, species reliant on sea-ice-derived carbon may be negatively affected by the changes in algal communities and timing of availability (Kohlbach et al. 2019). In fact, more southern latitudes of the Arctic have experienced a northward retraction of the range of Arctic cod and increased presence of capelin with climate warming and northward recession of sea ice (Florko et al. 2021). These changes can propagate up the entire food web and have detrimental impacts on higher trophic levels.

Ringed seals are generalist and opportunistic feeders with a taxonomically and functionally diverse diet of fish, crustaceans, and other invertebrates from benthic, sympagic, and pelagic habitats environments (Mclaren 1958, Young & Ferguson 2014). As a mobile predator with dietary flexibility over space and time, changes in their diet can be indicators of biological productivity and ecosystem change (Born et al. 2004, Young & Ferguson 2014, Yurkowski et al.

2018, de la Vega et al. 2021; Young & Ferguson 2013; Yurkowski et al. 2016). Ringed seal diets could be indicators of latitudinal shifts in food web dynamics that coincide with sea-ice conditions, such as the shift from sea-ice to phytoplankton-based food webs. At the southern periphery of the ringed seal's range in Hudson Bay, a longer ice covered season can dampen a seasonal pulse in phytoplankton derived resources and negatively impact body condition and breeding success (Laidre et al. 2008, Young & Ferguson 2013). On the other hand, an observed long-term shift in forage fish availability, from ice-associated fish such as Arctic cod to pelagic species such as capelin, has negatively impacted ringed seal demographics in Hudson Bay (Ferguson et al. 2005, Provencher 2012). A similar temporal shift in ringed seal diets to increasingly available capelin correlated with increased sea surface temperature and decreased sea-ice coverage has been observed in more northern Cumberland Sound (Yurkowski et al. 2018). In high Arctic Grise Fjord, Nunavut, Canada and Qaanaaq, Greenland where seals experience heavier ice conditions and longer ice-covered seasons, Arctic cod dominate the diet of ringed seals (Holst et al. 2001). Space-for-time studies across the ringed seals' range could yield similar patterns to the temporal shifts of the lower latitudes and identify food web shifts with latitude and sea-ice dynamics that could result with continued climate change (Hayden et al. 2019).

Our objective was to assess differences in ringed seal diet associated with latitudinal variation in sea-ice conditions by comparing $\delta^{13}C$ and $\delta^{15}N$ in ringed seal muscle and liver tissue, and HBIs in liver tissue from the low (Arviat, Nunavut, Canada: 61.1°N), intermediate (Pond Inlet, Nunavut, Canada: 72.7°N), and high (Grise Fjord, NU: 76.4°N; Qaanaaq, GL: 77.5°N) Arctic from May-February in 2016-2018 (Fig. 3.1). We used $\delta^{13}C$, $\delta^{15}N$, and HBIs to investigate source of diet and trophic dynamics in ringed seal samples from the low to high Arctic to help understand how varying sea-ice conditions and sea-ice derived production over the study locations may influence the feeding characteristics of ringed seals (Brown et al. 2014b a). We hypothesized that latitudinal variation in ringed seal diets will reflect regional sea-ice conditions, with signals indicative of sea-ice-derived production at higher latitudes. We predicted an increased proportion of sympagic carbon (IP_{25} and IIb) rather than pelagic signals (IIIa-d), increased $\delta^{13}C$, and decreasing pelagic carbon signal in a relative carbon source index with increasing latitude, indicative of increased sea-ice derived primary production in the diet as latitude increases. Our predictions would be due to increased reliance on sea-ice derived production at high latitudes and an enhanced benthic environment due to strong benthic-sympagic coupling with a shorter open water period and less pelagic primary production. We also predicted that at higher latitudes, ringed seal diets will exhibit increased $\delta^{15}N$ and a higher relative trophic position indicative of increased fish consumption and/or increased food web complexity (Yurkowski et al. 2016a, 2020a).

Methods

Sample collection and study sites

Muscle (n = 110) and liver (n = 107) tissue samples were collected from ringed seals by Inuit subsistence hunters as part of the community-based monitoring partnership coordinated by Fisheries and Oceans Canada (Winnipeg, Manitoba, Canada). Muscle tissue has a slower turnover rate (~4 months) than liver (~1-2 months) and together allowed for investigation into short and medium term diet variation (Vander Zanden et al. 2015). Samples were collected from a range of latitudes to represent low, intermediate, and high-Arctic regions: Arviat (61.1°N; 42 muscle and 40 liver), Pond Inlet (72.7°N; 34 muscle and liver), and Grise Fjord (76.4°N; 16

muscle and 15 liver) in Nunavut, Canada, plus Qaanaaq, Greenland (77.5°N; 18 muscle and liver) (Fig. 3.1; Table 3.1). Arviat in low Arctic western Hudson Bay experiences seasonal sea-ice coverage with complete ice coverage in December until ice break up begins in June followed by an open-water season from July to November that begins to freeze back up in late October and November (Wang et al. 1994, Laidre et al. 2020). Pond Inlet is more intermediate in latitude and typically experiences ice break up later in June or early July with a shorter open water period and complete ice coverage beginning in November (Welch et al. 1992, Galley et al. 2012). Grise Fjord and Qaanaaq in the high Arctic Smith Sound and Jones Sound regions do not experience ice breakup until late July, and ice cover has fully returned in early November with a shorter open water season between August and October with some ice remaining throughout the year (Vibe 1950, Born et al. 2004, Laidre et al. 2020). However, the presence of the North Water Polynya in southern Smith Sound and Northern Baffin Bay produces an area that is relatively ice free compared to the rest of the region (Holst et al. 2001, Born et al. 2004). The regions of western Hudson Bay, Eclipse Sound/Lancaster Sound, and Smith Sound/Jones Sound formed a model gradient of sea-ice conditions that fits inside the broad latitudinal range of the ringed seal (Fig. 3.1)

Samples were collected in 2018 for most locations, but we used samples from 2016-2017 for Pond Inlet as none were available for 2018 from that community. Samples were collected in the summer and fall open-water season (July-November) when seals are known to be foraging more intensively to build up fat reserves (Young & Ferguson 2013b). However, Qaanaaq seals were collected in May during ice-breakup. Further, Pond Inlet seals were collected from a larger range of months (May-November) and four seals were collected in January and February during the ice-covered season. Sex was recorded by hunters during collection, and seals from most locations were aged by Matson's Laboratory LLC (Missoula, MT, USA) by counting annual growth layer groups in cementum of the lower right canine (Stewart 1996, Young & Ferguson 2014, Yurkowski et al. 2016b). Teeth were not collected from Qaanaaq seals, and therefore we estimated age using a regression fit to growth models (Winship et al. 2001, Young & Loseto 2010, Luque et al. 2014). We used age estimates to classify seals as pup (<1 year of age), subadult (1-5 years of age), or adult (>6 years of age) (Stewart 1996, Young & Loseto 2010, Yurkowski et al. 2016b).

Stable isotope analysis

We measured stable isotope ratios of ringed seal liver and muscle samples at the Freshwater Institute, Fisheries and Oceans Canada (Winnipeg, MB, Canada). Muscle and liver tissue specimens were subsampled into pieces < 5g, freeze dried for 48 hours, homogenized using a mortar and pestle, then lipid extracted using a solution of 2:1-chloroform:methanol using a modified method from Bligh & Dyer (1959). Lipid-extracted tissue was then weighed into tin capsules at ~400µg using a microbalance, then combusted to measure $\delta^{13}C$ and $\delta^{15}N$ with a continuous flow isotope ratio mass spectrometer (Delta V Plus; Thermo Scientific) interfaced with an elemental analyzer (ECS 4010; Costech Instruments) and connected via a Conflo IV interface (Thermo Scientific).

The $\delta^{13}C$ and $\delta^{15}N$ values are expressed in per mil (‰) deviation from the standards of atmospheric nitrogen for nitrogen and Vienna Pee Dee Belemnite for carbon in delta (δ) notation with the equation: $\delta X = [(R_{sample}/R_{standard}) - 1] \times 1000$, where $X = {}^{13}C$ or ${}^{15}N$ and $R = {}^{13}C/{}^{12}C$ or ${}^{15}N/{}^{14}N$ (Bond & Hobson 2012). Precision and accuracy were validated based on certified reference materials (USGS40: $\delta^{13}C = -26.39 \pm 0.09‰$, $\delta^{15}N = -4.52 \pm 0.12‰$; USGS41a: $\delta^{13}C =$

36.55 ± 0.08‰, $\delta^{15}N$ = 47.55 ± 0.15‰). Measurements of USGS40 ranged from -26.27 to -26.64‰ for $\delta^{13}C$ and from -4.29 to -4.77‰ for $\delta^{15}N$ between runs, and among runs, was -26.390 ± 0.056‰ for $\delta^{13}C$ and -4.52 ± 0.084‰ for $\delta^{15}N$. Measurements of USGS41a ranged from 36.29 to 36.78‰ for $\delta^{13}C$ and from 47.19‰ to 47.80‰ for $\delta^{15}N$ between runs, and among runs, was 36.55 ± 0.11‰ for $\delta^{13}C$ and was 47.55 ± 0.15‰ for $\delta^{15}N$. A duplicate was run for every 10th seal sample and the standard deviations were < 0.06‰ for $\delta^{13}C$ and < 0.20 ‰ for $\delta^{15}N$. Carbon to Nitrogen ratios (C:N) were inspected and only one muscle sample was > 3.51 and only four liver samples were > 3.71, an indicator that lipid content in the tissues were low (~ < 5%) and there was likely no impact of lipid on $\delta^{13}C$ (Post et al. 2007) (Table 3.1).

We used the $\delta^{15}N$ of ringed seals to estimate their relative trophic position ($TP_{consumer}$) in each location. $TP_{consumer}$ depends on the trophic enrichment factor for ^{15}N ($\Delta^{15}N_{consumer}$), which differs between muscle and liver (Hobson et al. 1996). Therefore, we first estimated the relative trophic position for Arctic cod (TP_{fish}), approximately one trophic level lower than ringed seals, using a generally derived $\Delta^{15}N_{fish}$, with *Calanus* spp. (or *Calanus hyperboreus* when species-specific distinction was made) as the baseline ($TP_{baseline} = 2$), as *Calanus* is shown to be a reliable consumer of phytoplankton (McMeans et al. 2013b, Yurkowski et al. 2016b). We used published $\delta^{15}N$ values of Arctic cod ($\delta^{15}N_{fish}$) and *Calanus* ($\delta^{15}N_{baseline}$) from each location (Hobson and Welch 1992, Hobson et al. 2002, Chambellant et al. 2013) (Table 3.2) to calculate TP_{fish} using equation 1a (derived from Brown et al. 2014a, Yurkowski et al. 2016b).

$$TP_{fish} = TP_{baseline} + \frac{(\delta^{15}N_{fish} - \delta^{15}N_{baseline})}{\Delta^{15}N_{fish}} \text{ (Eq. 1a)}$$

We then used the TP_{fish} as the baseline to estimate $TP_{consumer}$ using liver values and again using muscle values in equation 1b, with $\Delta^{15}N_{consumer}$ of 3.1‰ for phocid liver and 2.4‰ for phocid muscle (Hobson et al. 1996, Caut et al. 2009)

$$TP_{consumer} = TP_{fish} + \frac{(\delta^{15}N_{consumer} - \delta^{15}N_{fish})}{\Delta^{15}N_{consumer}} \text{(Eq. 1b)}$$

The relative carbon source in seal diets ($RC_{consumer}$) was calculated with equation 2, using $\delta^{13}C$ of seals ($\delta^{13}C_{consumer}$) and $\delta^{13}C$ values of *Calanus* ($\delta^{13}C_{baseline}$) at each study site (Hobson and Welch 1992, Hobson et al. 2002, Chambellant et al. 2013, Pedro et al. 2020). Since *Calanus* is a pelagic filter feeder, higher relative carbon source values indicated relatively more pelagic feeding, whereas lower values indicated more benthic and/or sea-ice based carbon in seal diets (Kohlbach et al. 2019, Pedro et al. 2020).

$$RC_{consumer} = \frac{\delta^{13}C_{consumer}}{\delta^{13}C_{baseline}} \text{(Eq. 2)}$$

To account for the effect of the oceanic Suess effect on $\delta^{13}C$ introduced by difference in collection year between the literature values of *Calanus*/Arctic Cod (1988-2007) and ringed seals (2016-2018) collected for this study, 0.011‰ yr^{-1} of difference was added to the $\delta^{13}C$ literature values of *Calanus*/Arctic Cod (de la Vega et al. 2019). We also added 0.3‰ to the Hudson Bay *Calanus* values reported in Chambellant et al. (2013) to remove a carbonate correction in that study, for consistency with all other samples and since acidification to correct for carbonates has a negligible effect on *Calanus* (Pomerleau et al. 2014).

Highly branched isoprenoid (HBI) analysis

Freeze dried and homogenized liver samples were used for HBI analysis because more than 70% of HBIs in vertebrates are stored in the liver (Brown et al. 2014b). The samples from Arviat and Pond Inlet were shipped to the Scottish Association for Marine Sciences (SAMS), Scottish Marine Institute (Oban, Argyll, UK), for HBI analysis while the samples from Grise Fjord and Qaanaaq were analyzed at the Freshwater Institute (FWI), Fisheries and Oceans

Canada (Winnipeg, MB, Canada). The methods used to extract the samples were identical between SAMS and FWI. Samples were weighed to ~0.46-1.0g of homogenized tissue and HBIs extracted according to Belt et al. (2012). Then 5µl of an internal standard was added (9-octylheptadec-8-ene; 10 µL; 10 µg mL^{-1}) followed by saponification in a methanolic KOH solution (4mL H2O : MeOH, 1 : 9; 20% KOH) for 60 minutes at 80°C. Next, 4ml of hexane was added and the sample was vortexed for 1 minute, centrifuged (1minute, 2000rpm) three times before transferring supernatant solutions containing non-saponifiable lipids (NSLs) to a clean glass test tube, dried with N_2, and resuspended in 0.5ml of hexane. Finally, samples were fractionated with 6ml of hexane using column chromatography with silica gel (SiO_2; 0.5g). The remaining purified, non-polar lipid extracts containing HBIs were analyzed using gas chromatography-mass spectrometry (with a 30 m DB-5 analytical column) according to Belt et al. (2012) for samples at SAMS. For samples at FWI, gas chromatography-mass spectrometry was still used (Agilent 7890B attached to a 5977B MSD) but set up in a precolumn backflush mode (a 4-m uncoated fused silica precolumn connected via Agilents "purged ultimate anion" to the same 30 m DB-5 analytical column). HBIs were quantified by the mass spectral intensity for each HBI in selective ion monitoring mode (IP_{25}: *m/z* 350.3, II: *m/z* 348.3, III: *m/z* 346.3). Each HBI was normalized according to the intensities of all 3 HBIs using an equation known as the H-Print (Brown & Belt 2017) that provides a percent of HBI contributions from planktonic diatoms to sea-ice diatoms.

$$H - Print\ (\%) \ = \frac{III}{IP_{25} + II + III}\ X\ 100 \text{ (Eq. 3)}$$

An H-print calibration was then used to calculate the estimated proportion of sea-ice derived carbon as a percentage of total marine carbon in ringed seal livers, which we refer to as sympagic carbon (%) (Brown et al. 2018, Kohlbach et al. 2019).

$$Sympagic\ carbon\ (\%) = 101.8 - 1.02\ \times H - Print\ \text{(Eq. 4)}$$

Statistical analysis

We used linear mixed effects models (LMMs) to investigate spatial differences in ringed seal diet, with eight separate models for $\delta^{13}C$, $\delta^{15}N$, relative carbon source, and trophic position in muscle and liver. To investigate spatial changes in sympagic carbon (%), we used a generalized linear model (GLM) with a Beta distribution and a logistic link function (Ferrari & Cribari-Neto 2004, Zuur & Ieno 2016). In all models we used location and age class as fixed effects and month of capture as a random effect except in sympagic carbon, muscle $\delta^{13}C$, and muscle relative carbon source, where a GLM was run because preliminary analyses indicated that month had no effect on the models. Sex was not included in our models as other studies have not found sex differences in ringed seal diet and our preliminary data exploration supported this conclusion (Holst et al. 2001, Young et al. 2010, Young & Ferguson 2014).

Locations were compared using Tukey post-hoc analysis (Appendix 1). P-values for LMMs were calculated using the conditional F-statistic for degrees of freedom with the Kenward-Roger correction and an F-statistic for GLMs. Intraclass correlation ($\sigma_{randomeffect}$), marginal (R^2_m) and conditional (R^2_c) pseudo R^2 values were computed for LMMs and pseudo R^2 was calculated for GLMs (Nakagawa & Schielzeth 2013, Zuur & Ieno 2016). Models were validated and model assumptions were tested by examining the residuals (Zuur & Ieno 2016, Hartig 2020). To investigate the correlation between the variation in sympagic carbon and $\delta^{13}C$, we used the non-parametric Spearman rho rank-based correlation coefficient because sympagic carbon is proportional ranging from 0 to 1 (0-100%). Results for all tests were considered significant at $\alpha = 0.05$. All statistical analyses were performed using R version 3.4.2 (R Core

Team 2020) and models were fitted using “betareg”, “glmmTMB”, and “lme4” (Bates et al. 2015; Brooks et al. 2017; Cribari-Neto and Zeileis 2010).

Results

Stable isotope analysis

Location was a significant predictor of $\delta^{13}C$ in liver ($F_{3,12.45}$ = 38.5, $p < 0.0001$, R^2_m = 0.826, R^2_c = 0.855) (Fig. 3.2) and muscle ($F_{3,104}$ = 201.5, $p < 0.0001$, R^2 = 0.851) (Fig. 3.3). Tukey post-hoc tests determined that mean $\delta^{13}C$ of Arviat ringed seals in liver (-21.1 ± 0.06‰) and muscle (-21.5 ± 0.08‰) was significantly lower than Pond Inlet (-19.5 ± 0.05‰ for liver; $t_{12.43}$ = -7.65, $p < 0.0001$; -19.8 ± 0.06‰ for muscle; t_{104} = -16.22, $p < 0.0001$), Grise Fjord (-18.3 ± 0.18‰ for liver; $t_{12.14}$ = -10.67, $p < 0.0001$; -18.8 ± 0.16‰ for muscle; t_{-104} = -19.74, $p < 0.0001$), and Qaanaaq (-19.0 ± 0.07‰ for liver, $t_{6.28}$ = -6.73, $p = 0.002$; -19.1 ± 0.08‰ for muscle, t_{104} = -18.02, $p < 0.0001$). Pond Inlet was also significantly lower than Grise Fjord in liver ($t_{49.75}$ = -6.95, $p < 0.0001$) and muscle (t_{104} = -6.90, $p < 0.0001$), and Qaanaaq in muscle (t_{104} = -4.480, $p < 0.0001$).

In liver, none of our selected variables including location ($F_{3,63.4}$ = 0.726, $p = 0.541$, R^2_m = 0.096, R^2_c = 0.485) were significant predictors of $\delta^{15}N$ (Fig. 3.2). For muscle, location ($F_{3,36.23}$ = 3.03, $p = 0.042$) and age class ($F_{2,101.7}$ = 4.16, $p = 0.018$) were significant predictors of $\delta^{15}N$ (R^2_m = 0.249, R^2_c = 0.481) (Fig. 3.3). A Tukey’s post-hoc test found no significant differences between locations despite a trend for lower muscle $\delta^{15}N$ in Qaanaaq (15.9 ± 0.09‰) than Grise Fjord (16.7 ± 0.13‰; $t_{23.8}$ = 2.655, $p = 0.062$). Muscle $\delta^{15}N$ was also significantly higher in adults than pups ($t_{103.6}$ = -2.521, $p = 0.035$) and there was a trend towards higher muscle $\delta^{15}N$ in adults than subadults ($t_{99.7}$ = -2.335, $p = 0.056$).

Relative carbon source and highly branched isoprenoids

Location was a significant predictor of relative carbon source in liver ($F_{3,12.94} = 75.58$, $p < 0.0001$, $R^2_m = 0.891$, $R^2_c = 0.910$) and muscle ($F_{3,104} = 325.7$, $p < 0.0001$, $R^2 = 0.902$) (Fig. 3.4). Tukey post-hoc tests determined that Arviat ringed seals in liver (1.05 ± 0.003) and muscle (1.06 ± 0.004) was higher than Pond Inlet (0.98 ± 0.003 for liver, $t_{12.96} = 7.85$, $p <0.0001$; 0.983 ± 0.003 for muscle, $t_{104} = 16.60$, $p < 0.0001$), Grise Fjord (0.88 ± 0.009 for liver, $t_{12.65} = 13.9$, $p < 0.0001$; 0.899 ± 0.008 for muscle, $t_{104} = 25.45$, $p < 0.0001$), and Qaanaaq (0.92 ± 0.003 for liver, $t_{6.54} = 9.53$, $p = 0.0002$; 0.916 ± 0.004 for muscle, $t_{104} = 24.09$, $p < 0.0001$). Pond Inlet ringed seals also had a higher relative carbon than Grise Fjord liver ($t_{50.84} = 11.5$, $p < 0.0001$) and muscle ($t_{104} = 12.19$, $p < 0.0001$), and Qaanaaq liver ($t_{8.79} = 5.50$, $p = 0.002$) and muscle ($t_{104} = 12.19$, $p < 0.0001$). Location was also a significant predictor of sympagic carbon (%) ($F_{3,104} = 109.8$ $p < 0.0001$, $R^2 = 0.774$) (Fig. 3.5). A Tukey post-hoc test determined that sympagic carbon was significantly lower in Arviat (22.0 ± 2.73%) than Pond Inlet (84.4 ± 2.27%; $t_{104} = -21.26$, $p < 0.0001$), Grise Fjord (89.9 ± 2.08%; $t_{104} = -20.70$, $p < 0.0001$), and Qaanaaq (81.0 ± 2.24%; $t_{104} = -16.91$, $p < 0.0001$). Sympagic carbon and $\delta^{13}C$ were also positively correlated to each other (Spearmans's $\rho = 0.71$, $p < 0.001$, $n = 106$).

Relative trophic position

For trophic position location was a significant predictor in liver ($F_{3,63.4} = 13.2$, $p < 0.0001$, $R^2_m = 0.537$, $R^2_c = 0.737$) and muscle ($F_{3,36.23} = 18.6$, $p < 0.0001$, $R^2_m = 0.546$, $R^2_c = 0.687$) while age class ($F_{2,101.7} = 4.16$, $p = 0.018$) was also a significant predictor in muscle (Fig.

3.6). A Tukey post-hoc test determined that Arviat ringed seals had a lower trophic position in liver (3.78 ± 0.02) than Pond Inlet (4.40 ± 0.05, $t_{71.0}$ = -2,80, $p = 0.033$), Grise Fjord (4.73 ± 0.06, $t_{69.3}$ = -5.31, $p < 0.0001$), and Qaanaaq (4.76 ± 0.03, $t_{41.6}$ = -4.02, $p = 0.001$). Pond Inlet liver was also lower in trophic position than Grise Fjord ($t_{96.9}$ = -4.85, $p < 0.0001$) and Qaanaaq ($t_{41.8}$ = -2.90, $p = 0.029$). A Tukey post-hoc test determined that in muscle, Arviat (3.82 ± 0.04; $t_{38.2}$ = -5.996, $p < 0.0001$) and Pond Inlet (4.26 ± 0.06; $t_{83.2}$ = -7.145, $p < 0.0001$) were lower than Grise Fjord (4.93 ± 0.06), while Qaanaaq (4.57 ± 0.04) trended towards being lower than Grise Fjord ($t_{23.8}$ = 2.655, $p = 0.062$). We also found that in muscle, pups had a lower trophic position than adults ($t_{103.6}$ = -2.521, $p = 0.035$) and subadults showed a trend towards being lower than adults ($t_{99.7}$ = -2.335, $p = 0.056$).

Discussion

In this study, complementary diet biomarker analyses showed an increase in sympagic carbon, an increase in $\delta^{13}C$, and a decrease in relative carbon source with latitude indicating less pelagic carbon in higher latitudes compared to low latitude. Agreement between our different analyses presents evidence of a shift in carbon source contribution to ringed seal diets over a large-scale latitudinal gradient, from a higher contribution of phytoplankton-derived carbon in the low Arctic to sympagic carbon in the high Arctic. Further, trophic position in seals from the high Arctic was higher compared to the low Arctic, indicating increased fish consumption, or changing food web structure with latitude. The pattern we observed agrees with other studies that have seen similar temporal effects and suggests future changes to Arctic food webs as a result of sea-ice loss may be reflected in the diets of high Arctic ringed seals (Brown et al. 2014a). We also found an increase δ^{15}N and trophic position from pups to adults, but the effect was small compared to the spatial trend we observed.

δ^{13}C increased with latitude and relative pelagic carbon decreased with increasing latitude. Together, these indices suggest a higher contribution of phytoplankton-based carbon to ringed seal diets at low latitude with a shift to a more sympagic or benthic diet in the intermediate and high Arctic (Pedro et al. 2020). However, proportion of sympagic carbon in ringed seal diets also increased with latitude and was highly correlated with δ^{13}C, which indicates that our results are likely driven by a higher relative contribution of sympagic carbon to the diets of ringed seals in the intermediate and high Arctic and more reliance on phytoplankton-based food webs for ringed seals at lower latitudes (Brown et al. 2014a, Kohlbach et al. 2019). Benthic feeding could also be playing a role by strong benthic-sympagic coupling where organic matter export from the sympagic environment to the benthic environment is promoting a rich benthic food web for ringed seals Our results show that complementary analysis of δ^{13}C and HBIs can help understand the sources of carbon that are present at the base of Arctic food webs and are contributing to the diet of Arctic marine predators, with implications for previous studies that have attributed an increase in δ^{13}C in diets to increased benthic carbon (Holst et al. 2001, Brown et al. 2014a, Pomerleau et al. 2016, Pedro et al. 2020).

Although location did not influence δ^{15}N in liver and had a small effect in muscle, when corrected for prey baseline and Δ^{15}N, our results indicated that trophic position increased with latitude in both liver and muscle. The conflict between δ^{15}N and trophic position highlight the importance of correcting for variation in baselines when comparing δ^{15}N between locations in consumers. The increase in trophic position with latitude may be driven by increased consumption of forage fish at higher trophic positions such as Arctic cod at higher latitudes, consistent with previous studies (Holst et al. 2001, Born et al. 2004, Yurkowski et al. 2016b). The increase in trophic position may also be driven by low Arctic food webs being composed of shorter food chains with less zooplankton complexity in the lower trophic levels, while the high Arctic may have longer food chains with increased zooplankton complexity in the lower trophic levels (Young & Ferguson 2014, Yurkowski et al. 2016b, de la Vega et al. 2021b). In this case, high Arctic food webs would have more Arctic-associated invertebrates that display more carnivory near the base of food webs, while the low Arctic would have more small and omnivorous or herbivorous Atlantic-associated invertebrates with fewer trophic interactions at the base of the food web (Dalpadado et al. 2016, Møller & Nielsen 2020, de la Vega et al. 2021b).

Differences in sea-ice conditions and phenology between our low and high Arctic locations are likely a major driver in the patterns we have observed (Arrigo & van Dijken 2015). Not only is physical sea-ice habitat for algae and sympagic grazers important, but correct timing to match with spring availability of sun, temperature increases, nutrients and timing of zooplankton and fish to take advantage of increased sea-ice algae production (Søreide et al. 2010, Brown et al. 2014a).Further, if landfast sea ice remains later, it can help drive tight sympagic-benthic coupling over coastal shelves to promote rich benthic food webs (Kohlbach et al. 2019). Our study supports that the heavier ice conditions and longer ice-covered seasons of the high Arctic seem to be sufficient to drive a higher contribution of sympagic/benthic carbon to the diet of ringed seals throughout the year (Brown et al. 2014a, Lowther et al. 2017). Transient sea-ice coverage in western Hudson Bay may not be present and stable for long enough into the spring and summer to promote rich sympagic-benthic coupled food webs compared to higher latitude locations. The longer open water season in western Hudson Bay would promote high levels of phytoplanktonic productivity contributing to the diet of ringed seals and other marine predators (Carroll et al. 2013, Arrigo & van Dijken 2015). A shorter open water season at higher latitudes would limit phytoplankton production, especially a seasonal pulse in the spring and summer (Yurkowski et al. 2018). Similar patterns were found in ringed seals over a long-term temporal gradient in Cumberland Sound, Nunavut, Canada and Svalbard, Norway, where phytoplanktonic carbon in ringed seal diets increased with lower sea-ice concentrations and longer open-water periods (Brown et al. 2014a, Lowther et al. 2017). Other environmental conditions may contribute to the patterns we have observed, such as air temperature and sea surface temperature, but latitude and sea-ice conditions are strongly tied to these variables and together they contribute shifts in ringed seal diets we have observed over our large spatial gradient (Young & Ferguson 2014).

Over this large-scale latitudinal gradient, factors that act on smaller scales can introduce uncertainty into the patterns we observed. For example, Qaanaaq experiences warmer currents and upwelling on the eastern side of Smith Sound, which can create sea-ice conditions and phenology, phytoplankton blooms, and species assemblages more indicative of more southern latitudes (Vibe 1950, Holst et al. 2001, Born et al. 2004). These conditions may help explain some results from Qaanaaq (77.5°N) that we would predict for latitudes lower than Grise Fjord (76.4°N) on the western side of Smith Sound and more like intermediate Pond Inlet (72.7°N). Moreover, the difference in currents and upwelling between Qaanaaq and Grise Fjord could also influence nutrient availability and impact the composition of primary production and prey availability between the two locations (Vibe 1950, Holst et al. 2001). Independent of sea ice, other oceanographic and geographical conditions such as bathymetry (coastal/shelf/pelagic), freshwater input (rivers/glaciers), and nutrient availability could play a role in the patterns we observed. For example, we observed Pond Inlet seals with diet biomarker characteristics closer to higher latitude locations which could be influenced by Eclipse Sound being a constrained basin that promotes the formation and persistence of landfast ice later into the spring.

Uncertainties were also introduced by temporal and spatial sampling constraints in our study. Due to availability of samples, Pond Inlet samples were from 2016-2017, whereas samples from every other site were collected in 2018. Further, seasonal sea-ice dynamics and seasonal dietary variation in ringed seal diets could have introduced variation to our data (Young & Ferguson 2013a, Brown et al. 2014a). Spatially, our study sites are not a perfect latitudinal gradient and were chosen in areas where ringed seal harvests exist. Further, ringed seals are highly mobile during the open water season and seals diets in our locations likely reflect a larger area than the community of capture (Ogloff et al. 2021). For example, Pond Inlet is closer to our high latitude locations than our low latitude location and ringed seals from Pond Inlet may also have fed in the Lancaster Sound or northern Baffin Bay region prior to capture. However, the large-scale latitudinal signal we observed was consistent among the complementary biomarker analyses we conducted and stronger than the small variations that were introduced by sampling limitations.

Climate change and future sea-ice recession could shift the base of high Arctic food webs from mostly sympagic production and high sympagic-benthic coupling to more phytoplankton-based production like observed at lower latitudes (Arrigo & van Dijken 2015, Yurkowski et al. 2020a). These changes are expected to have many impacts on Arctic species and restructuring of Arctic marine food webs, including decreased abundance of Arctic species such as Arctic cod and increased abundance of temperate species such as capelin and harp seals (Young & Ferguson 2014, Yurkowski et al. 2018, Ogloff et al. 2019). Early changes to ecosystem structure and function could be detected by diet biomarkers of seals from higher Arctic locations changing to resemble what we observed in lower latitude locations, such as more phytoplanktonic and pelagic carbon contributing to consumer diets and lower trophic position associated with less-complex phytoplankton communities and a potential decrease of Arctic cod in the diet (Carroll et al. 2013, de la Vega et al. 2021b). Demographic responses and a diet shift to more temperate capelin and sand lance has been already been observed in the southern edge of the range of ringed seals in Hudson Bay (Ferguson et al. 2017b). We demonstrate the potential of ringed seals to be sentinel species indicative of large scale ecosystem change over space and time as highly mobile and high trophic level predators integrating resources spatially, temporally, and up the food web (Young & Ferguson 2014, de la Vega et al. 2021a).

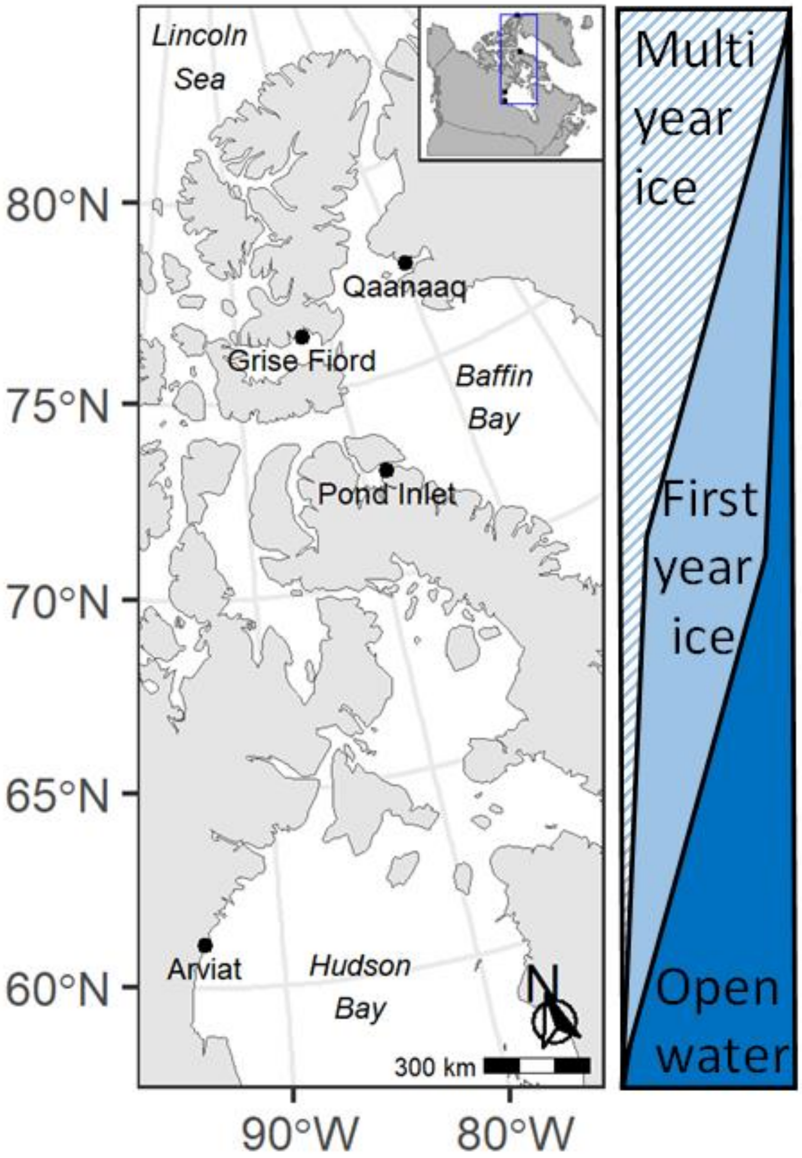

Figure 3.1. Main: A latitudinal gradient of sea-ice conditions from the eastern Canadian and western Greenland Arctic. Arviat, Nunavut (61.1°N) represents low latitude western Hudson Bay, Pond Inlet, Nunavut (72.7°N) represents intermediate latitude Eclipse Sound/Lancaster Sound, and Grise Fjord, Nunavut (76.4°N) and Qaanaaq, Greenland (77.5°N) represent high latitude Smith Sound/Jones Sound. Right: Conceptual representation of the increase in sea-ice conditions from low to high Arctic that reflects the latitudinal gradient that is the basis for this study.

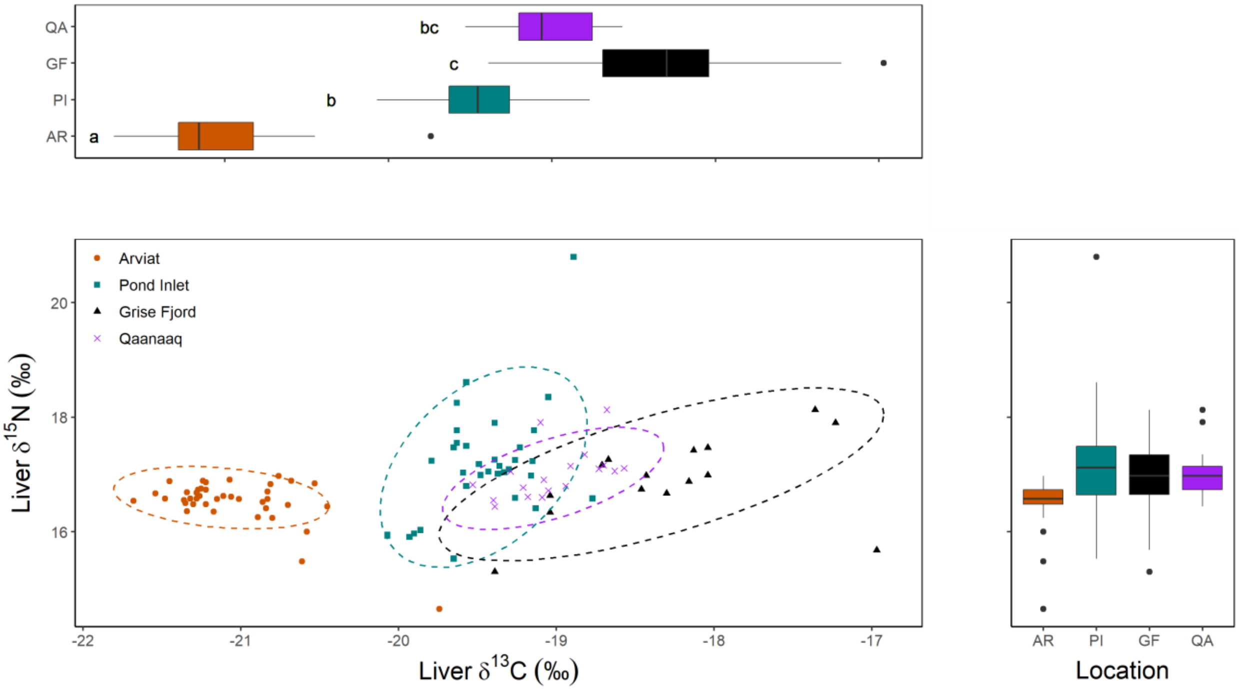

Figure 3.2. δ^{13}C and δ^{15}N for ringed seal liver samples collected in 2018 from Arviat, NU, Grise Fjord, NU, and Qaanaaq, GL, and in 2016-2017 from Pond Inlet, NU (Table 3.1). Main: biplot of δ^{13}C and δ^{15}N with dashed ellipses representing the 95% confidence intervals of multivariate t-distributions for each location. Top: Boxplot of δ^{13}C for each location. Letters represent separate groups determined by Tukey post-hoc analysis. Right: Boxplot of δ^{15}N for each location.

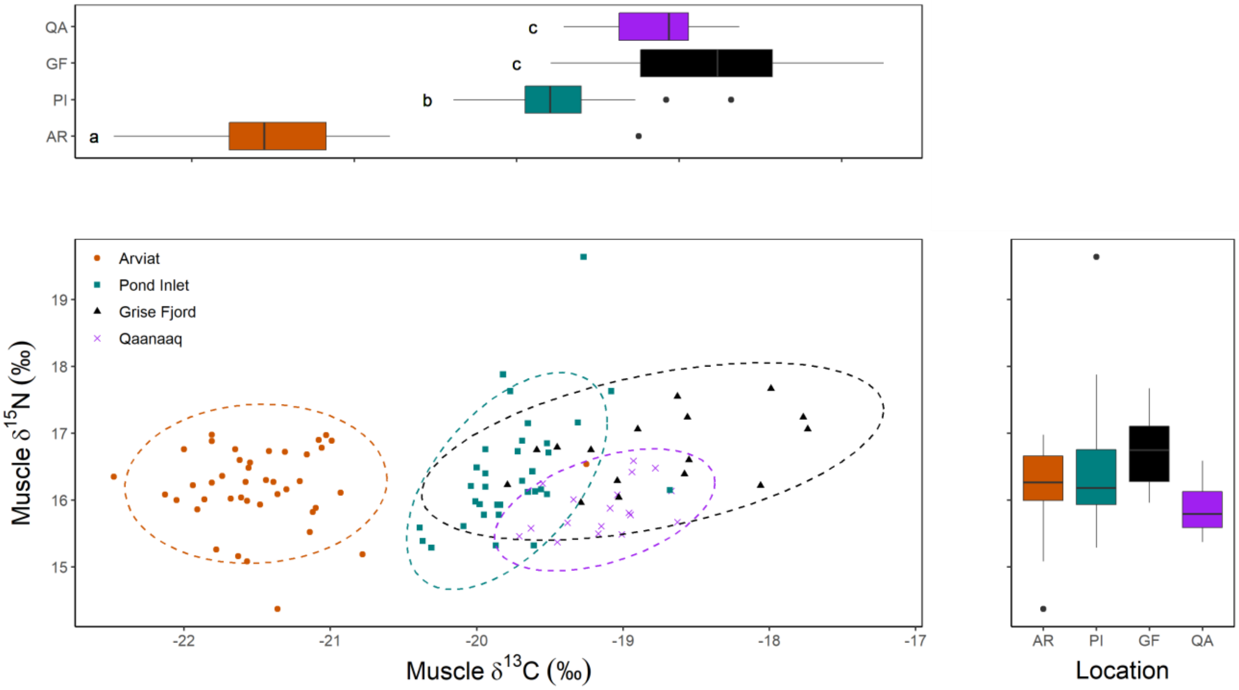

Figure 3.3. δ^{13}C and δ^{15}N for ringed seal muscle samples collected in 2018 from Arviat, NU, Grise Fjord, NU, and Qaanaaq, GL, and in 2016-2017 from Pond Inlet, NU (Table 3.1). Main: biplot of δ^{13}C and δ^{15}N with dashed ellipses representing the 95% confidence intervals of multivariate t-distributions for each location. Top: Boxplot of δ^{13}C for each location. Letters represent separate groups determined by Tukey post-hoc analysis. Right: Boxplot of δ^{15}N for each location.

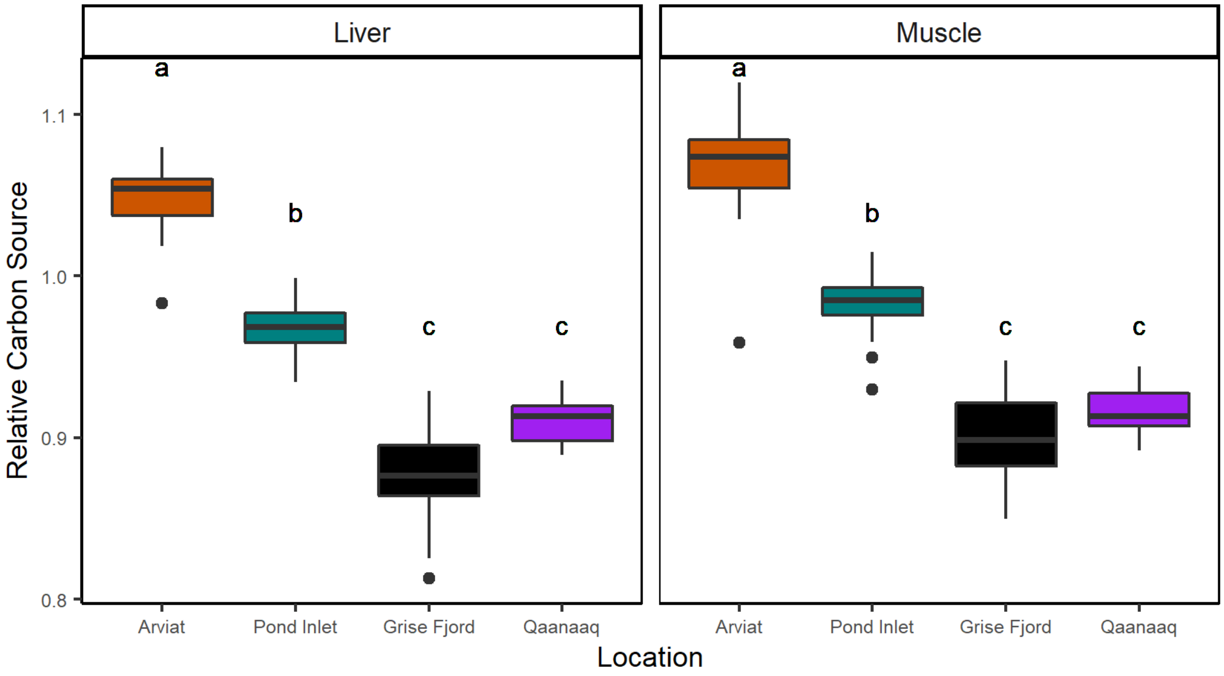

Figure 3.4. Relative carbon source index from seal liver and muscle samples collected from each study area (higher values indicate relatively more phytoplanktonic feeding and lower values indicate more benthic/sympagic feeding). Letters represent separate groups determined by Tukey post-hoc analysis.

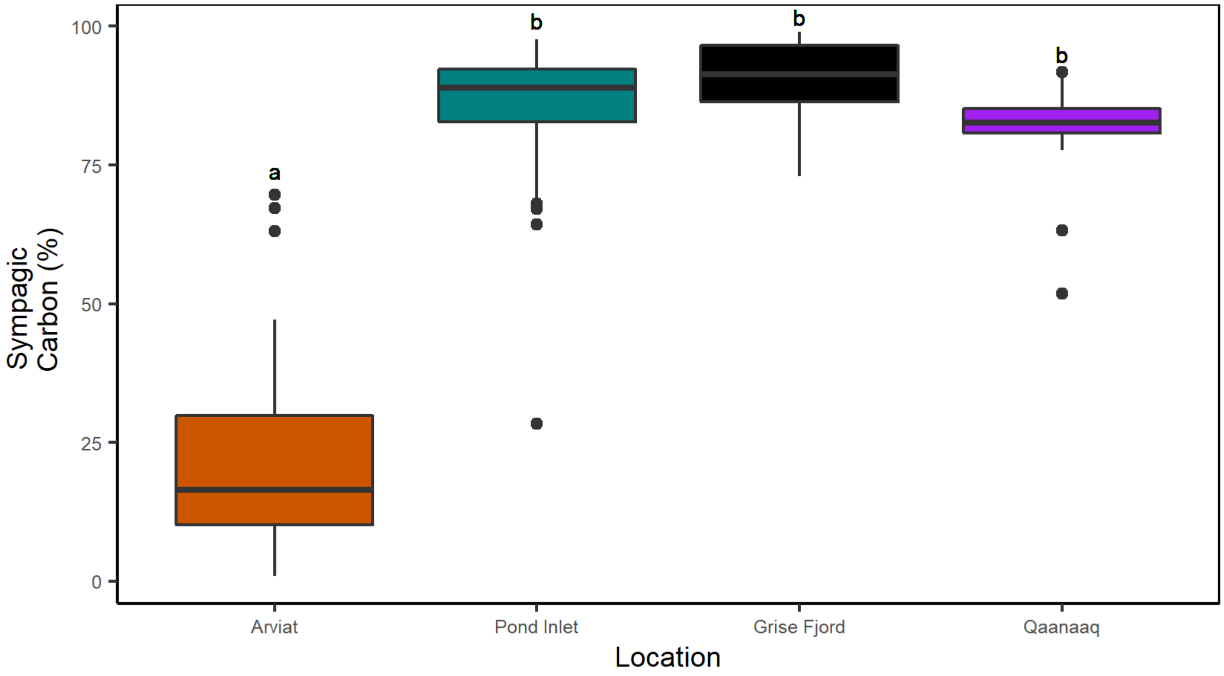

Figure 3.5. Boxplot of sympagic carbon (%) as a percentage of total marine carbon in ringed seal diets for each location in this study (Table 3.1). Letters represent separate groups determined by Tukey post-hoc analysis.

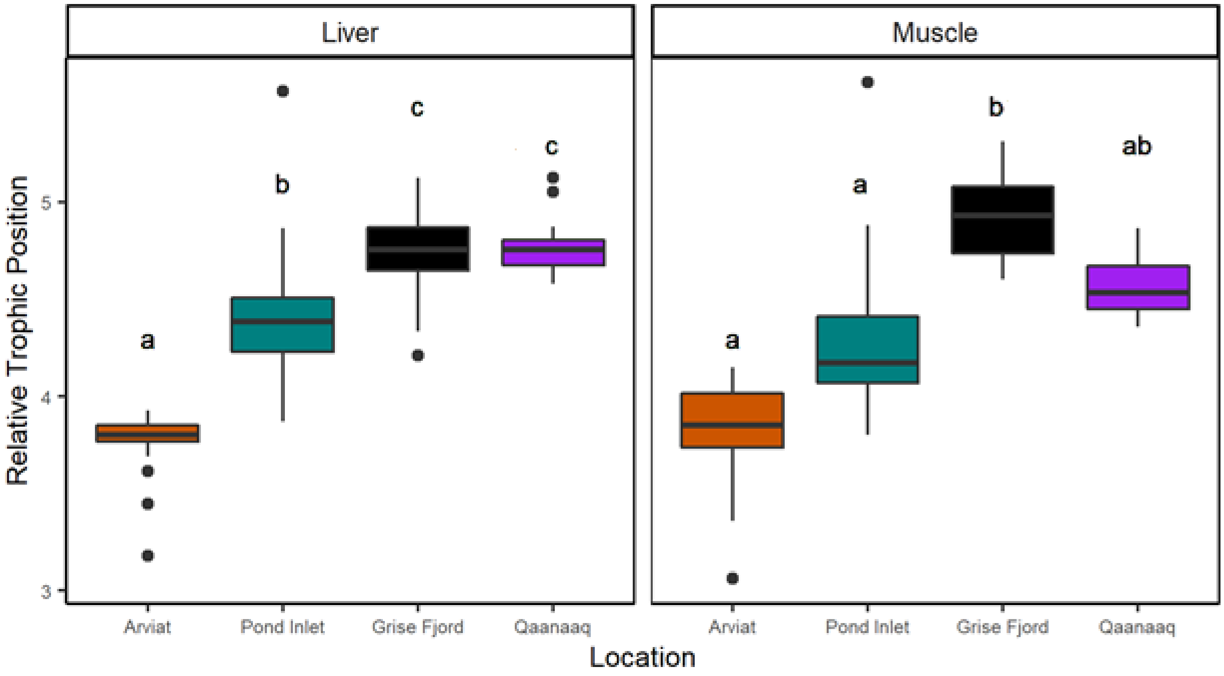

Figure 3.6. Relative trophic positions calculated (see Eq. 1 Methods) for ringed seal liver and muscle using *Calanus* literature values as a baseline (TP = 2) from Arviat, NU (Chambellant et al. 2013a), Lancaster Sound, NU for Pond Inlet (Hobson, Keith A., and Welch 1992), and the North Water Polynya for Grise Fjord, NU and Qaanaaq, NU (Hobson et al. 2002) (Table 3.1). Letters represent separate groups determined by Tukey post-hoc analysis.

Table 3.1. Summary of means (SE) of δ^{15}N, δ^{13}C, sympagic carbon, relative carbon source, relative trophic position, and Carbon/Nitrogen ratio for each tissue type from biomarker analysis of ringed seals in this study.

		Muscle						Liver						
		N	δ^{15}N (‰)	δ^{13}C (‰)	C/N ratio	Relative Carbon	Trophic Position	N	δ^{15}N (‰)	δ^{13}C (‰)	C/N ratio	Relative Carbon	Trophic Position	Sympagic carbon (%)
Low latitude	Arviat	42	16.5 (0.06)	-21.5 (0.08)	3.36 (0.01)	1.08 (0.003)	3.82 (0.04)	40	16.2 (0.09)	-21.1 (0.06)	3.48 (0.02)	1.05 (0.003)	3.78 (0.02)	22.0 (2.73)
Intermediate latitude	Pond Inlet	34	17.2 (0.17)	-19.8 (0.06)	3.26 (0.01)	1.00 (0.003)	4.26 (0.06)	34	16.4 (0.15)	-19.5 (0.05)	3.46 (0.02)	0.98 (0.003)	4.40 (0.05)	84.4 (2.27)
High latitude	Grise Fjord	16	16.9 (0.19)	-18.8 (0.16)	3.22 (0.02)	0.91 (0.008)	4.93 (0.06)	15	16.7 (0.13)	-18.3 (0.18)	3.32 (0.02)	0.88 (0.009)	4.73 (0.06)	89.9 (2.08)
	Qaanaaq	18	17.0 (0.10)	-19.1 (0.08)	3.21 (0.01)	0.92 (0.004)	4.57 (0.04)	18	15.9 (0.09)	-19.0 (0.07)	3.47 (0.02)	0.92 (0.003)	4.76 (0.03)	81.0 (2.24)

Table 3.2. Means (SE) of $\delta^{15}N$, $\delta^{13}C$ for prey samples. $\delta^{13}C$ was corrected to account for decreasing $\delta^{13}C$ in the atmosphere over time according to de la Vega et al. (2019)(Chambellant et al. 2013a, Quay et al. 2017)(Chambellant et al. 2013a, Quay et al. 2017) and to remove a carbonate correction made by Chambellant et al. (2013).

Latitude	Location	Year	Species	N	$\delta^{13}C$	$\delta^{15}N$	Reference
Low	Western Hudson Bay	2004-2007	*Calanus* spp.	19	-19.9 (0.3)	10.6 (1.0)	Chambellant et al. 2013
			Boreogadus saida	27	-18.6 (0.8)	14.7 (1.3)	
Intermediate	Lancaster Sound – Barrow Strait	1988-1990	*Calanus hyperboreus*	6*	-20.0 (0.4)	9.20 (0.5)	Hobson and Welch 1992
			Boreogadus saida	26	-18.4 (1.0)	15.2 (0.7)	
High	North Water Polynya	1998	*Calanus hyperboreus*	80	-20.7 (0.1)	7.90 (0.1)	Hobson et al. 2002
			Boreogadus saida	8	-19.0 (0.1)	14.1 (0.2)	

*each sample was composed of several individuals

References

Arrigo KR, van Dijken GL (2015) Continued increases in Arctic Ocean primary production. Prog Oceanogr 136:60–70.

Bates D, Maechler M, Bolker B, Walker S (2015) Fitting Linear Mixed Effects Models Using lme4. Journal of Stat Softw 67:1-48. doi:10.18637/jss.v067.i01.

Belt ST, Brown TA, Rodriguez AN, Sanz PC, Tonkin A, Ingle R (2012) A reproducible method for the extraction, identification and quantification of the Arctic sea ice proxy IP 25 from marine sediments. Anal Methods 4:705–713.

Bengtsson O, Lydersen C, Kovacs KM, Lindström U (2020) Ringed seal (*Pusa hispida*) diet on the west coast of Spitsbergen, Svalbard, Norway: during a time of ecosystem change. Polar Biol 43:773–788.

Bond AL, Hobson KA (2012) Reporting stable-isotope ratios in ecology: Recommended terminology, guidelines and best practices. Waterbirds 35:324–331.

Born EW, Teilmann J, Acquarone M, Riget FF (2004) Habitat use of ringed seals (*Phoca hispida*) in the North Water area (North Baffin Bay). Arctic 57:129–142.

Brown TA, Alexander C, Yurkowski DJ, Ferguson SH, Belt ST (2014a) Identifying variable sea ice carbon contributions to the Arctic ecosystem: A case study using highly branched isoprenoid lipid biomarkers in Cumberland Sound ringed seals. Limnol Oceanogr 59:1581–1589.

Brown TA, Belt ST (2017) Biomarker-based H-Print quantifies the composition of mixed sympagic and pelagic algae consumed by *Artemia* sp. J Exp Mar Bio Ecol 488:32–37.

Brown TA, Galicia MP, Thiemann GW, Belt ST, Yurkowski J, Dyck MG (2018) High contributions of sea ice derived carbon in polar bear (*Ursus maritimus*) tissue. PLoS ONE

13:1–13.

Brown TA, Yurkowski DJ, Ferguson SH, Alexander C, Belt ST (2014b) H-Print: A new chemical fingerprinting approach for distinguishing primary production sources in Arctic ecosystems. Environ Chem Lett 12:387–392.

Carroll SS, Horstmann-dehn L, Norcross BL (2013) Diet history of ice seals using stable isotope ratios in claw growth bands. Can J Zool 202:191–202.

Caut S, Angulo E, Courchamp F (2009) Variation in discrimination factors (Δ15N and Δ13C): The effect of diet isotopic values and applications for diet reconstruction. J Appl Ecol 46:443–453.

Chambellant M, Stirling I, Ferguson SH (2013) Temporal variation in western Hudson Bay ringed seal *Phoca hispida* diet in relation to environment. Mar Ecol Prog Ser 481:269–287.

Cribari-Neto F, Zeileis A (2010) Beta Regression in R. J Stat Softw 34:1-24. doi: 10.18637/jss.v034.i02.

Dalpadado P, Hop H, Rønning J, Pavlov V, Sperfeld E, Buchholz F, Rey A, Wold A (2016) Distribution and abundance of euphausiids and pelagic amphipods in Kongsfjorden, Isfjorden and Rijpfjorden (Svalbard) and changes in their relative importance as key prey in a warming marine ecosystem. Polar Biol 39:1765–1784.

Dey CJ, Richardson E, Mcgeachy D, Iverson SA (2017) Increasing nest predation will be insufficient to maintain polar bear body condition in the face of sea ice loss. Glob Chang Biol 23:1821–1831.

Ferguson SH, Stirling I, McLoughlin P (2005) Climate change and ringed seal (*Phoca hispida*) recruitment in western Hudson Bay. Mar Mammal Sci 21:121–135.

Ferguson SH, Young BG, Yurkowski DJ, Anderson R, Willing C, Nielsen O (2017)

Demographic, ecological, and physiological responses of ringed seals to an abrupt decline in sea ice availability. PeerJ 5:e2957.

Ferrari SLP, Cribari-Neto F (2004) Beta regression for modelling rates and proportions. J Appl Stat 31:799–815.

Fossheim M, Primicerio R, Johannesen E, Ingvaldsen RB, Aschan MM, Dolgov AV (2015) Recent warming leads to a rapid borealization of fish communities in the Arctic. Nat Clim Chang 5:673–677.

Frainer A, Primicerio R, Kortsch S, Aune M, Dolgov AV, Fossheim M, Aschan MM (2017) Climate-driven changes in functional biogeography of Arctic marine fish communities. Proc Natl Acad Sci U S A 114:12202–12207.

Galley RJ, Else BGT, Howell SEL, Jennifer V, Galley RJ, Else BGT, Howell SEL, Lukovich J V, Barber DG (2012) Landfast Sea Ice Conditions in the Canadian Arctic : 1983-2009. Arctic 65:133–144.

Hartig F (2020) DHARMa: Residual Diagnostics for Hierarchical (Multi-Level / Mixed) Regression Models. R package version 0.3.3.0. https://CRAN.R-project.org/package=DHARMa

Hayden B, Harrod C, Thomas SM, Eloranta AP, Myllykangas JP, Siwertsson A, Præbel K, Knudsen R, Amundsen PA, Kahilainen KK (2019) From clear lakes to murky waters – tracing the functional response of high-latitude lake communities to concurrent ‘greening’ and ‘browning’. Ecol Lett 22:807–816.

Hobson KA, Welch HE (1992) Determination of trophic relationships within a high Arctic marine food web using δ13C and δ15N analysis. Mar Ecol Prog Ser 84:9–18.

Hobson KA, Ambrose WG, Renaud PE (1995) Sources of primary production, benthic-pelagic coupling, and trophic relationships within the Northeast Water Polynya: insights from δ13C and δ15N analysis. Mar Ecol Prog Ser 128:1–10.

Hobson KA, Fisk A, Karnovsky N, Holst M, Gagnon JM, Fortier M (2002) A stable isotope (δ^{13}C, δ^{15}N) model for the North Water food web: Implications for evaluating trophodynamics and the flow of energy and contaminants. Deep Res Part II Top Stud Oceanogr 49:5131–5150.

Hobson KA, Schell DM, Renouf D, Noseworthy E (1996) Stable carbon and nitrogen isotopic fractionation between diet and tissues of captive seals. Can J Fish Aquat Sci 53:528–533.

Holst M, Stirling I, Hobson KA (2001) Diet Of Ringed Seals (*Phoca Hispida*) On The East And West Sides Of The North Water Polynya, Northern Baffin Bat. Mar Mammal Sci 17:888–908.

Kamil Barton (2020). MuMIn: Multi-Model Inference. R package version 1.43.17. https://CRAN.R-project.org/package=MuMIn

Kohlbach D, Ferguson SH, Brown TA, Michel C (2019) Landfast sea ice−benthic coupling during spring and potential impacts of system changes on food web dynamics in Eclipse Sound, Canadian Arctic. Mar Ecol Prog Ser 627:33–48.

Kortsch S, Primicerio R, Fossheim M, Dolgov AV, Aschan MM (2015) Climate change alters the structure of arctic marine food webs due to poleward shifts of boreal generalists. Proceedings Biol Sci 282:1–9.

de la Vega C, Jeffreys RM, Tuerena R, Ganeshram R, Mahaffey C (2019) Temporal and spatial trends in marine carbon isotopes in the Arctic Ocean and implications for food web studies. Glob Chang Biol 25:4116–4130.

de la Vega C, Mahaffey C, Tuerena RE, Yurkowski DJ, Ferguson SH, Stenson GB, Nordøy ES, Haug T, Biuw M, Smout S, Hopkins J, Tagliabue A, Jeffreys RM (2021a) Arctic seals as tracers of environmental and ecological change. Limnol Oceanogr Lett 6:24–32.

de la Vega C, Mahaffey C, Yurkowski DJ, Norman L, Simpson E, Smout S, Ferguson SH, Jeffreys RM (2021b) Biomarkers in Ringed Seals Reveal Recent Onset of Borealization in the High- Compared to the Mid-Latitude Canadian Arctic. Front Mar Sci 8: 700687.

Laidre KL, Atkinson SN, Regehr E V, Stern HL, Born EW, Wiig Ø, Lunn NJ, Dyck M, Heagerty P, Cohen BR (2020) Transient benefits of climate change for a high-Arctic polar bear (*Ursus maritimus*) subpopulation. Glob Chang Biol 1–15.

Laidre KL, Stirling I, Lowry LF, Wiig Ø, Heide-Jørgensen MP, Ferguson SH (2008) Quantifying the sensitivity of Arctic marine mammals to climate-induced habitat change. Ecol Appl 18:97–125.

Lenth RV (2021) emmeans: Estimated Marginal Means, aka Least-Squares Means. R package version 1.5.4. https://CRAN.R-project.org/package=emmeans.

Lowther AD, Fisk A, Kovacs KM, Lydersen C (2017) Interdecadal changes in the marine food web along the west Spitsbergen coast detected in the stable isotope composition of ringed seal (*Pusa hispida*) whiskers. Polar Biol 0:0.

Luque SP, Ferguson SH, Breed GA (2014) Spatial behaviour of a keystone Arctic marine predator and implications of climate warming in Hudson Bay. J Exp Mar Bio Ecol 461:504–515.

Mclaren IA (1958) The Biology of the Ringed Seal (*Phoca hispida Schreber*) in the Eastern Canadian Arctic. Ottawa, Fish Res Board Can. 97 pp.

McMeans BC, Rooney N, Arts MT, Fisk AT (2013) Food web structure of a coastal Arctic marine ecosystem and implications for stability. Mar Ecol Prog Ser 482:17–28.

Møller EF, Nielsen TG (2020) Borealization of Arctic zooplankton—smaller and less fat zooplankton species in Disko Bay, Western Greenland. Limnol Oceanogr 65:1175–1188.

Brooks ME, Kristensen K, van Benthem KJ, Magnusson A, Berg CW, Nielsen A, Skaug HJ, Maechler M, Bolker BM (2017) glmmTMB Balances Speed and Flexibility Among Packages for Zero-inflated Generalized Linear Mixed Modeling. The R Journal, 9:378-400.

Nakagawa S, Schielzeth H (2013) A general and simple method for obtaining R2 from generalized linear mixed-effects models. Methods Ecol Evol 4:133–142.

Ogloff WR, Ferguson SH, Fisk AT, Marcoux M, Hussey NE, Jaworenko A, Yurkowski DJ (2021) Long-distance movements and associated diving behaviour of ringed seals (*Pusa hispida*) in the eastern Canadian Arctic . Arct Sci 18:1–18.

Ogloff WR, Yurkowski DJ, Davoren GK, Ferguson SH (2019) Diet and isotopic niche overlap elucidate competition potential between seasonally sympatric phocids in the Canadian Arctic. Mar Biol 166:1–12.

Overland JE, Wang M (2013) When will the summer Arctic be nearly sea ice free ? 40:2097–2101.

Pedro S, Fisk AT, Ferguson SH, Hussey NE, Kessel ST, McKinney MA (2020) Broad feeding niches of capelin and sand lance may overlap those of polar cod and other native fish in the eastern Canadian Arctic. Polar Biol 43:1707–1724.

Pomerleau C, Stern GA, Pućko M, Foster KL, Macdonald RW, Fortier L (2016) Pan-Arctic concentrations of mercury and stable isotope ratios of carbon (δ^{13}C) and nitrogen (δ^{15}N) in marine zooplankton. Sci Total Environ 551–552:92–100.

Pomerleau C, Winkler G, Sastri A, Nelson RJ, Williams WJ (2014) The effect of acidification and the combined effects of acidification/lipid extraction on carbon stable isotope ratios for sub-Arctic and Arctic marine zooplankton species. Polar Biol 37:1541–1548.

Post DM, Layman CA, Arrington DA, Takimoto G, Quattrochi J, Montaña CG (2007) Getting to the fat of the matter: Models, methods and assumptions for dealing with lipids in stable isotope analyses. Oecologia 152:179–189.

Post E, Bhatt US, Bitz CM, Brodie JF, Fulton TL, Hebblewhite M, Kerby JT, Kutz S, Stirling I, Walker DA (2013) Ecological Consequences of Sea-Ice Decline. Science (80) 341:519–524.

Provencher JF (2012) Seabird diet indicates changing Arctic marine communities in eastern Canada. Mar Ecol Prog Ser 454:171-182

Quay P, Sonnerup R, Munro D, Sweeney C (2017) Anthropogenic CO^2 accumulation and uptake rates in the Pacific Ocean based on changes in the $^{13}C/^{12}C$ of dissolved inorganic carbon. Global Biogeochem Cycles 31:59–80.

Søreide JE, Leu EVA, Berge Jør, Graeve M, Falk-Petersen S (2010) Timing of blooms, algal food quality and *Calanus glacialis* reproduction and growth in a changing Arctic. Glob Chang Biol 16:3154–3163.

R Core Team (2020) R: A language and environment for statistical computing. R Foundation for Statistical Computing, Vienna, Austria. URL https://www.R-project.org/.

Stewart BE (1996) Counts Of Growth Layer Groups In Cementum And Dentine In Ringed Seals (*Phoca Hispida*). Mar Mamm Sci 12:383-401.

Vibe C (1950) The marine mammals and the marine fauna in Thule District (Northwest Greeenland) with observations on ice conditions 1939-41. Medd. om Grønland. 150:93–97.

Wang J, Mysak LA, Ingram RG (1994) Interannual variability of sea-ice cover in Hudson Bay, Baffin Bay and the Labrador Sea. Atmos - Ocean 32:421–447.

Welch HE, Bergmann MA, Siferd TD, Martin KA, Curtis MF, Crawford RE, Conover RJ, Hop H (1992) Energy Flow through the Marine Ecosystem of the Lancaster Sound Region , Arctic Canada. Arctic 45:343–357.

Winship AJ, Trites AW, Calkins DG (2001) Growth in body size of the steller sea lion (*Eumetopias jubatus*). J Mammal 82:500–519.

Wickham H (2016) ggplot2: Elegant Graphics for Data Analysis. Springer-Verlag New York.

Wisz MS, Pottier J, Kissling WD, Pellissier L, Damgaard CF, Dormann CF, Forchhammer MC, Grytnes J, Guisan A, Heikkinen RK, Høye TT, Ockinger E, Schmidt NM, Termansen M, Wardle DA, Aastrup P, Svenning J (2013) The role of biotic interactions in shaping distributions and realised assemblages of species : implications for species distribution modelling. Biol Rev 88:15–30.

Young BG, Ferguson SH (2013) Seasons of the ringed seal : pelagic open-water hyperphagy , benthic feeding over winter and spring fasting during molt. Wild Res 40:52–60.

Young BG, Ferguson SH (2014) Using stable isotopes to understand changes in ringed seal foraging ecology as a response to a warming environment. Mar Mammal Sci 30:706–725.

Young BG, Loseto LL, Ferguson SH (2010) Diet differences among age classes of Arctic seals: Evidence from stable isotope and mercury biomarkers. Polar Biol 33:153–162.

Yurkowski DJ, Brown TA, Blanchfield PJ, Ferguson SH (2020a) Atlantic walrus signal latitudinal differences in the long-term decline of sea ice-derived carbon to benthic fauna in the Canadian Arctic: Climate change and imperiled ice carbon. Proc R Soc B Biol Sci 287.

Yurkowski DJ, Ferguson S, Choy ES, Loseto LL, Brown TM, Muir DCGG, Semeniuk CADD, Fisk AT (2016a) Latitudinal variation in ecological opportunity and intraspecific competition indicates differences in niche variability and diet specialization of Arctic marine predators. Ecol Evol 6:1666–1678.

Yurkowski DJ, Ferguson SH, Semeniuk CAD, Brown TM, Muir DCG, Fisk AT (2016b) Spatial and temporal variation of an ice-adapted predator's feeding ecology in a changing Arctic marine ecosystem. Oecologia 180:631–644.

Yurkowski DJ, Hussey NE, Ferguson SH, Fisk AT (2018) A temporal shift in trophic diversity among a predator assemblage in a warming Arctic. R Soc Open Sci 5: 180259.

Yurkowski DJ, Richardson ES, Lunn NJ, Muir DCG, Johnson AC, Derocher AE, Ehrman AD, Houde M, Young BG, Debets CD, Sciullo L, Thiemann GW, Ferguson SH (2020b) Contrasting Temporal Patterns of Mercury, Niche Dynamics, and Body Fat Indices of Polar Bears and Ringed Seals in a Melting Icescape. Environ Sci Technol 54:2780–2789.

Vander Zanden MJ, Clayton MK, Moody EK, Solomon CT, Weidel BC (2015) Stable isotope turnover and half-life in animal tissues: A literature synthesis. PLoS One 10:1–16.

Zuur AF, Ieno EN (2016) A protocol for conducting and presenting results of regression-type analyses. Methods Ecol Evol 7:636–645.

Chapter 4: Marine mammal biodiversity and rare narwhal (*Monodon monoceros*) observations near northern Ellesmere Island, Canada

Carlyle, CG, Florko KRN, Young BG, Yurkowski DJ, Michel C, Ferguson SH (2021) Ecosphere 12(6):e03534. 10.1002/ecs2.3534.

Abstract

Climate-driven decline of sea ice has increased international interest in understanding the ecology of seldom studied high-Arctic regions projected to retain the last summer sea ice. Arctic marine mammals are vulnerable to future environmental change due to their high dependence on sea ice. We completed aerial surveys in August 2019 to document the occurrence and location of marine mammals within the recently designated Tuvaijuittuq Marine Protected Area, which acts as a last refuge for ice-associated species. We present photographic evidence of narwhals (*Monodon monoceros*), Atlantic walruses (*Odobenus rosmarus*), bearded seals (*Erignathus barbatus*), and ringed seals (*Pusa hispida*) in Archer Fjord, northern Ellesmere Island, Nunavut, Canada (81° 14’ N - 81° 49’ N). We discuss these observations in the context of historical records and more recent opportunistic sightings from the region to support the hypothesis of an expansion north of the currently accepted range of narwhal. The diversity and number of observations of marine mammals in Archer Fjord is a striking contrast to the relative scarcity of the rest of the surveyed region, with very few observations of ringed seals throughout the more northerly study area. Our observations highlight opportunities to further explore other places such as Archer Fjord and that may now host unique marine mammal biodiversity in the region, including narwhal.

Key words: Aerial survey; Arctic; Atlantic walrus; bearded seal; climate change; high latitude; range; ringed seal; sea ice.

The low accessibility and high costs of field research in the high Arctic have resulted in few observations and limited knowledge of animal biodiversity and distribution in these remote areas (Mallory et al. 2018). A rapid climate-driven recession of sea ice has generated international interest in understanding how these high-latitude systems will respond to further change. For example, a multinational agreement was reached in 2018 that banned commercial fishing in the Central Arctic Ocean until there is sufficient ecological knowledge of the region. Arctic marine mammals are especially vulnerable to future environmental changes due to their dependence on sea-ice habitat for activities such as hunting, breeding, and molting (Laidre et al. 2008). In response to increased interest to protect high-latitude sea-ice habitat that serves as the last place of refuge for pagophilic (ice-associated) marine mammal species, such as narwhal (*Monodon Monoceros*), Atlantic walruses (*Odobenus rosmarus rosmarus*), ringed seals (*Pusa hispida*), and polar bears (*Ursus maritimus*), the Canadian government designated the Tuvaijuittuq Marine Protected Area by Ministerial Order in August 2019. Concurrently, large-scale multi-year research projects such as the Multidisciplinary Arctic Program (MAP)-Last Ice led by Fisheries and Oceans Canada (DFO), have been conducting research into this little-studied area. Results are anticipated to fill gaps in knowledge on high-Arctic ecosystem structure and function and inform decision makers on the effectiveness and enhancement of conservation initiatives such as Tuvaijuittuq (Lange et al. 2019).

Before 2018, information on marine mammals in Tuvaijuittuq has been primarily based on opportunistic sightings from explorer records (Greely 1886; Peary 1910), which often lack key biological context such as abundance, sex, age classes, and behavior. In August 2015 in Petermann Fjord, Greenland, an area adjacent to the south-eastern portions of Tuvaijuittuq, an ice breaker-based survey observed ringed seals, bearded seals (*Erignathus barbatus*), harp seals

(*Pagophilus groenlandicus*), and polar bears (Lomac-McNair et al. 2018; Lomac McNair et al. 2019). In August 2018, MAP-Last Ice completed the first summer aerial surveys to document marine mammal occurrence within Tuvaijuittuq and observed Atlantic walruses in Archer Fjord – an area much farther north than their previously recorded range (Yurkowski et al. 2019). To build on these findings, we conducted aerial surveys in August 2019 where we observed a broader diversity of marine mammal species than in August 2018, and most notably, narwhal farther north than their currently recognized range in Canada (Hobbs et al. 2019; Lowry et al. 2017). A DeHavilland Twin Otter flying at a target speed and altitude of 110 knots and 305m was equipped with a Nikon D810 digital single-lens reflex (DSLR) camera and a 35mm lens mounted in a port in the belly of the aircraft. Images were captured directly below the aircraft, covering a 312m wide strip with ~40% overlap between successive images. In total, 57 survey transects were flown covering 1054 km^2 (Appendix B: Fig. B.1; see Yurkowski et al. (2019) for more details). We photographed 29 individual narwhals (seven adult males, seven adult females, one yearling, and 14 unknowns due to submergence on 14 August 2019), three Atlantic walrus (18 August 2019), 30 ringed seals (14 & 18 August 2019), and four bearded seals (14 August 2019) along 2 transects covering 84.12 km^2 Archer Fjord and Lady Franklin Bay (Fig. 4.1, Fig. 4.2; Appendix B: Table B.1, Fig. B.1). There was also a visual observer recording wildlife sightings and environmental observations. The visual observer spotted 25 narwhals (14 August 2019; some of which were likely outside of the view of the camera), 36 Atlantic walrus (21 individuals on 14 August 2019, 15 individuals on 18 August 2019) that dove into the water before the plane passed over them and were also outside of the view of the camera, and 18 seals (11 individuals on 14 August 2019, seven individuals on 18 August 2019) along the same 2 transects in Archer Fjord and Lady Franklin Bay (Fig. 4.2). The data was insufficient to estimate density for narwhals, Atlantic walrus, and bearded seals. In addition to marine mammals, gulls (family Laridae) were also observed in Archer Fjord. Environmental conditions during our time in Archer Fjord on 14 August were open water to light drift ice cover (0-10%), calm sea state (0-1 Beaufort Sea Scale), and no cloud cover (0%), fog, or precipitation. On 18 August, conditions shifted to more drift or light pack sea ice cover (10-40%), calm or light breeze sea state (0-2 Beaufort Sea Scale), heavy cloud cover (100%), light fog, and light precipitation.

The currently accepted northern extent of narwhal range in Canada is to approximately 80° 30’ N in the Nares Strait (Hobbs et al. 2019; Lowry et al. 2017), but systematic surveys have not observed narwhals north of ~79° 30’ N in Kane Basin (Doniol-Valcroze et al. 2015). However, historical records report “a number of narwhals” (at least five but total number of individuals not reported) as far north as Hall Basin (~81° 30’ N) and a tusk recovered as far as Floeberg Beach (~82° 27’ N) in 1881 (Greely 1886). A narwhal hunted at Cape Union (~82° 15’ N) in 1909 (Peary 1910) also suggests common occurrence in Hall Basin and potential to reach the Lincoln Sea. Additionally, an ice breaker expedition not equipped to survey for marine mammals, opportunistically observed a group of up to 30 narwhals from a helicopter in the southeastern region of the Petermann Fjord adjacent to the Petermann Glacier front, Greenland in August 2012 (K. Lomac-McNair, pers. comm., July 2020). Our novel observations at 81° 18’ N indicate summer habitat use of Archer Fjord by an aggregation of narwhals with a yearling approximately 175 km north of the previously surveyed range of narwhals in Canada (Doniol-Valcroze et al. 2015). Together with historical records, our observations of this narwhal aggregation that included a yearling, support the northern extent of the narwhal’s range in Canada to include Archer Fjord, Lady Franklin Bay, and Hall Basin (COSEWIC 2004; Fig. 4.2).

Observations of numerous narwhals in Archer fjord identifies knowledge gaps about their ecology and population status in the area. First, the presence of narwhal in Archer Fjord may be an annual summer occurrence, but lack of long-term monitoring in the area may have precluded discovery of this baseline information. Alternatively, these observations may represent an ecological range shift. However, the short timeframe of our survey precludes conclusions concerning narwhal habitat use and reliance on this area, our observations of 29 individuals and a yearling near the head of Archer Fjord, and the opportunistic observations of a large group well within Petermann Fjord in 2012 suggests important habitat use of the area throughout summer. The lack of information on the number of individuals observed and ecological context from explorer records makes it difficult to conclude whether these sightings represent ecologically important and recurrent use, or transient visits to the area. Second, genetic and movement ecology would determine where these high-Arctic aggregations fit into the management context of the eight currently defined summering stocks of the high-Arctic Baffin Bay population of narwhal (Hobbs, et al. 2019). This aggregation may be a part of the northernmost stock (Smith Sound) which is vital information for responsible co-management with Inuit from Canada and Greenland that hunt narwhals for cultural and subsistence purposes.

The number of Atlantic walrus individuals observed in Archer Fjord in 2019 (n = 21 visual and 3 photographic) was higher than 2018 (n = 7 visual and 1 photographic) (Yurkowski et al. 2019). The presence and observations of numerous Atlantic walruses in Archer Fjord for two consecutive years support the range extension of the current Atlantic walrus distribution proposed by Yurkowski et al. (2019). The number of seal observations in Archer Fjord was also greater in 2019 (n = 34 seals) compared to the 2018 surveys (n = 3). The difference in observations between the two years could have been due to the earlier 2018 surveys (one week).

Tuvaijuittuq is characterized by heavy year-round sea ice conditions and a very dynamic sea ice cover (Moore et al. 2019). Interannual differences in sea-ice conditions in Tuvaijuittuq and the connected Canadian high-Arctic region, (i.e., Kennedy Channel and Kane Basin) could have also influenced the difference in marine mammal biodiversity and number of observations between 2018 and 2019. Tuvaijuittuq and the connected Kennedy Channel and Kane Basin region experienced lighter sea-ice conditions in 2019 compared to 2018 (Appendix B: Fig. B.2). In particular, the sea-ice conditions from Smith Sound and Kane Basin in the south to Hall Basin and Nares Strait in the north likely acts as a choke point moderating the ability of marine mammals such as narwhal and Atlantic walrus to reach Archer Fjord (COSEWIC 2004; Higdon and Ferguson 2009; Yurkowski et al. 2019). An earlier sea-ice breakup in 2019 may have also changed the timing and biomass of phytoplankton blooms and increased the summer availability of marine resources in the region (e.g., Arrigo and van Dijken 2015). This could support an increased abundance of marine mammals that require abundant food resources in the summer months to support their high annual metabolic and nutritional requirements.

During our two surveys in August 2018 (Yurkowski et al. 2019) and 2019 (this study), narwhals, Atlantic walruses, and bearded seals were only observed within the two transects covering Archer Fjord and Lady Franklin Bay (Appendix B: Fig. B.1). Although ringed seals were observed in some of the 55 transects outside Archer Fjord in 2019 (none in 2018) and considerably farther north (~82° 50’ N 59° 13’ W), there were very few sightings in this large region compared to the 30 individuals observed within Archer Fjord. The numerous observations and aggregations of many marine mammal species in Archer Fjord suggests this area is a seasonal oasis of relatively higher productivity in the high Arctic. Future work examining environmental properties such as bathymetry, temperature, and sea-ice dynamics, as well as the resulting biological productivity may help researchers understand how Archer Fjord and Lady Franklin Bay can support the habitat requirement of narwhals, Atlantic walruses, bearded seals, and ringed seals in the summer at the northern limits of their ranges. The findings of multi-year high-Arctic research programs (e.g., MAP-Last Ice) highlight the need for continued monitoring of marine mammals at the northern edge of their range to help understand the mechanisms of biodiversity, distribution shifts, and demographic changes in a rapidly changing Arctic.

Acknowledgments

This research is part of the Multidisciplinary Arctic Program (MAP) – Last Ice, funded by Fisheries and Oceans Canada and with logistical support generously provided by Polar Continental Shelf Program, Environment and Climate Change Canada and Department of National Defence at Canadian Forces Station (CFS) Alert. Special thanks to Major Tonja Kerr, Commanding Officer (CO) and Master Warrant Office (MWO) Dwayne Fox, Station Warrant Officer (SWO). We also thank the Hunters and Trappers Association of Resolute Bay and Grise Fjord for their support to the project. Specifically, we thank Uluriak Amarualik of Resolute Bay for her participation in the surveys. We thank our Kenn Borek Ltd. crew – Captain Troy McKerral, First Officer Jorge Barreto, and Engineer Travis Griesbecht. CGC and KF are supported by NSERC with additional support from the W. Garfield Weston Foundation to CGC.

References

Arrigo, K.R., and G.L. van Dijken. 2015. Continued increases in Arctic Ocean primary production. Progress in Oceanography 136:60–70.

COSEWIC. 2004. COSEWIC assessment and update status report on the Narwhal *Monodon monoceros* in Canada. Committee on the Status of Endangered Wildlife in Canada, Ottawa, Ontario, Canada.

Doniol-Valcroze, T., J.F. Gosselin, D. Pike, J. Lawson, N. Asselin, K. Hedges, and S.H. Ferguson. 2015. Abundance estimates of narwhal stocks in the Canadian high-Arctic in 2013. DFO Canadian Science Research Document 2015/060. Fisheries and Oceans Canada, Ottawa, Ontario, Canada.

Greely, A.W. 1886. Natural history notes. Appendix VII. Pages 359-371 *in* A.W. Greely. *Three years of Arctic service; an account of the Lady Franklin Bay Expedition of 1881-84 and the attainment of the farthest north.* Vol. 2. Richard Bentley and Son, London, England.

Hobbs, R.C., R.R. Reeves, J.S. Prewitt, G. Desportes, K. Breton-Honeyman, T. Christensen, J.J. Citta, S.H. Ferguson, K.J. Frost, E. Garde, M. Gavrilo, M. Ghazal, D.M. Glazov, J.F. Gosselin, M. Hammill, R.G. Hansen, L. Harwood, M.P. Heide Jørgensen, G. Inglangasuk, K.M. Kovacs, V.V. Krasnova, D.M. Kuznetsova, D.S. Lee, V. Lesage, D.I. Litovka, E.D. Lorenzen, L.F. Lowry, C. Lydersen, C.J.D. Matthews, I.G. Meschersky, A. Mosnier, G. O’Corry-Crowe, L. Postma, L.T. Quakenbush, O.V. Shpak, M. Skovrind, R.S. Suydam, and C.A. Watt. 2019. Global review of the conservation status of monodontid stocks. Marine Fisheries Review 81:3-4.

Higdon, J.W. and S.H. Ferguson. 2009. Loss of Arctic sea ice causing punctuated change in sightings of killer whales (Orcinus orca) over the past century. Ecological Applications 19(5):1365-1375.

Laidre, K.L., I. Stirling, L.F. Lowry, O. Wiig, M.P. Heide-Jørgenson, and S.H. Ferguson. 2008. Quantifying the sensitivity of Arctic marine mammals to climate-induced habitat change. Ecological Applications 18(2):97-125.

Lange, B.A., C. Haas, J. Charette, C. Katlein, K. Campbell, S. Duerksen, P. Coupel, P. Anhaus, A. Jutila, P.O.G. Tremblay, C.G. Carlyle, and C. Michel. 2019. Contrasting ice algae and snow-dependent irradiance relationships between first-year and multiyear sea ice. Geophysical Research Letters 46(19):10834-10843.

Lomac-McNair, K., M. Jakobsson, A. Mix, F. Freire, K. Hogan, L. Mayer, and M.A. Smultea 2018. Seal occurrence and habitat use during summer in Petermann Fjord, Northwestern Greenland. Arctic 71(3):334-348.

Lomac-McNair, K., J.P. Andrade, E. Esteves. 2019. Seal and polar bear behavioural response to an icebreaker vessel in northwest Greenland. Human-Wildlife Interactions 13(2):277-289.

Lowry, L., K.L. Laidre, and R. Reeves. 2017. *Monodon monoceros*. The IUCN Red List of Threatened Species 2017: e.T13704A50367651.en. https://dx.doi.org/10.2305/IUCN.UK.2017-3.RLTS.T13704A50367651.en.

Mallory, M.L., H.G. Gilchrist, M. Janssen, H.L. Major, F. Merkel, J.F. Provencher, and H. Strøm 2018. Financial costs of conducting science in the Arctic: examples from seabird research. Arctic Science 4(4):624-633.

Moore, G.W.K., A. Schweiger, J. Zhang, and M. Steele. 2019. Spatiotemporal variability of sea ice in the Arctic's Last Ice Area. Geophysical Research Letters 46:11,237-11,243.

Peary, R.E. 1910. *The North Pole*. Hodder and Stoughton, London, England.

Yurkowski, D.J., C.G. Carlyle, U. Amarualik, B.A. Lange, A. Platt, J.W. Higdon, D.B. Stewart, A. Ferguson, S.H. Ferguson, and C. Michel 2019. Novel Observations of Atlantic walruses (*Odobenus rosmarus rosmarus*) in Archer Fjord, northern Ellesmere Island, Nunavut, Canada. Polar Biology 42:1193-1198.

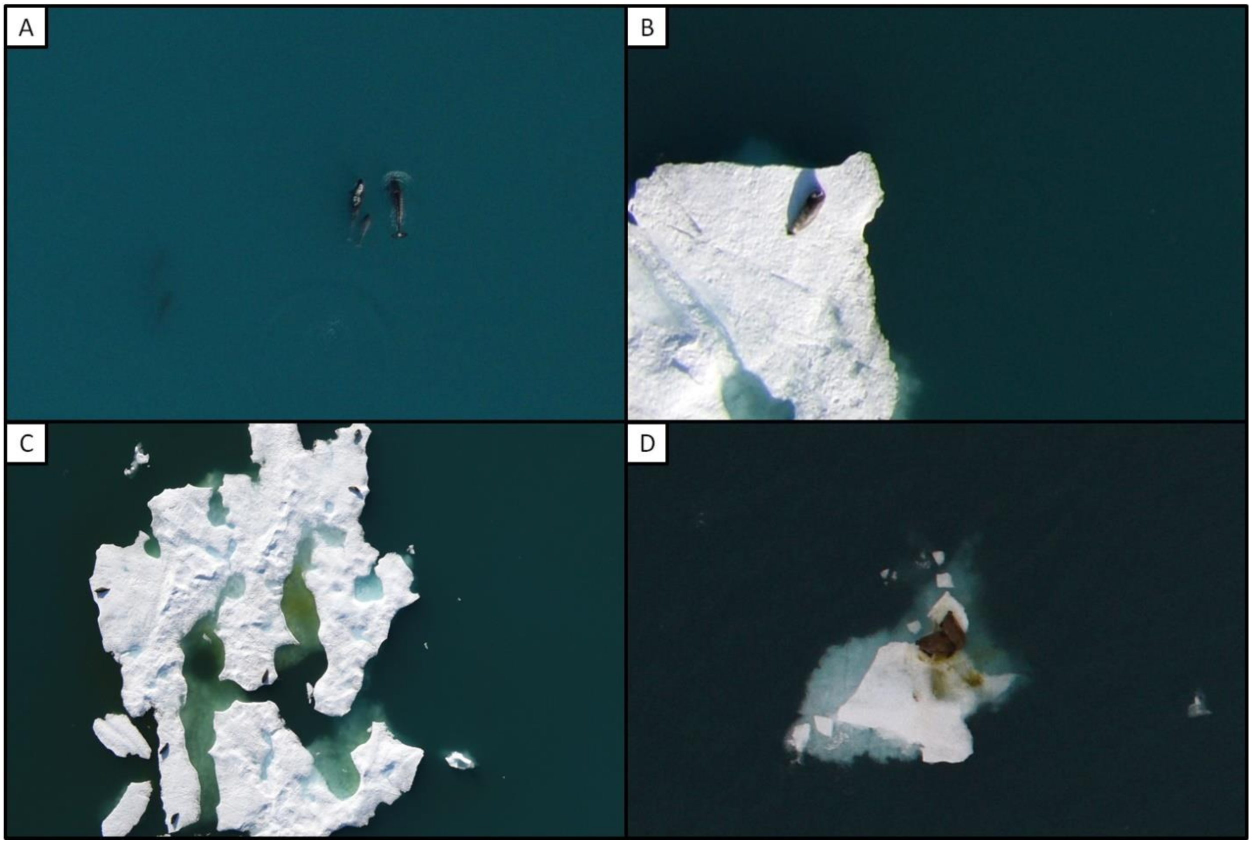

Figure 4.1. Close-up images of (A) a group of five narwhals including a yearling, (B) a bearded seal, and (C) six ringed seals taken in Archer Fjord and Lady Franklin Bay on 14 August 2019. (D) Close-up image of two Atlantic walruses taken in Archer Fjord on 18 August 2019.

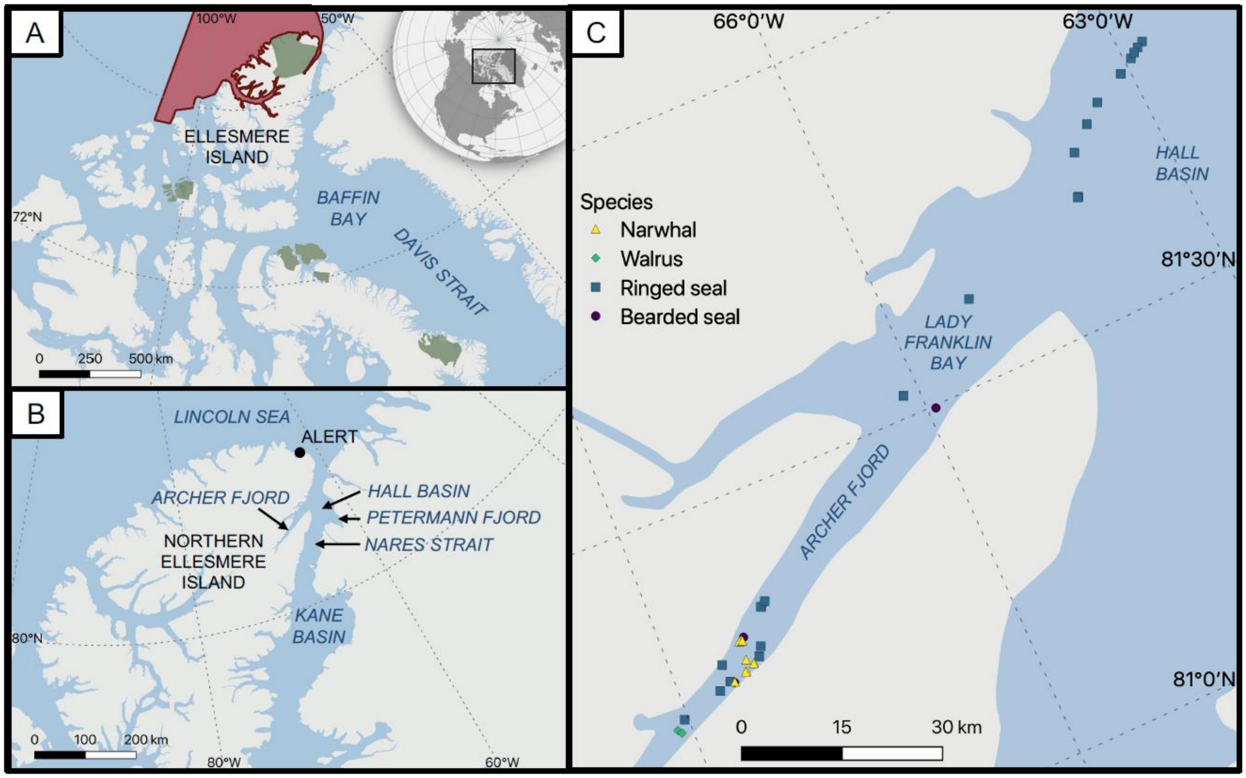

Figure 4.2. (A) The eastern Canadian and western Greenland Arctic. The area covered by the TMPA is indicated in red and the area covered by national parks is indicated in green (shapefiles from Natural Resources Canada at https://open.canada.ca/data). (B) Study region and place names mentioned in text. (C) Location of the marine mammals observed in Archer Fjord, Nunavut, Canada on 14 and18 August 2019. Map was generated using QGIS version 3.6.2 (http://www.qgis.org/en/site/).

Chapter 5: General conclusion

In this thesis, we examined the abundance and feeding of ringed seals over an unprecedented latitudinal gradient while also documenting the biodiversity and occurrence of marine mammals from the first systematic aerial surveys in the high Arctic “Last Ice Area”. We observed considerable plasticity in the density and diet of ringed seals from low to high Arctic and propose that these patterns are directly linked to the different sea-ice conditions experienced over this latitudinal gradient. The observed decrease in ringed seal density in the high Arctic that mirrors a decrease in preferred first-year ice and increase in multiyear ice availability suggests that the immediate response of ringed seals to sea-ice loss will not be uniform across their range, as preferred first-year ice will increase in the north but will be lost in the south in conjunction with more open water. The predicted loss of preferred first-year ice in the low Arctic threatens the breeding and molting habitat of ringed seals and has led to circumpolar countries being proactive and recommending the ringed seal be listed as “special concern” (Kelly et al. 2010, COSEWIC 2019). Moreover, the positive impacts associated with a decrease in multiyear ice in the high Arctic would cease if multiyear ice is completely replaced by first year ice, which is projected to happen by the middle of the century. (Overland & Wang 2013, Laidre et al. 2020).

When comparing ringed seal diets across our latitudinal gradient, results showed a distinct shift from more reliance on pelagic carbon in the low Arctic to a higher proportion of sympagic carbon in their diet in the high Arctic. We also found that ringed seals show an increase in relative trophic position from low to high latitude, which previous studies suggest could be a result of increased consumption of ice-associated fish such as Arctic cod, or increased zooplankton community complexity (Yurkowski et al. 2016b). Therefore, ringed seals diets can be used to examine future shifts in the composition of primary productivity, zooplankton, and fish communities in Arctic food webs (Fossheim et al. 2015, Dalpadado et al. 2016, de la Vega et al. 2021b). A shift in composition of primary production and zooplankton communities could also have negative impacts on ringed seals. As top predators, ringed seals are more vulnerable to ecosystem and biomass changes in the lower trophic levels. The higher trophic position of the high Arctic ringed seals make them more vulnerable due to predator-prey mass ratios and energy transfer efficiency up a trophic pyramid (Yurkowski et al. 2016b, Møller & Nielsen 2020).

A seasonal effect on pelagic versus sympagic carbon in the diet of ringed seals may also be present, but we did not have enough samples from different months to test for seasonal diet shifts (Brown et al. 2017). As a random effect, month had high intraclass correlation with our trophic position measurements in both muscle and liver, which suggests temporal variability in prey, trophic structure or physiological effects due to moulting or fasting of ringed seals (Young & Ferguson 2014). However, we found little correlation with month for liver and none in muscle for our carbon source metrics, suggesting negligible seasonal variation in the carbon source in ringed seal diets. Moreover, our samples from high Arctic Grise Fjord were collected from July to September, which would capture ringed seal diets from the open water period and these individuals still had a higher sympagic carbon contribution than the low Arctic during a similar time. These summer Grise Fjord samples also had less pelagic carbon than winter samples from the intermediate Arctic and high Arctic Qaanaaq, which would be biased towards a signal of less pelagic production. Therefore, seasonal effects do not seem to influence our observation of a high amount of sympagic carbon contributing to ringed seal diets in the high Arctic. Previous studies found a seasonal fluctuation in sympagic carbon that correlates with sea ice and daily sunlight in Cumberland Sound, Nunavut (Brown et al. 2014a). Unique properties in Cumberland Sound such as a polynya may increase the seasonal impact of sunlight on biological productivity

(Brown et al. 2014a). Future studies with adequate seasonal sampling could investigate the interaction between space and time in the diet of ringed seals across a latitudinal gradient. For example, the contribution of sea-ice derived carbon to ringed seal diets throughout the year could be different in low Arctic Arviat with transient sea-ice coverage compared to high Arctic Grise Fjord with almost year-round sea-ice coverage.

Our study also did not consider other factors that could impact the management and conservation of ringed seals with continued sea-ice loss in the Arctic. We did not consider the impact that increased prevalence of more temperate competitors such as harp seals (*Pagophilus groenlandicus*) in the Arctic may have on ringed seals (Ogloff et al. 2019). Continued sea-ice recession is also leading to rapid increases in human activities in the Arctic, including shipping and ice breaking (Post et al. 2013, Yurkowski et al. 2019b). Shipping and ice breaking have the potential to increase disturbance and mortality in ringed seals through increased noise, destruction of sea-ice habitat, and collisions, especially in our low and intermediate study sites covering Hudson Bay and Eclipse Sound (Stewart et al. 2010, Hauser et al. 2018). Anthropogenic disturbance and shipping can impact the distribution and foraging ecology of ringed seals and future studies could investigate the role that they play in the patterns we observed.

In this study we characterized how ringed seals respond to regional variation in sea-ice conditions from a perspective of habitat change and food web variation to gain a more complete picture of how sea-ice loss may impact this species. We also established a survey design and a baseline estimate for longitudinal monitoring studies of the abundance of ringed seals and other marine mammals in the high Arctic “Last Ice Area”. This “Last Ice Area” composed of the Canadian Arctic Archipelago and northern Greenland is expected to contain summer sea ice longer than any other Arctic region and has been identified as a refuge for ice-dependent species (Moore et al. 2019, Schweiger et al. 2020). This poorly studied region has now been targeted for extensive research to gain a holistic ecosystem understanding of this unique high Arctic region and identify critical habitat for protection (Lange et al. 2019, Yurkowski et al. 2019a, Carlyle et al. 2021). Our information on high Arctic ringed seal abundance and diets can be combined with information on sea ice, primary production, and the entire food web to help characterize this ecosystem in the context of its unique ice habitat.

Generally, changes to the Arctic environment are likely to cause some level of adaptation, demographic, and population consequences to ringed seals. The flexibility in their abundance and diet in this study demonstrates that ringed seals may also have a limited capacity to respond to shifts in sea-ice habitat and food webs. The response of ringed seals to changes in sea-ice conditions and prey availability could have impacts on other Arctic species. For example, a shorter ice-covered season and a switch to more pelagic foraging could change time spent by ringed seals in the sea-ice environment and create a mismatch in the polar bear-ringed seal relationship, since polar bears rely on hunting ringed seals in the sea-ice environment for most of their diet (Yurkowski et al. 2020b). The culture and subsistence of people across the Arctic is also tightly linked to annual harvests of ringed seals. Changes to the demographics, distribution, and behaviour of ringed seals impact the reliability and success of these hunts, as they rely on traditional knowledge of spatial and temporal availability of seals. We provide information on how a key Arctic predator adjusts to varying environmental conditions, which will aid management to mitigate the effects of climate change and human development in the Arctic, and develop effective co-management with northern people for sustainable harvests that are vital to food security and cultural identity (Laidre et al. 2015).

References

Brown TA, Alexander C, Yurkowski DJ, Ferguson SH, Belt ST (2014) Identifying variable sea ice carbon contributions to the Arctic ecosystem: A case study using highly branched isoprenoid lipid biomarkers in Cumberland Sound ringed seals. Limnol Oceanogr 59:1581–1589.

Brown TA, Chrystal E, Ferguson SH, Yurkowski DJ, Watt C, Hussey NE, Kelley TC, Belt ST (2017) Coupled changes between the H-Print biomarker and δ15N indicates a variable sea ice carbon contribution to the diet of Cumberland Sound beluga whales. Limnol Oceanogr 62:1606–1619.

Carlyle CG, Florko KRN, Young BG, Yurkowski DJ, Michel C, Ferguson SH (2021) Marine mammal biodiversity and rare narwhal (*Monodon monoceros*) observations near northern Ellesmere Island, Canada . Ecosphere 12.

COSEWIC. (2019). COSEWIC assessment and update status report on the ringed seal *Pusa hispida* in Canada. Committee on the Status of Endangered Wildlife in Canada, Ottawa. xii + 82 pp.

Dalpadado P, Hop H, Rønning J, Pavlov V, Sperfeld E, Buchholz F, Rey A, Wold A (2016) Distribution and abundance of euphausiids and pelagic amphipods in Kongsfjorden, Isfjorden and Rijpfjorden (Svalbard) and changes in their relative importance as key prey in a warming marine ecosystem. Polar Biol 39:1765–1784.

Fossheim M, Primicerio R, Johannesen E, Ingvaldsen RB, Aschan MM, Dolgov A V. (2015) Recent warming leads to a rapid borealization of fish communities in the Arctic. Nat Clim Chang 5:673–677.

Hauser DDW, Laidre KL, Stern HL (2018) Vulnerability of Arctic marine mammals to vessel traffic in the increasingly ice-free Northwest Passage and Northern Sea Route. PNAS 115:7618-7622.

de la Vega C, Mahaffey C, Yurkowski DJ, Norman L, Simpson E, Smout S, Ferguson SH, Jeffreys RM (2021) Biomarkers in Ringed Seals Reveal Recent Onset of Borealization in the High- Compared to the Mid-Latitude Canadian Arctic. Front Mar Sci 8:700687.

Kelly, B.P., Bengston, J.L., Boveng, P.L., Cameron, M.F., Dahle, S.P., Jansen, J.K., Logerwell, E.A., Overland, J.E., Sabine, G.L., Waring, G.T., & Wilder, J.M. (2010). Status Review of the Ringed Seal (*Phoca hispida*). U.S. Dept. Commer., NOAA Tech. Memo. NMFS-AFSC-212, 250p.

Laidre KL, Atkinson SN, Regehr E V, Stern HL, Born EW, Wiig Ø, Lunn NJ, Dyck M, Heagerty P, Cohen BR (2020) Transient benefits of climate change for a high-Arctic polar bear (*Ursus maritimus*) subpopulation. Glob Chang Biol 1–15.

Laidre KL, Stern H, Kovacs KM, Lowry L, Moore SE, Regehr E V, Ferguson SH, Wiig Ø, Boveng P, Angliss RP, Born EW, Litovka D, Quakenbush L, Lydersen C, Vongraven D, Ugarte F (2015) Arctic marine mammal population status, sea ice habitat loss, and conservation recommendations for the 21st century. Cons Biol 29:724–737.

Lange BA, Haas C, Charette J, Katlein C, Campbell K, Duerksen S, Coupel P, Anhaus P, Jutila A, Tremblay POG, Carlyle CG, Michel C (2019) Contrasting Ice Algae and Snow-Dependent Irradiance Relationships Between First-Year and Multiyear Sea Ice. Geophys Res Lett 46:10834–10843.

Møller EF, Nielsen TG (2020) Borealization of Arctic zooplankton—smaller and less fat zooplankton species in Disko Bay, Western Greenland. Limnol Oceanogr 65:1175–1188.

Moore GWK, Schweiger A, Zhang J, Steele M (2019) Spatiotemporal Variability of Sea Ice in the Arctic's Last Ice Area. Geophys Res Lett 46:11237–11243.

Ogloff WR, Yurkowski DJ, Davoren GK, Ferguson SH (2019) Diet and isotopic niche overlap elucidate competition potential between seasonally sympatric phocids in the Canadian Arctic. Mar Biol 166:1–12.

Post E, Bhatt US, Bitz CM, Brodie JF, Fulton TL, Hebblewhite M, Kerby JT, Kutz S, Stirling I, Walker DA (2013) Ecological Consequences of Sea-Ice Decline. Science (80) 341:519–524.

Schweiger AJ, Steele M, Zhang J, Moore GWK, Laidre KL (2020) Accelerated sea ice loss in the Wandel Sea points to a change in the Arctic' s Last Ice Area. Commun Earth Environ:1–11.

Stewart EJ, Tivy A, Howell SEL, Dawson J, Draper D (2010) Cruise tourism and sea ice in Canada's Hudson Bay Region. Arctic 63:57–66.

Young BG, Ferguson SH (2014) Using stable isotopes to understand changes in ringed seal foraging ecology as a response to a warming environment. Mar Mammal Sci 30:706–725.

Yurkowski DJ, Carlyle CG, Amarualik U, Lange BA, Platt A, Higdon JW, Stewart DB, Ferguson A, Ferguson SH, Michel C (2019a) Novel observations of Atlantic walruses (*Odobenus rosmarus rosmarus*) in Archer Fjord, northern Ellesmere Island , Nunavut , Canada. Polar Biol 42:1193–1198.

Yurkowski DJ, Ferguson SH, Semeniuk CAD, Brown TM, Muir DCG, Fisk AT (2016) Spatial and temporal variation of an ice-adapted predator's feeding ecology in a changing Arctic marine ecosystem. Oecologia 180:631–644.

Yurkowski DJ, Young BG, Dunn JB, Ferguson SH (2019b) Spring distribution of ringed seals (*Pusa hispida*) in eclipse sound and Milne Inlet, Nunavut: Implications for potential ice-breaking activities. Arct Sci 5:54–61.

Appendix A: Statistical tables and supplementary figures

Table A.1. Summary biometrics for ringed seal liver (L) and muscle (M) sampled from the low (Arviat, NU), intermediate (Pond Inlet, NU), and high (Grise Fjord, NU and Qaanaaq, GL) Artic from 2016-2018.

Latitude	Location	N	Age Class (Pup: Juvenile: Adult)	Sex (Female: Male:Unknown)	Year (2018: 2017: 2016:)	Month
Low	Arviat	L – 40 M – 42	L - 8:16:16 M - 8:17:17	L - 14:19:7 M - 16:19:7	L - 40:0:0 M - 42:0:0	L - Oct: 40 M - Oct: 42
Intermediate	Pond Inlet	34	11:13:10	12:19:3	0:24:10	Jan: 1, Feb: 3, May: 2, June: 11, July: 4, Aug: 3, Sept: 2, Oct: 4, Nov: 3, Dec: 1
High	Grise Fjord	L - 15 M – 16	L - 6:3:6 M - 6:3:7	L - 7:7:1 M - 8:7:1	L - 15:0:0 M - 16:0:0	L - July: 7, Aug: 7, Sept: 1 M- July: 8, Aug: 7, Sept: 1
	Qaanaaq	18	1:7:10	9:9:0	18:0:0	May: 18
Total		L - 107 M – 110	L - 26:39:42 M - 26:40:44	L - 42:54:11 M - 45:54:11	L - 73:24:10 M - 76:24:10	L - Jan: 1, Feb: 3, May: 20, June: 11, July: 11, Aug: 10, Sept: 3, Oct: 44, Nov: 3, Dec: 1 M - Jan: 1, Feb: 3, May: 20, June: 11, July: 12, Aug: 10, Sept: 3, Oct: 46, Nov: 3, Dec: 1

Table A.2. Estimated regression values, standard errors, Kenward-Roger adjusted degrees of freedom, z-values, and p-values for the LMM comparing $\delta^{13}C$ in liver ($\delta^{13}C$ ~ location + age class + (1 | month), n = 107). Estimated value for $\text{sigma}_{\text{Month}}$ is 0.164.

	Estimate	Std. Error	df	z-value	P-value
Intercept	-20.8	0.162	10.05	-128.9	< 0.001
LocPI	1.38	0.151	14.45	9.139	< 0.001
LocGF	2.48	0.195	14.13	12.73	< 0.001
LocQA	1.85	0.227	7.392	8.146	< 0.001
AgeClassSubadult	-0.11	0.105	101.0	-1.008	0.316
AgeClassAdult	-0.04	0.106	99.95	-0.413	0.681

Table A.3. Estimated values, standard errors, Kenward-Roger corrected degrees of freedom, t-statistic, and p-values for Tukey post-hoc analysis comparing the means for each location for $\delta^{13}C$ in liver.

Contrast	Estimate	Standard error	df	t-value	p-value
AR – PI	-1.384	0.181	12.43	-7.648	< 0.0001
AR – GF	-2.480	0.232	12.14	-10.674	< 0.0001
AR – QA	-1.846	0.274	6.28	-6.731	< 0.005
PI – GF	-1.096	0.158	49.75	-6.953	< 0.0001
PI – QA	-0.462	0.217	8.52	-2.123	0.2205
GF – QA	-0.634	0.265	9.24	2.476	0.1295

Table A.4. Estimated regression values, standard errors, t-values, and p-values for the GLM comparing $\delta^{13}C$ in muscle ($\delta^{13}C$ ~ location + age class, n = 110).

	Estimate	Std. Error	t-value	P-value
Intercept	-21.4	0.110	-195.1	< 0.001
LocPI	1.71	0.105	16.22	< 0.001
LocGF	2.66	0.135	19.74	< 0.001
LocQA	2.31	0.128	18.02	< 0.001
AgeClassSubadult	-0.151	0.117	-1.288	0.201
AgeClassAdult	-0.045	0.115	-0.566	0.573

Table A.5. Estimated values, standard errors, t-statistic, and p-values for Tukey post-hoc analysis comparing the means for each location for $\delta^{13}C$ in muscle.

Contrast	Estimate	Standard error	t-value	p-value
AR – PI	-1.708	0.105	-16.22	< 0.0001
AR – GF	-2.662	0.135	-19.74	< 0.0001
AR – QA	-2.314	0.128	-18.02	< 0.0001
PI – GF	-0.954	0.138	-6.902	< 0.0001
PI – QA	-0.606	0.135	-4.480	< 0.0001
GF – QA	0.348	0.159	2.187	0.1267

Table A.6. Estimated regression values, standard errors, Kenward-Roger adjusted degrees of freedom, t-values, and p-values for the LMM comparing $\delta^{15}N$ in liver ($\delta^{15}N$ ~ location + age class + (1 | month), n = 107). Estimated value for $\text{sigma}_{\text{Month}}$ is 0.430.

	Estimate	Std. Error	df	z-value	P-value
Intercept	17.29	0.327	30.16	52.80	< 0.001
LocPI	-0.426	0.281	75.86	-1.519	< 0.133
LocGF	-0.491	0.362	74.41	-1.357	< 0.179
LocQA	-0.540	0.458	47.67	-1.117	< 0.245
AgeClassSubadult	0.151	0.165	98.38	0.914	0.363
AgeClassAdult	0.273	0.168	99.09	1.627	0.107

Table A.7. Estimated values, standard errors, Kenward-Roger corrected degrees of freedom, t-statistic, and p-values for Tukey post-hoc analysis comparing the means for each location for $\delta^{15}N$ in liver.

Contrast	Estimate	Standard error	df	t-value	p-value
AR – PI	-0.4259	0.300	71.0	1.421	0.4906
AR – GF	-0.4914	0.388	69.3	1.268	0.5861
AR – QA	-0.5396	0.501	41.6	1.077	0.7050
PI – GF	-0.0655	0.252	96.9	0.260	0.9938
PI – QA	-0.1137	0.403	41.8	0.282	0.9921
GF – QA	-0.0482	0.469	45.2	0.103	0.9996
Pup – Subadult	-0.151	0.166	97.7	-0.906	0.6377
Pup – Adult	-0.273	0.169	98.6	-1.609	0.2468

Subadult – Adult	-0.122	0.137	95.5	-0.886	0.6502

Table A.8. Estimated regression values, standard errors, Kenward-Roger adjusted degrees of freedom, z-values, and p-values for the LMM comparing $\delta^{15}N$ in muscle ($\delta^{15}N$ ~ location + age class + (1 | month), n = 110). Estimated value for $sigma_{Month}$ is 0.310.

	Estimate	Std. Error	df	z-value	P-value
Intercept	16.47	0.293	23.42	56.17	< 0.001
LocPI	-0.360	0.263	47.09	-1.372	0.1765
LocGF	0.136	0.337	45.08	0.404	0.6878
LocQA	-1.030	0.417	25.13	-2.473	< 0.05
AgeClassSubadult	0.108	0.162	102.9	0.665	0.5077
AgeClassAdult	0.422	0.164	103.7	2.568	< 0.05

Table A.9. Estimated values, standard errors, Kenward-Roger corrected degrees of freedom, t-statistic, and p-values for Tukey post-hoc analysis comparing the means for each location for $\delta^{15}N$ in muscle.

Contrast	Estimate	Standard error	df	t-value	p-value
AR – PI	0.360	0.291	40.1	1.239	0.6063
AR – GF	-0.136	0.374	38.2	-0.364	0.9832
AR – QA	1.030	0.472	20.2	2.184	0.1614
PI – GF	-0.497	0.244	83.2	-2.032	0.1847

PI – QA	0.670	0.378	22.2	1.772	0.3126
GF – QA	1.167	0.439	23.8	2.655	0.0623
Pup – Subadult	-0.108	0.165	102.6	-0.656	0.7894
Pup – Adult	-0.422	0.167	103.6	-2.521	< 0.05
Subadult – Adult	-0.314	0.134	99.7	-2.335	0.0556

Table A.10. Estimated regression values, standard errors, Kenward-Roger adjusted degrees of freedom, z-values, and p-values for the LMM comparing relative carbon source in liver (RC ~ location + age class + (1 | month), n = 107). Estimated value for $\text{sigma}_{\text{Month}}$ is 0.168.

	Estimate	Std. Error	df	z-value	P-value
Intercept	1.037	0.008	10.38	130.6	< 0.001
LocPI	-0.070	0.007	15.07	-9.357	< 0.001
LocGF	-0.158	0.010	14.72	-16.56	< 0.001
LocQA	-0.128	0.011	7.700	-11.51	< 0.001
AgeClassSubadult	0.005	0.005	101.0	0.997	0.321
AgeClassAdult	0.002	0.005	100.1	0.425	0.672

Table A.11. Estimated values, standard errors, Kenward-Roger corrected degrees of freedom, t-statistic, and p-values for Tukey post-hoc analysis comparing the means for each location for relative carbon source in liver.

Contrast	Estimate	Standard error	df	t-value	p-value
AR – PI	0.070	0.009	12.96	7.854	< 0.0001
AR – GF	0.158	0.011	12.65	13.93	< 0.0001
AR – QA	0.128	0.013	6.54	9.531	< 0.0005
PI – GF	0.090	0.008	50.84	11.54	< 0.0001
PI – QA	0.059	0.011	8.79	5.499	< 0.005
GF – QA	-0.030	0.013	9.53	-2.401	0.143

Table A.12. Estimated regression values, standard errors, t-values, and p-values for the GLM comparing relative carbon source in muscle (RC ~ location + age class, n = 110).

	Estimate	Std. Error	t-value	P-value
Intercept	1.067	0.005	-197.8	< 0.001
LocPI	-0.086	0.005	-16.60	< 0.001
LocGF	-0.169	0.007	-25.45	< 0.001
LocQA	-0.152	0.006	-24.09	< 0.001
AgeClassSubadult	0.007	0.006	1.270	0.207
AgeClassAdult	-0.003	0.006	-0.593	0.555

Table A.13. Estimated values, standard errors, t-statistic, and p-values for Tukey post-hoc analysis comparing the means for each location for relative carbon source in muscle.

Contrast	Estimate	Standard error	t-value	p-value
AR – PI	0.086	0.005	16.60	< 0.0001

AR – GF	0.169	0.007	25.45	< 0.0001
AR – QA	0.152	0.006	24.09	< 0.0001
PI – GF	0.083	0.007	12.19	< 0.0001
PI – QA	0.066	0.007	9.941	< 0.0001
GF – QA	-0.017	0.008	-2.134	0.1424

Table A.14. Estimated regression values, standard errors, Kenward-Roger adjusted degrees of freedom, z-values, and p-values for the LMM comparing relative trophic position in liver (TP ~ location + age class + (1 | month), n = 107). Estimated value for sigma$_{\text{Month}}$ is 0.431.

	Estimate	Std. Error	df	z-value	P-value
Intercept	4.029	0.106	30.16	38.16	< 0.001
LocPI	0.271	0.091	75.86	2.993	< 0.005
LocGF	0.664	0.117	74.41	5.685	< 0.001
LocQA	0.650	0.148	47.67	4.386	< 0.001
AgeClassSubadult	0.049	0.053	98.38	0.914	0.363
AgeClassAdult	0.088	0.054	99.09	1.627	0.107

Table A.15. Estimated values, standard errors, Kenward-Roger corrected degrees of freedom, t-statistic, and p-values for Tukey post-hoc analysis comparing the means for each location for relative trophic position in liver.

Contrast	Estimate	Standard error	df	t-value	p-value
AR – PI	-0.271	0.097	71.0	-2.800	< 0.05

AR – GF	-0.664	0.125	69.3	-5.313	< 0.0001
AR – QA	-0.649	0.162	41.6	-4.015	< 0.005
PI – GF	-0.393	0.081	96.9	-4.848	< 0.0001
PI – QA	-0.378	0.130	41.8	-2.903	< 0.05
GF – QA	0.016	0.151	45.2	0.103	0.9996

Table A.16. Estimated regression values, standard errors, Kenward-Roger adjusted degrees of freedom, z-values, and p-values for the LMM comparing relative trophic position in muscle (TP ~ location + age class + (1 | month), n = 110). Estimated value for sigma$_{\text{Month}}$ is 0.310.

	Estimate	Std. Error	df	z-value	P-value
Intercept	3.94	0.122	23.42	32.23	< 0.001
LocPI	0.207	0.109	47.09	1.893	0.0645
LocGF	0.935	0.141	45.08	6.656	< 0.001
LocQA	0.449	0.174	25.13	2.585	< 0.05
AgeClassSubadult	0.045	0.068	102.9	0.665	0.508
AgeClassAdult	0.176	0.069	103.7	2.568	< 0.05

Table A.17. Estimated values, standard errors, Kenward-Roger corrected degrees of freedom, t-statistic, and p-values for Tukey post-hoc analysis comparing the means for each location for relative trophic position in muscle.

Contrast	Estimate	Standard error	df	t-value	p-value
AR – PI	-0.207	0.121	40.1	-1.709	0.3324

AR – GF	-0.935	0.156	38.2	-5.996	< 0.0001
AR – QA	-0.447	0.197	20.2	-2.283	0.1352
PI – GF	-0.728	0.102	83.2	-7.145	< 0.0001
PI – QA	-0.242	0.158	22.2	-1.534	0.4352
GF – QA	0.486	0.183	23.8	2.655	0.0623
Pup – Subadult	-0.045	0.069	102.6	-0.656	0.7894
Pup – Adult	-0.176	0.070	103.6	-2.521	< 0.05
Subadult – Adult	-0.131	0.056	99.7	-2.335	0.0556

Table A.18. Estimated regression values, standard errors, t-values, and p-values for the GLM comparing sympagic carbon in liver (Beta[sympagic carbon] ~ location + age class, n = 107).

	Estimate	Std. Error	t-value	P-value
Intercept	-1.046	0.187	-5.579	< 0.001
LocPI	2.901	0.187	15.55	< 0.001
LocGF	3.302	0.258	12.79	< 0.001
LocQA	2.693	0.216	12.47	< 0.001
AgeClassSubadult	-0.302	0.201	-1.500	0.1336
AgeClassAdult	-0.366	0.200	-1.829	0.0675

Table A.19. Estimated values, standard errors, t-statistic, and p-values for Tukey post-hoc analysis comparing the means for each location for sympagic carbon in liver.

Contrast	Estimate	Standard error	t-value	p-value
AR – PI	-0.615	0.028	-7.648	< 0.0001
AR – GF	-0.663	0.032	-10.674	< 0.0001
AR – QA	-0.584	0.035	-6.731	< 0.0001
PI – GF	-0.048	0.029	-6.953	0.3458
PI – QA	-0.031	0.033	-2.123	0.7952
GF – QA	-0.078	0.036	2.476	0.1268

Table A.20. Estimated regression values, standard errors, t-statistic, and p-values for the GLM investigating spatial differences in ringed seal density (Seals/km^2). (Gamma[Density] ~ location, n = 5).

	Estimate	Std. Error	t-value	P-value
Intercept	14.359	3.846	3.733	0.0649
LocationIntermediate	-12.636	3.874	-3.262	0.0825
LocationLow	-12.163	3.935	-3.091	0.0907

Table A.21. Estimated values, standard errors, t-statistic, and p-values for Tukey post-hoc analysis comparing the mean ringed seal density for each survey location.

Contrast	Estimate	Standard error	t-value (z?)	p-value
High - intermediate	12.636	3.874	3.262	< 0.005
High - low	12.163	3.935	3.091	< 0.005

Intermediate – low	-0.474	0.952	-0.498	0.8614

Table A.22. Estimated regression values, standard errors, t-statistic, and p-values for the simple linear regression investigating the relationship between ringed seal density (Seals/km^2) and total ice concentration (%). (Density ~ total ice concentration, n = 5).

	Estimate	Std. Error	f-value	P-value
Intercept	0.81708	2.47722	0.330	0.763
TotalIceConcentation	-0.00483	0.02563	-0.188	0.863

Table A.23. Estimated regression values, standard errors, t-statistic, and p-values for the simple linear regression investigating the relationship between ringed seal density (Seals/km^2) and first-year ice concentration (%). (Density ~ first-year ice concentration, n = 5).

	Estimate	Std. Error	f-value	P-value
Intercept	0.003094	0.075184	0.041	0.9698
FirstYearIce	0.005867	0.001048	5.601	0.0112

Table A.24. Estimated regression values, standard errors, t-statistic, and p-values for the simple linear regression investigating the relationship between ringed seal density (Seals/km^2) and multiyear ice concentration (%). (Density ~ multiyear ice concentration, n = 5).

	Estimate	Std. Error	f-value	P-value
Intercept	0.559306	0.067771	8.253	0.00373
MultiyearIce	-0.005653	0.001228	-4.604	0.01927

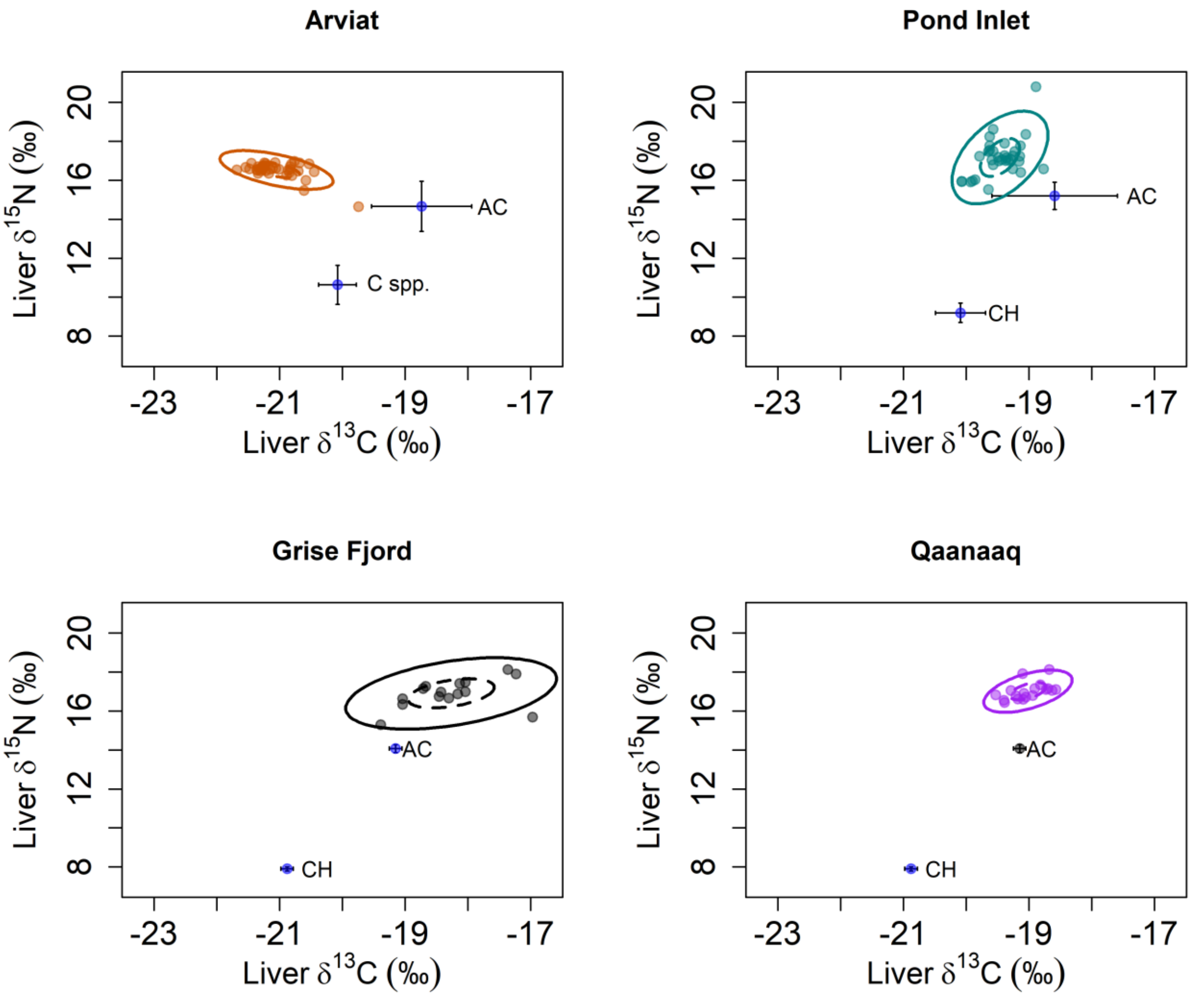

Figure A.1. δ^{13}C and δ^{15}N for ringed seal liver samples collected in 2018 from Arviat, NU, Grise Fjord, NU, and Qaanaaq, GL, and in 2016-2017 from Pond Inlet, NU with dashed ellipses representing the 95% confidence intervals of multivariate t-distributions for each location and with prey baselines (AC = Arctic Cod, CH = *Calanus hyperboreus*, C spp. = *Calanus* spp.) used for relative carbon source and relative trophic position calculations in each location (Hobson, Keith A., and Welch 1992, Hobson et al. 2002, Chambellant et al. 2013b) (Table 3.2).

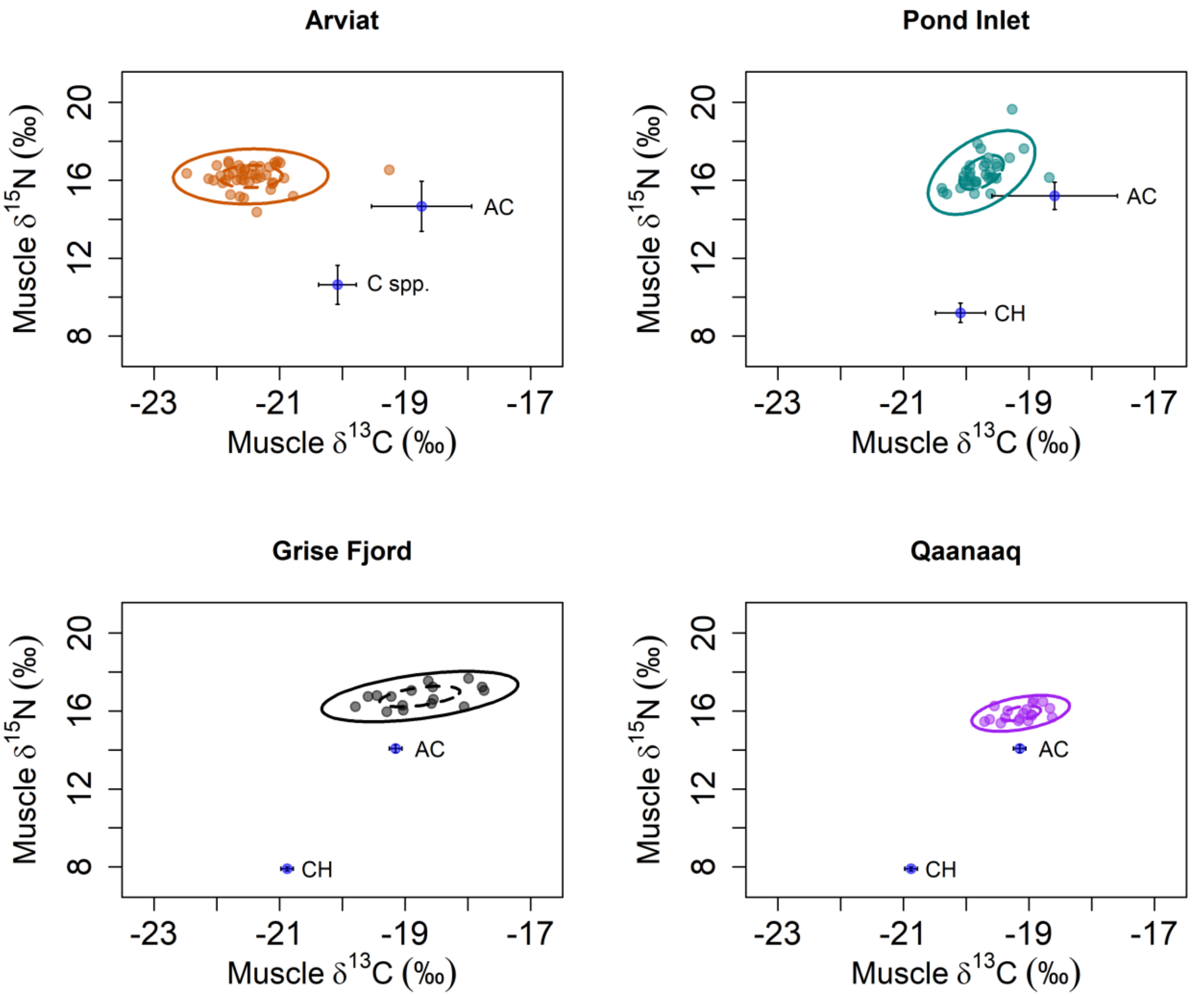

Figure A.2. δ^{13}C and δ^{15}N for ringed seal muscle samples collected in 2018 from Arviat, NU, Grise Fjord, NU, and Qaanaaq, GL, and in 2016-2017 from Pond Inlet, NU with dashed ellipses representing the 95% confidence intervals of multivariate t-distributions for each location and with prey baselines (AC = Arctic Cod, CH = *Calanus hyperboreus*, C spp. = *Calanus* spp.) used for relative carbon source and relative trophic position calculations in each location (Hobson, Keith A., and Welch 1992, Hobson et al. 2002, Chambellant et al. 2013b) (Table 3.2).

Appendix B: Supporting tables and figures from Chapter 4

Table B.1: Date, time, count, and GPS location associated with all photographed sightings of marine mammals on the two transect lines covering Archer Fjord and Lady Franklin Bay, Nunavut, Canada on 14 and 18 August, 2019.

Date	**Time (UTC)**	**Species**	**Count**	**GPS Position†**
14 August 2019	18:29:39	Ringed seal	1	81.67, 63.94
14 August 2019	18:29:41	Ringed seal	1	81.67, 63.95
14 August 2019	18:40:41	Bearded seal	1	81.50, 65.92
14 August 2019	18:52:30	Ringed seal	3	81.30, 68.18
14 August 2019	18:53:59	Ringed seal	1	81.27, 68.54
14 August 2019	18:54:27	Ringed seal	1	81.26, 68.66
14 August 2019	18:57:57	Narwhal	1	81.29, 68.35
14 August 2019	18:59:02	Ringed seal	2	81.28, 68.23
14 August 2019	18:59:21	Narwhal	6	81.28, 68.29
14 August 2019	18:59:23	Narwhal	2 (one repeat)	81.28, 68.29
14 August 2019	18:59:51	Narwhal	1	81.27, 68.38
14 August 2019	18:59:55	Narwhal	2	81.27, 68.39
14 August 2019	19:00:33	Narwhal	6	81.26, 68.51
14 August 2019	19:00:35	Bearded seal	1	81.26, 68.51
14 August 2019	19:16:22	Ringed seal	6	81.24, 69.03
14 August 2019	19:19:13	Ringed seal	1	81.29, 68.56
14 August 2019	19:22:10	Ringed seal	1	81.34, 68.05
14 August 2019	19:22:24	Bearded seal	1	81.35, 68.00
14 August 2019	19:26:06	Narwhal	6	81.31, 68.32
14 August 2019	19:26:10	Narwhal	1	81.31, 68.33
14 August 2019	19:26:14	Narwhal	1	81.31, 68.34
14 August 2019	19:28:05	Narwhal	2	81.31, 68.32
14 August 2019	19:28:07	Narwhal	2	81.31, 68.31

14 August 2019	19:28:17	Bearded seal	1	81.32, 68.29
14 August 2019	19:29:53	Ringed seal	1	81.34, 68.05
14 August 2019	19:30:07	Ringed seal	1	81.35, 68.00
14 August 2019	19:42:01	Ringed seal	2	81.53, 66.15
14 August 2019	19:47:51	Ringed seal	1	81.61, 65.25
14 August 2019	19:56:50	Ringed seal	1	81.75, 63.58
14 August 2019	20:00:27	Ringed seal	1	81.80, 62.93
18 August 2019	17:33:04	Ringed seal	1	81.82, 62.77
18 August 2019	17:33:23	Ringed seal	1	81.81, 62.83
18 August 2019	17:33:38	Ringed seal	1	81.81, 62.89
18 August 2019	17:34:43	Ringed seal	1	81.79, 63.09
18 August 2019	17:36:16	Ringed seal	1	81.77, 63.40
18 August 2019	17:38:40	Ringed seal	1	81.73, 63.79
18 August 2019	18:08:57	Atlantic walrus	1	81.23, 69.13
18 August 2019	18:20:54	Atlantic walrus	2	81.23, 69.10

† Latitude in decimal degrees north, longitude in decimal degrees west.

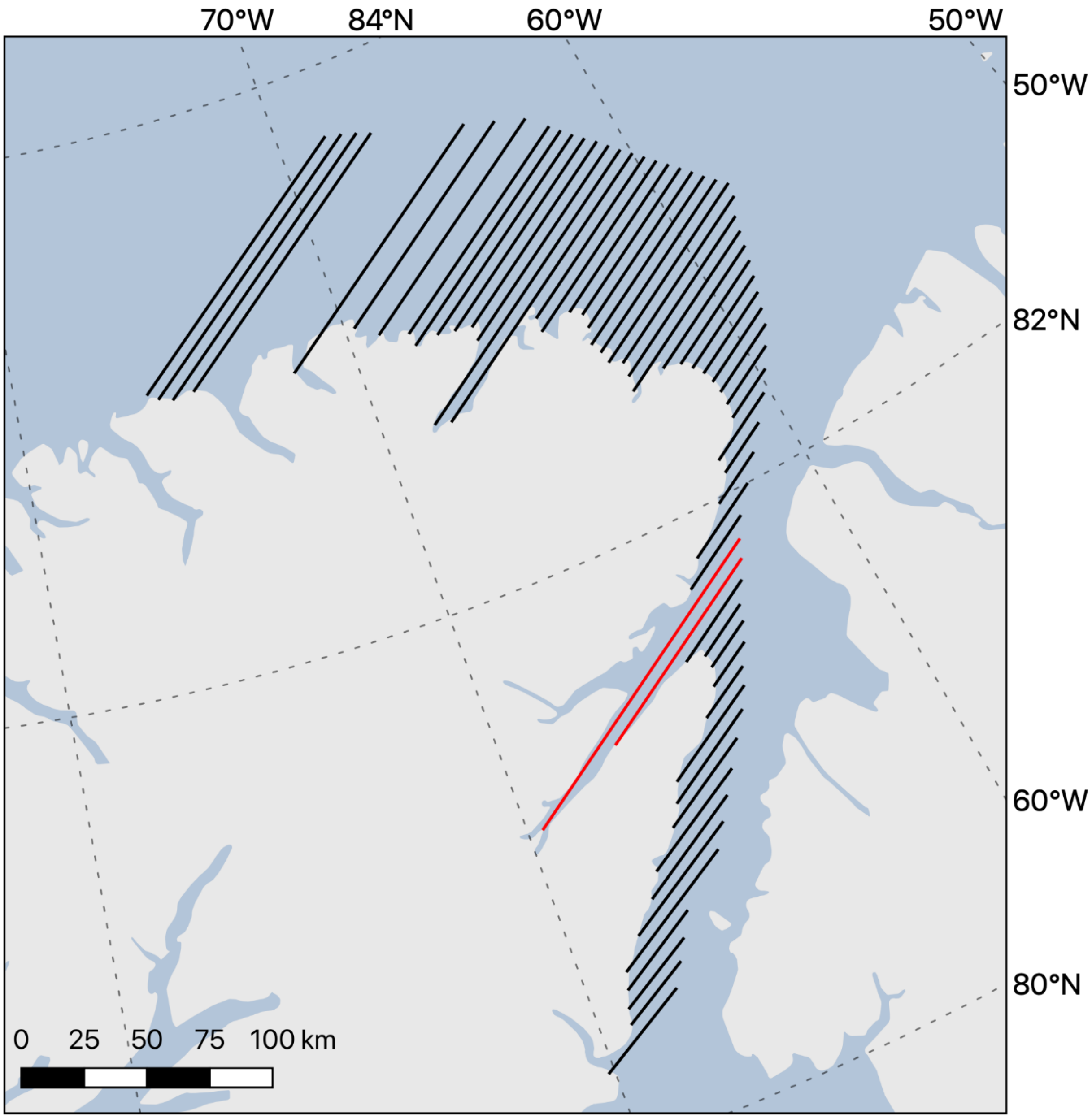

Figure B.1. All 57 transect lines flown for the marine mammal aerial surveys based out of Alert, Nunavut from 14 to 18 August 2019. Solid red lines indicate the transects that cover Archer Fjord and Lady Franklin Bay, Nunavut, Canada. Solid black lines indicate the 55 transects that do not cover Archer Fjord and Lady Franklin Bay. Map was generated using QGIS version 3.6.2 (http://www.qgis.org/en/site/).

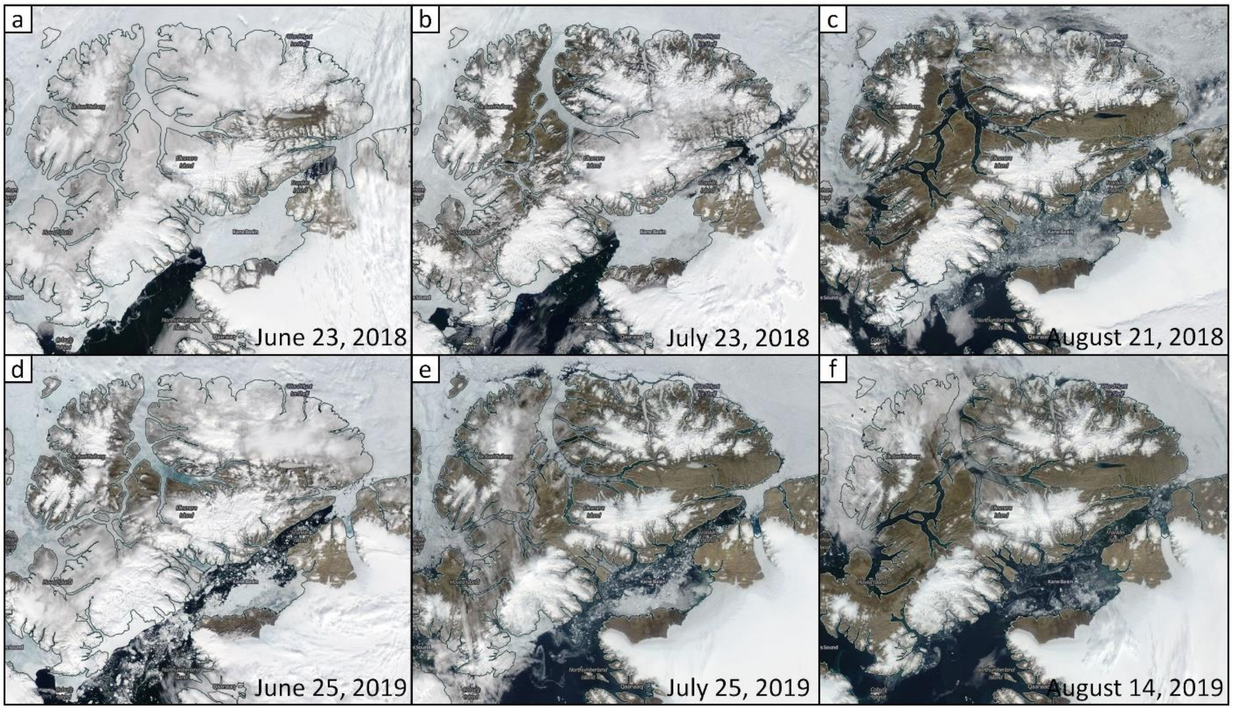

Figure B.2. MODIS satellite imagery of the sea-ice conditions of the eastern Canadian and western Greenland high-Arctic surrounding our study area for (a) 23 June 2018, (b) 23 July 2018, (c) 21 August 2018, (d) 25 June 2019, (e) 25 July 2019, and (f) 14 August 2019 (accessed from NASA Worldview at https://go.nasa.gov/39IdDgE). Variable dates between years are due to cloud cover and visibility, and approximately correspond to the survey start date (c and f), one month before the survey date (b and e), and two months before the survey date (a and d) for 2018 and 2019.